THESIS

EVALUATING CHANNEL MORPHOLOGIC CHANGES AND BED-MATERIAL TRANSPORT USING AIRBORNE LIDAR, UPPER COLORADO RIVER, ROCKY MOUNTAIN NATIONAL PARK, COLORADO

Submitted by

Joseph F. Mangano

Department of Geosciences

In partial fulfillment of the requirements

For the Degree of Master of Science

Colorado State University

Fort Collins, Colorado

Summer 2014

Master's Committee:

Advisor: Sara Rathburn

Ellen Wohl
Brian Bledsoe

Copyright by Joseph F. Mangano 2014

All Rights Reserved

ABSTRACT

EVALUATING CHANNEL MORPHOLOGIC CHANGES AND BED-MATERIAL TRANSPORT USING AIRBORNE LIDAR, UPPER COLORADO RIVER, ROCKY MOUNTAIN NATIONAL PARK, COLORADO

A debris flow associated with the 2003 breach of Grand Ditch in Rocky Mountain National Park, Colorado provided an opportunity to determine controls on channel geomorphic responses following a large sedimentation event. Due to the remote site location and high spatial and temporal variability of processes controlling channel response, repeat airborne lidar surveys in 2004 and 2012 were used to capture conditions along the upper Colorado River and tributary Lulu Creek i) one year following the initial debris flow, and ii) following two bankfull flows (2009 and 2010) and a record-breaking long duration, high intensity snowmelt runoff season (2011). Locations and volumes of aggradation and degradation were determined using lidar differencing. Channel and valley metrics measured from the lidar surveys included water surface slope, valley slope, changes in bankfull width, sinuosity, braiding index, channel migration, valley confinement, height above the water surface along the floodplain, and longitudinal profiles.

Reaches of aggradation and degradation along the upper Colorado River are influenced by valley confinement and local controls. Aggradational reaches occurred predominantly in locations where the valley was unconfined and valley slope remained constant through the length of the reach. Channel avulsions, migration, and changes in sinuosity were common in all unconfined reaches, whether aggradational or degradational. Bankfull width in both aggradational and degradational reaches showed greater changes closer to the sediment source, with the magnitude of change decreasing downstream. Local variations in channel morphology, site specific channel conditions, and the distance from the

sediment source influence the balance of transport supply and capacity and, therefore, locations of aggradation, degradation, and associated morphologic changes. Additionally, a complex response initially seen in repeat cross-sections is broadly supported by lidar differencing, although the differencing captures only the net change over eight years and not annual changes. Lidar differencing shows great promise because it reveals vertical and horizontal trends in morphologic changes at a high resolution over a large area.

Repeat lidar surveys were also used to create a sediment budget along the upper Colorado River by means of the morphologic inverse method. In addition to the geomorphic changes detected by lidar, several levels of attrition of the weak clasts within debris flow sediment were applied to the sediment budget to reduce gaps in expected inputs and outputs. Bed-material estimates using the morphologic inverse method were greater than field-measured transport estimates, but the two were within an order of magnitude. Field measurements and observations are critical for robust interpretation of the lidar-based analyses because applying lidar differencing without field control may not identify local controls on valley and channel geometry and sediment characteristics. The final sediment budget helps define variability in bed-material transport and constrain transport rates through the site, which will be beneficial for restoration planning. The morphologic inverse method approach using repeat lidar surveys appears promising, especially if lidar resolution is similar between sequential surveys.

ACKNOWLEDGMENTS

I'd like to start by thanking my advisor, Dr. Sara Rathburn, for her continued support over the last two years. I've enjoyed the long hours with her in the field or in her office, discussing my project, geology in general, and our shared love of delicious food. Courses that I took from Dr. Ellen Wohl and Dr. Brian Bledsoe helped prepare me for this work, and I'm thankful to have them both on my committee. Funding for this project was generously provided by several sources: Rocky Mountain National Park, American Water Resources Association – Colorado Section, the Geological Society of America, the Colorado Scientific Society, CSU Warner College of Natural Resources, and CSU Department of Geosciences. Many people assisted me in the field over the past two years, including Quin Scanlon, Dave Dust, Karen Jackson, Katherine Lininger, Jenn Davis, Michael Garcia, Jonathan Garber, and Scott Shahverdian. Dave Dust quickly process several field surveys. My CSU 'flamily' provided continued support, suggestions, and laughter over the last two years, both in the office and at countless potlucks. My immediate and extended family, especially my parents Vince and Nancy, have provided endless emotional support and encouragement throughout my entire life – I love you all so much. Lastly, I'd like to thank my instructors and friends at the City of Fort Collins Pottery Studio for providing me a creative outlet during a stressful year, and for teaching me to use sediment in a way different than I ever had before.

DEDICATION

To Jana Mabry, who's been saying since high school, "You'll make a great geologist, JoJo." You've been a dear teacher, mentor, and friend for many years.

TABLE OF CONTENTS

LIST OF TABLES

LIST OF FIGURES

1. INTRODUCTION

Airborne light detection and ranging (LiDAR) has recently become a promising research tool in the field of geomorphology (Marcus and Fonstad, 2010). The ability to quickly survey large tracts of land at sub-meter resolution with high vertical accuracy has allowed researchers to quantitatively and qualitatively assess landscapes in a way never before possible (Notebaert et al., 2008). Since its advent in the 1990s, airborne LiDAR (hereafter referred to as lidar) has become instrumental to geomorphic studies of landform measurements (Scheidl et al., 2008), geomorphic surface mapping (Jones et al., 2007; James et al., 2007), fish habitat identification (Jones, 2006), and hydrologic modeling (Marks and Bates, 2000; French, 2002; Jones et al., 2008). Recently, access to sequential lidar surveys of a study site has improved as survey collection becomes more financially practical and post-processing capabilities become more user-friendly (Marcus and Fonstad, 2010). Differencing between sequential lidar surveys can identify topographic changes and quantify active geomorphic processes over large temporal and spatial scales. The use of lidar differencing is especially beneficial in fluvial landscapes, which can be spatially and temporally dynamic, spatially extensive (Marcus and Fonstad, 2010), and commonly remote. Although aerial photographs have been routinely used for decades to monitor lateral adjustments in river channel morphology (i.e., Lane, 2000), lidar differencing reveals changes in the vertical dimension that are not possible without the collection of vast amounts of additional field data. The use of lidar differencing is especially useful in evaluating the morphologic response of a river system recently disturbed by a large sedimentation event by extracting metrics of channel change while the system adjusts to the influx of sediment (Hoffman and Gabet, 2007). Additionally, lidar differencing can be used to reliably quantify volumes of aggradation and degradation within different reaches of a disturbed river. In this way, sediment transport is determined using the inverse method, where transport is backed out of channel morphologic changes (Martin and Church, 1995; Ham and Church, 2000; Surian and Cisotto, 2007; Rumsby et al., 2008). In cases where sediment disturbances and associated channel change cause significant ecosystem damage within managed lands, lidar differencing and the inverse method hold great

promise in facilitating restoration plans. By understanding the geomorphic processes at a disturbed site, restoration plans can be tailored to suit the needs of the recovering system.

1.1 Background

1.1.1 Sediment Disturbances in Mountain Rivers

Infrequent sedimentation events, such as floods and mass movements, are a recognized component of the disturbance regime of mountain rivers (Benda and Dunne, 1997). Because of the high connectivity between hillslopes and channels in most mountainous settings (Cavalli et al., 2013), extreme influxes of sediment from a disturbance may cause initial, drastic changes to the channel morphology. These changes may include channel and floodplain aggradation, channel widening, channel incision, a transition to a braided planform, channel slope adjustments upstream and downstream of constricting deposits, and changes in the sediment size of bed material (Madej and Ozaki, 1996; Miller and Benda, 2000, Rathburn and Wohl, 2003; Hoffman and Gabet, 2007). Disturbed reaches are commonly unstable, with the potential to drastically adjust planform and transport large amounts of stored sediment during future high flows. Over time, a system may recover to a more stable planform and channel geometry that can adequately transport the existing sediment and water regimes.

Many field and flume case studies exist that document various responses of a mountain river system following a large sediment input. Pitlick (1993) showed that different reaches of the Fall River, Colorado were never in the same phase of adjustment following a dam-outburst flood and associated sediment input. As degradation occurred in upstream reaches, aggradation occurred in the lower reaches. Madej and Ozaki (1996) noted aggradation followed by degradation and widening at cross-sections as a result of increase sediment from poor land use practices upstream. Miller and Benda (2000) documented channel widening, braiding, and fining of the bed initially after a sediment pulse caused by debris flows, followed by channel coarsening, construction of coarse grained terraces, and formation of new side channels. After the sediment wave passed, abundant channel incision into the recent deposits occurred.

Sutherland et al. (2000) saw dissipation of a landslide-caused sediment wave at a site where resistant banks prevented width adjustments and the channel was relatively uniform, whereas Hoffman and Gabet (2007) noted increased width and braiding of downstream reaches following numerous debris flows in a recently burned watershed. Flume experiments of Madej et al. (2009) indicated that moderate sediment inputs only increased bed elevation while retaining bed armoring, but no planform changes occurred. Finally, Andrews (2010) noted that post-fire sedimentation caused channel widening, but the introduction of wood created variable, local channel changes.

The location and timing of sediment transport and storage along a river following a large sediment influx is influenced by variations in flow, sediment texture, and channel and valley morphology (Lisle, 2010; Buffington, 2012). Geomorphically effective flows, or those flows that are both large in discharge and long in duration, are important for mobilizing, reworking, and transporting sediment that ultimately results in significant channel change (Costa and O'Connor, 1995). The timing of geomorphically significant flows influences the sediment persistence or lag time of recovery following a sedimentation event (Madej, 2001). Humphries et al. (2012) demonstrated that lower magnitude peak flows cause translation and dispersion of the input sediment, long-duration high flows caused dispersion, and extremely high flows caused dispersion with some translation. Variations in channel type exert an especially strong control on the magnitude of morphologic changes in a river; the larger width and lower slopes in pool-riffle channels are known to be more sensitive to adjustments in upstream sediment flux than steep, confined step-pool channels (Wohl, 2014). Steep, confined reaches typically recover from sediment loading faster than lower-gradient unconfined reaches because the former have greater transport capacity and lower sediment storage (Megahan et al., 1980; Madej and Ozaki, 1996). Insufficient sediment storage in confined valley segments force virtually all of the material delivered to the channel to be transported downstream (Montgomery and Buffington, 1997). In unconfined valley reaches, where there is adequate room for the channel to adjust position, an increase in bedload input may cause local aggradation and increased braiding intensity (Ashmore, 1991). Because of these variations in channel and

valley morphology typical of heterogeneous landscapes, complex response (Schumm, 1973) may be the dominant fluvial response to sediment loading. Complex response occurs when a pulse of sediment is transported downstream during high stream flows, and degradation in one reach of a river may promote aggradation downstream. Over time, the aggraded reaches may start to degrade, promoting a similar cycle of aggradation further downstream.

Sediment disturbances may require restoration efforts to protect human health and property, to ensure adequate water quality, to reestablish a particular channel morphology or habitat, and/or to address ecosystem degradation (e.g. Fitzpatrick et al, 2009; Elliot and Capesius, 2009; among others). Acknowledging the natural variability that is inherent to all river systems enhances the need to stray from establishing restoration efforts that focus on a particular static endpoint (Wohl et al., 2005). Recent efforts have focused on restoring river systems to more natural processes while working within existing constraints of the system (Kondolf et al., 2006). In the context of large sedimentation events, restoration efforts should focus on the current and future processes of the system influenced by the large sediment influx. Mass aggradation commonly promotes channel instability (Hoffman and Gabet, 2007), where planform changes repeatedly occur because the sediment inputs temporarily overwhelm the transport capacity of the system. Additionally, extensive floodplain aggradation can disrupt the hydrologic connectivity between the channel and floodplain. By understanding the factors driving channel morphology of a reach prior to restoration planning, the underlying geomorphologic processes are more likely to be considered in restoration plans to ensure future process-form linkages and adjustments (Kondolf et al., 2006). Ultimately, restoration should be considered at the watershed scale, including upstream adjustments in water and sediment flux (Wohl et al., 2005), and incorporate characteristics of the river prior to intensive human alteration using least altered reference rivers or proxy data (Wohl, 2011; Rathburn et al., 2013).

Monitoring a pulse of sediment through a system can be difficult using traditional field methods, which commonly rely on repeat channel cross-sections (Lisle, 2010). Issues associated with field tracking

a sediment pulse include cross-section spacing, timing of surveys, site accessibility (both for location and timing), and the scale of morphologic changes resulting from the initial sedimentation event. Determining morphologic changes and estimating bed-material transport rates from lidar differencing is a useful approach to identify how a system is responding to a large influx of sediment and to aid restoration planning.

1.1.2 Lidar Analysis and Differencing

Digital elevation models (DEMs) are increasingly popular in geomorphic studies for both computational and visual assessments of a landscape. DEMs are stored as square-grid surfaces, with each grid cell containing an elevation value and the cell size depending on the resolution of the dataset (Wilson, 2011). DEMs at the resolution of 10-meter grids have been created from digitization of topographic maps and are easily accessible for most areas in the United States (www.nationalmap.gov). These coarse-resolution DEMs are most useful for large-scale studies because features smaller than the DEM pixel resolution cannot be identified (Notebaert et al., 2008).

Airborne lidar has become increasingly popular in creating high-resolution DEM surfaces over large areas. Airborne lidar acquisition requires flying over an area with a small plane that is equipped with high precision GPS and rapid scanning laser survey equipment. Swaths of laser pulses at rates sometimes exceeding 100,000 pulses per second are sent towards Earth's surface, and the timing, rate, and intensity of the reflected pulses are recorded (Scheidl et al., 2008). Traditional lidar, commonly referred to as 'red lidar' because it utilizes inferred lasers during scanning, is limited by its inability to penetrate water surfaces. This creates a void in lidar-derived surfaces, typically only showing the water surface elevation of a stream or lake but not the depth and bottom characteristics of the water bodies. Recent advances in 'green lidar', which can penetrate water, prove promising but are yet to be mainstream in the United States (Marcus and Fonstad, 2010). In some cases, bathymetric surveys have been combined with lidar surveys to reveal topography below the water surface.

Post-processing of the lidar survey points use algorithms and hand adjustments to classify the various returns as vegetation, water, last returns or other possible categories. Lidar DEMs composed of only points classified as last returns create bare-earth surfaces of the ground. The ability to remove vegetation and expose only the bare earth during lidar processing is highly beneficial, especially in densely vegetated landscapes (James et al., 2007). With elevation survey point densities greater than one point per square meter and DEMs produced on the scale of sub-meter resolution (Snyder, 2009), "lidar data are invaluable in revealing the subtle variation in topography that is typical of… river floodplains" (French, 2002). Notebaert et al. (2008) explicitly identifies the versatile use of lidar in studies pertaining to fluvial geomorphology. In combination with aerial photography (Lane, 2000; Smith and Pain, 2009), geomorphic measurements can be obtained in three dimensions from lidar surveys.

DEM differencing is quickly becoming a common method for determining geomorphic changes between two successive elevation surveys (James et al., 2011, Rumsby et al, 2008; Picco et al., 2013). A DEM of difference (DOD) can be created by simply subtracting an older elevation surface from a more recent one, exposing locations of vertical change on the landscape between surveys. Elevation surfaces created from various acquisition methods, including lidar, sonar, RTK-GPS, total station surveys, aerial photographs, and terrestrial laser scanning (commonly referred to as 'ground-based lidar'), all include inherent error that must be considered when creating a DOD (Wheaton et al., 2010; Milan et al., 2011). Earlier methods of reducing error in DEM differencing entailed determining a minimum level of detection that should be applied to an entire surface (or minimum levels of detection for different surface classifications) and exclude all geomorphic changes that fall short of the specified minimum level of detection (Fuller et al., 2003). This surface-wide approach to treating error in DODs is typically too simplistic, overestimating error in areas with high confidence in survey results and underestimating errors in localized, complex areas.

Recently, Wheaton et al. (2010) proposed using a fuzzy inference system to help distinguish true geomorphic change from noise in the DEM differencing process. A fuzzy inference system quantifies

error at a local scale, pixel-by-pixel, on each lidar surface used in creating a DOD. Fuzzy inference relies on a set of user-defined membership functions, where known survey metrics (i.e. surface slope, point density, point quality) are the inputs and the function outputs an appropriate error value. User-defined ranges of input values are lumped into descriptive groups such as 'high', 'medium', and 'low.' Each possible combination of input values is then assigned a descriptive output value, and a membership function of output values is used to assign an error value to that combination of inputs. These pixel-specific error values are then included in the DEM differencing computations. Minimizing survey error during DEM differencing strengthens confidence in quantifying landform changes over time.

1.1.3 Inverse Method of Sediment Transport

Theoretical and numerical models developed to understand bed-material transfer and deposition in a river are typically one-dimensional, and simplify the fully-dimensional response expected in nature (Lisle, 2010). Additionally, there is a known spatial and temporal variability of bedload transport by traditional direct field measurements (Knighton, 1998). The morphological approach to sediment budgeting has become an appealing method for determining bed-material transport rates on gravel-bed rivers (Brewer and Passmore, 2002). Bed material is defined as the material that makes up the bed of the river and adjacent gravel bars, and may include the bedload and material transported in the suspended load during high flows. Applying the morphologic inverse method requires knowledge of the volumetric change in sediment for a given reach, certain characteristics of the bed-material, and the identification of a site where a sediment transport rate is known (Ashmore and Church, 1998).

Measuring volumetric changes to apply the inverse method initially relied on repeat channel cross-section surveys (i.e. Martin and Church, 1995), which involved identifying morphologic changes at various cross-sections and extrapolating a uniform quantity of vertical change over an entire surface or reach. Knowing that the cross-section approach simplified volumetric change estimates, Fuller et al. (2003) used differencing from both cross-section surveys and field-derived DEMs on the same reach of

river to prove that the cross-section approach drastically underestimated volumetric changes. As technology advanced, aerial photogrammetry and RTK-GPS ground surveys became a means to create ground surface DEMs for inverse method applications (Gaeuman et al., 2003; Brasington et al., 2002), although Gaeuman et al. (2003) explicitly noted the inability of aerial photogrammetry to identify small vertical changes during differencing.

Lidar-derived DEMs, with their high resolution and accuracy, have strong potential for use in inverse method applications, especially in remote locations where traditional surveys are difficult to perform. Lidar differencing is a tool that can be used to confidently identify the location and timing of bed-material adjustments along an entire river system. Sediment flux through a reach can then be inversely derived by combining reach-scale changes in channel morphology with predicted upstream or downstream sediment transport (Church, 2006).

Initial upstream or downstream sediment volumes used in the inverse method may be influenced by changes in the grain size distribution of sediment during transport. Attrition is the breakdown of individual clasts as they move downstream, and rates of attrition are known to vary greatly between different rock types (O'Connor et al., 2014). Lisle (2010) suggests that attrition of bed-material may have a large influence in reducing the transport of debris flow deposits as bedload. Additionally, impacts during the mass-wasting process can weaken bed-material supplied from debris flows. Accounting for attrition may help reduce gaps in sediment budgets, especially in debris flow deposits that initiate in weak rock types (Sutherland et al., 2002).

1.1.4 Study Goal

The goal of this study is to use airborne lidar surveys that capture channel morphologic conditions immediately following an extreme sedimentation event within a mountainous headwater stream to determine controls on geomorphic response and constrain bed-material transport rates. Repeat lidar surveys are used to assess channel and planform adjustments resulting from geomorphically

significant stream flows that remobilized the introduced sediment. Additionally, lidar differencing was used to create a sediment budget that incorporates changes in planform geometry as an indicator of sediment transport. This will allow restoration planners to better understand spatial patterns of bed-material flux and ensure that future channel designs are adequate for transport of the delivered sediment load. Such a restoration approach will seek to maintain longitudinal, lateral, and vertical connectivity along the river (Kondolf et al., 2006), helping to guarantee a successful process-based restoration project.

1.2 Research Objectives and Hypotheses

This study will use a 2003 debris flow at the headwaters of the Colorado River in Rocky Mountain National Park, Colorado to examine channel morphologic response following a large sediment disturbance and multiple geomorphically significant flows, including a flow of record. The research focus is on determining channel morphologic changes that i) can be confidently identified from lidar surveys and ii) are beneficial in the support of practical restoration goals for the site, such as restoring hydrologic connectivity between the channel and floodplain.

1.2.1 Objective 1: Evaluating Channel Morphologic Changes

Metrics of change in channel geometry resulting from sediment disturbances can be extracted from the repeat lidar datasets and accompanying aerial photographs to determine the effectiveness of bankfull and greater stream flows. Of particular interest are the high-magnitude, long duration flows that remobilize upstream sediment deposits and reset or alter channel morphology. These geomorphically effective flows create an opportunity to understand the controls on geomorphic change caused by infrequent flows following a large sediment disturbance. Specific channel response reaches following high-magnitude flows are determined based on trends in geomorphic changes. Geomorphic changes are separated into two categories: i) locations of aggradation and degradation, and ii) changes in planform geometry.

Valley slope and confinement are commonly the dominant factors controlling locations of aggradation and degradation within fluvial systems (Figure 1). If valley geometry is not the main control, proximity to a sediment source, or a complex response, often exert local control on aggradation and degradation, and hence channel stability. The hypothesis related to aggradational and degradational locations following a sedimentation event is:

> H.1 – Aggradational response reaches correspond to low valley confinement and low valley slope, whereas erosional response reaches correspond to high valley confinement and high valley slope.

Changes in planform geometry are expected to be more distinguishable by lidar in pool-riffle reaches than along other reaches because more distinguishable changes are expected to occur where there is greater valley width, lower slope, and smaller bed material typical of pool-riffle reaches. Anticipated planform changes resulting from a sedimentation event include channel migration, sinuosity adjustments, transitions between multi-thread and single-thread channels, and changes in bankfull width (Figure 1). Hypotheses related to planform geometry changes include:

> H.2 – Locations of avulsions, channel migration, and changes in sinuosity within pool-riffle reaches following a sediment disturbance most closely correspond to reaches with low valley confinement.
>
> H.3 – Bankfull width changes within pool-riffle reaches following high stream flows are related to distance from a sediment source.

1.2.2 Objective 2: Sediment Transport Estimates

The second objective of this project is to use the morphologic inverse method (Church, 2006) to better constrain sediment transport rates on a river affected by an extreme sediment disturbance. Although fine sediment loading may substantially alter mountain rivers (Wohl and Cenderelli, 2000; Rathburn and Wohl, 2003), the emphasis in this analysis is on bed-material load, or that component of the grain size

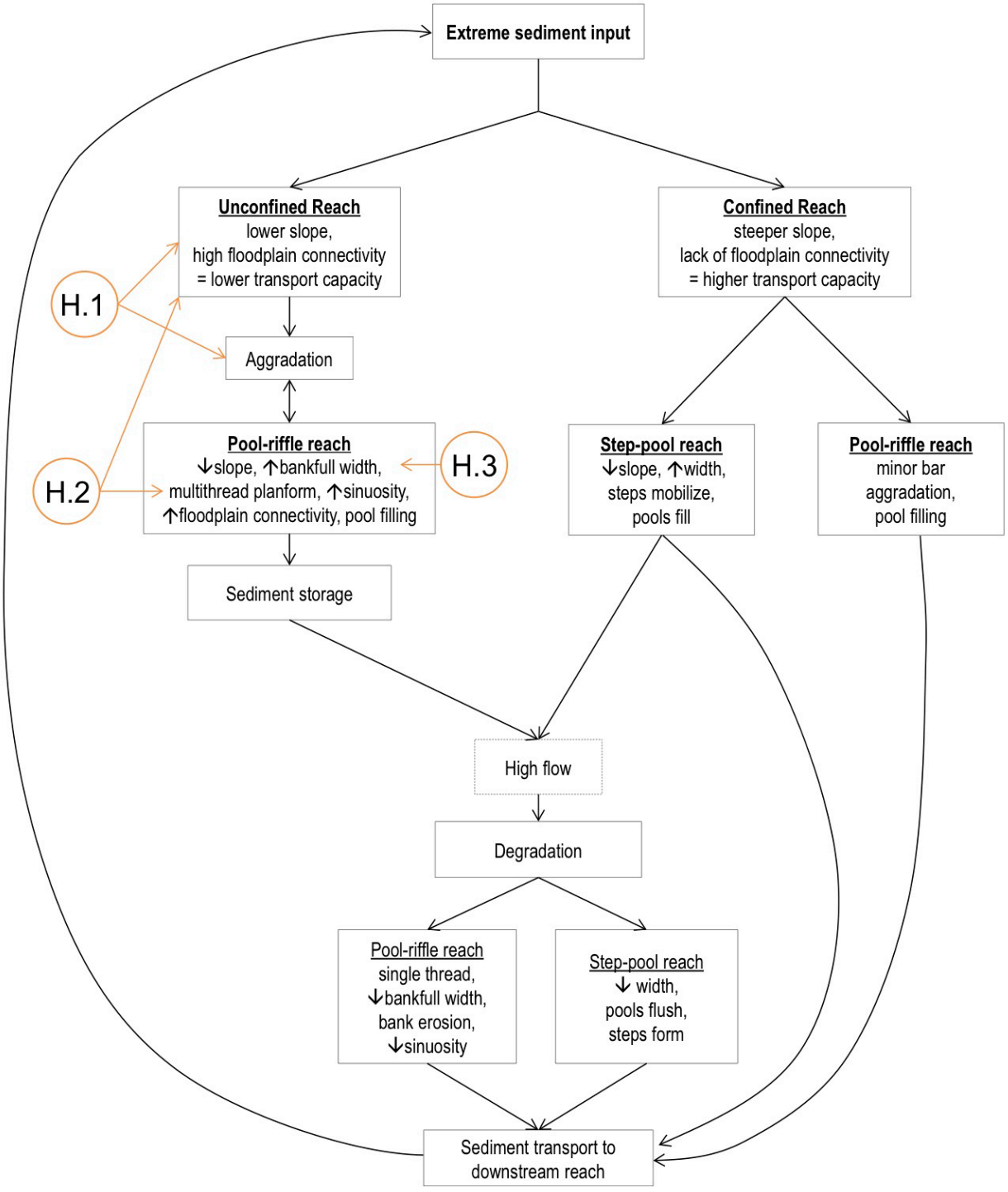

Figure 1: Conceptual model of morphologic response to a large sediment input, focusing on changes that are confidently identified from lidar surveys and are beneficial in the support of practical restoration goals for the site. Circles with letter "H" followed by a number indicate the research hypothesis to be tested within the conceptual model.

fraction that more readily alters channel form. Bedload transport rates measured in the field tend to be conservative estimates of sediment flux (Bunte et al, 2004). Therefore, geomorphic change detected by lidar can be used to estimate the transport of sediment through a river and create a more constrained sediment budget. The hypothesis related to bed-material transport estimates is:

> H.4 – Bed-material transport quantified by the morphologic inverse method more closely approximates field measurements of bed-material transport than calculated transport rates using applicable transport laws.

1.3 Study Area and Site History

The Colorado River is one of the major river systems in the western United States. Starting at the Continental Divide in Colorado, the Colorado River flows through several states before crossing into Mexico and reaching the Gulf of California. The Colorado River has a long history of water retention and diversion projects that affect the hydrologic and ecologic processes within and along the river (Adler, 2007). Although many of the larger and better-known projects on the Colorado River are lower in the basin (i.e., Lake Powell, Lake Mead), the headwaters of the Colorado River are also affected by smaller-scale diversion projects. The Grand Ditch (Figure 2), a 26-km-long trans-basin diversion, removes water from the Colorado River and its tributaries and transports it across the Continental Divide. A 2003 breach in Grand Ditch (hereafter referred to as the ditch), which initiated a 36,000 m^3 debris flow on the hillslope below the ditch, down Lulu Creek, and into the Colorado River, motivated research on how the Grand Ditch influences Colorado River ecology (Clayton and Westbrook, 2008), the magnitude of debris flows along the upper Colorado River valley (Grimsley, 2012), and the aggradational history and channel changes within the valley relative to the historical range of variability (Rubin et al., 2012; Rathburn et al., 2013). Prior to the ditch breach, Woods (2000) evaluated the influence that flow diversion has on the streams and wetlands in Rocky Mountain National Park. The area affected by the 2003 overtopping of the Grand Ditch and subsequent debris flow into tributary Lulu Creek and the Colorado River headwaters

form the basis of this study, focusing on the response of the river system following several geomorphically significant stream flows.

1.3.1 Upper Colorado River Valley

The Colorado River heads in Rocky Mountain National Park, Colorado at La Poudre Pass (2940 meters). It quickly drops nearly 200-meters of elevation over two kilometers through a steep, confined valley before entering the long, glacially carved upper Colorado River valley. The expansion of the valley floor promotes a highly sinuous, pool-riffle planform (Montgomery and Buffington, 1997) as the Colorado River flows south. Wetlands are common throughout the valley, especially upstream of constrictions in the valley caused by fans of debris flow material from the steep valley tributaries. The bedrock geology varies between the mountains that flank the opposing sides of the upper Colorado River valley (Cole and Braddock, 2009). The Never Summer Mountains form the west slopes of the valley, reaching elevations over 3,700 meters. This range is mostly composed of Oligocene-aged post-Laramide intrusive rocks (Cole and Braddock, 2009). Flanking the base of the Never Summer Mountains is a veneer of till from the upper Pleistocene Pinedale glaciation. The eastern slope of the Colorado River valley is primarily composed of Paleoproterozoic metamorphic rocks to the south and Oligocene-aged, post-Laramide intrusive rocks towards the north end of the valley. Unlike the west side of the valley, the east slopes mostly lack the large till deposits that flank the base of the mountains. A swath of hydrothermally altered rhyolite tuff runs northwest-southeast at the north end of the valley (Grimsley, 2012). The 2003 Grand Ditch debris flow mobilized substantial quantities of the light-colored, hydrothermally altered rhyolite tuff (Grimsley, 2012), making it easy to identify 2003-related debris flow material in the field. The remainder of the valley floor is composed of Pleistocene glacial deposits overlain by Quaternary alluvial sediments or older debris flow deposits at the base of steep tributary channels.

The upper Colorado River receives average annual precipitation of 110 cm (Capesius and Stephens, 2010), typically in the form of winter snowpack and summer thunderstorms (Woods, 2000).

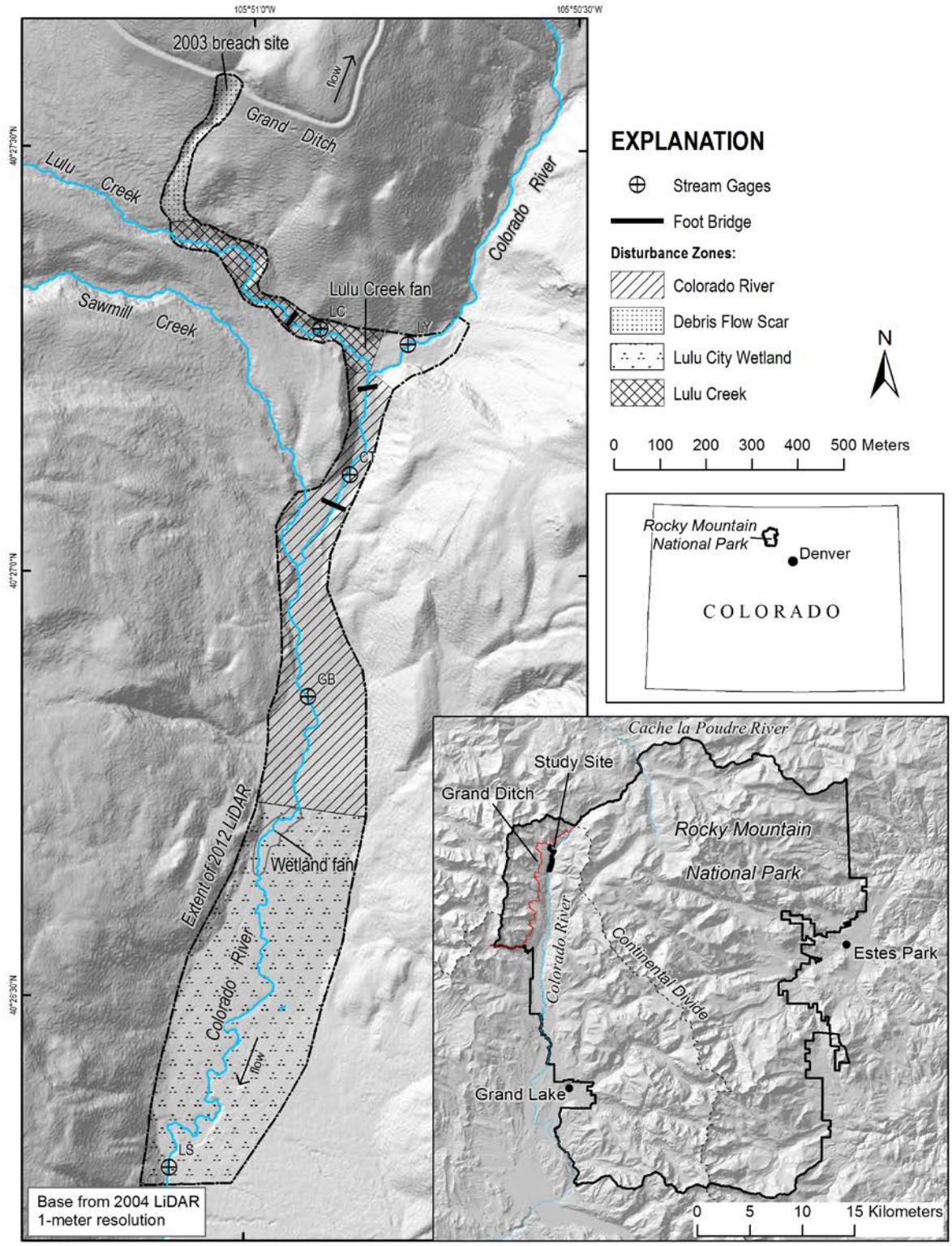

Figure 2: Site map showing extent of disturbance zones and locations of gages and footbridges.

High snowpack in the watershed promotes a classic snowmelt hydrograph, with high flows in the late spring and early summer from melting snow and base flows sustained by groundwater inputs the remainder of the year (Figure 3). Continuous discharge measurements on the Colorado River have been recorded from 1953 to present at the Baker Gulch gage [US Geological Survey (USGS) gage 09010500; Figure 3], located approximately 13-kilometers downstream from the study site. Mean annual discharge at the Baker Gulch gage is 2.30 m^3/s, with mean monthly flows of 10.3 m^3/s during the peak of the snowmelt season in June (Rathburn et al., 2013).

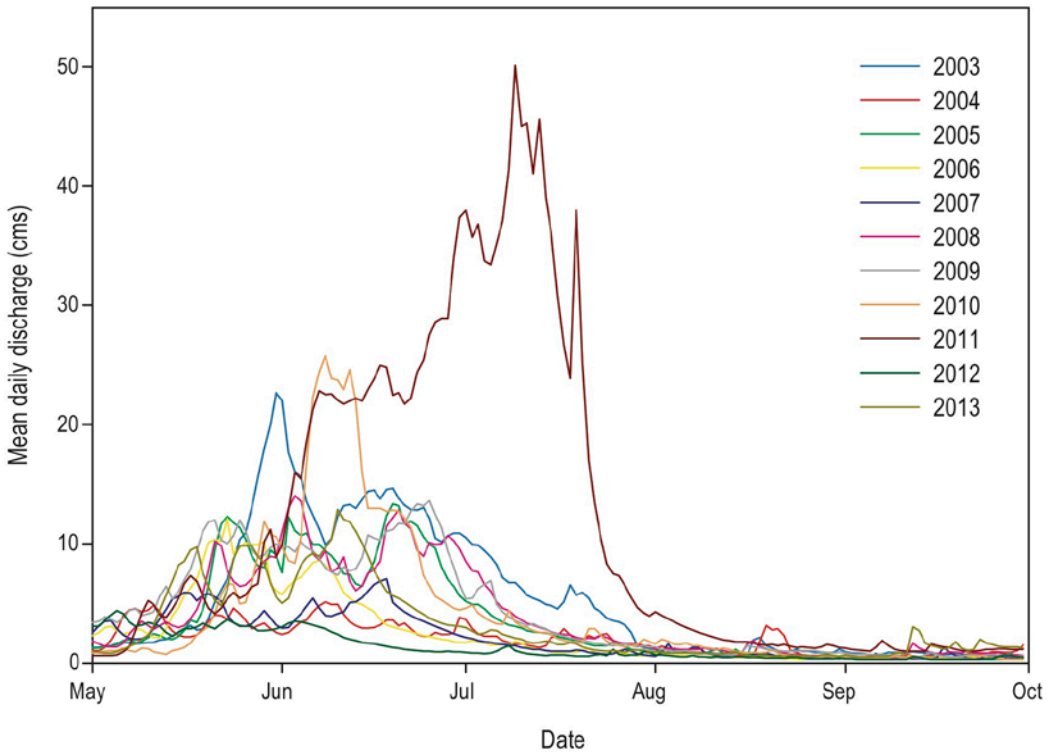

Figure 3: Daily maximum flows from the Baker Gulch gage (US Geological Survey gage 09010500), located approximately 13-kilometers downstream from the study site, for the summers of 2003 through 2013.

Grand Ditch, perched ~300 meters above the floor of the upper Colorado River valley, runs along the side of the Never Summer Mountains and transports water across the Continental Divide (Figure 2) at La Poudre Pass. Its primary purpose as a trans-basin diversion is to provide additional irrigation water to the eastern plains of Colorado via the Cache la Poudre River. The ditch intersects several large tributaries and, through a series of head gates, ditch operators can divert some or all tributary flow over the

Continental Divide when desired. Construction of the ditch began in 1896 and continued for 40 years before its total length of 26 kilometers was completed in 1936 (Woods, 2000). Built prior to the designation of Rocky Mountain National Park, its presence and function is grandfathered in by the park. The ditch is privately owned and maintained by the Water Supply and Storage Company of Fort Collins.

The Grand Ditch greatly influences the flow regime in the upper Colorado River (Woods, 2000). More than half the drainage area of the upper Colorado River is intercepted by Grand Ditch diversions. Flow diversion typically occurs when intersecting tributaries are running high as the snowpack melts during the late spring and early summer. During the peak of the snowmelt season, high flows commonly exceed the capacity of the Grand Ditch and excess flow is sent down the various tributaries; therefore, the Grand Ditch removes less than half of the annual discharge of the upper Colorado River (Woods, 2000). Notably, nearly all flow is diverted and tributaries below Grand Ditch commonly run dry during the receding limb of the snowmelt season. This reduction in magnitude and duration of high flows has negative implications for sediment transport and ecologic integrity of rivers (Poff et al., 1997). Frequency and duration of sediment-transporting flows are reduced when peak flows are minimized, and groundwater-surface water interactions may be disrupted. Clayton and Westbrook (2008) showed that reductions in flow and increased fluctuations in discharge over short time scales caused by flow diversion may have an adverse effect on downstream benthic invertebrate abundance along the upper Colorado River.

1.3.2 Effects of Debris Flow

In May 2003, a breach in Grand Ditch initiated a debris flow below the ditch and into the Colorado River system (Rubin, 2010). The debris flow first entered tributary Lulu Creek (Figure 2), depositing cobble- to boulder-sized material along the steep tributary valley and obliterating the previous single-thread, step-pool morphology of the creek. A large, unstable fan of coarse material was also deposited where Lulu Creek joins the Colorado River. An estimated 50% of the initial debris flow

material entered the Colorado River, causing extensive deposition of cobbles, gravels, and sand within and along the river while also transporting material over a kilometer downstream into the Lulu City wetland (Rathburn et al., 2013). In addition to extensive aggradation along the Colorado River, increased braiding and some pool infilling were noted. Initial trends in channel morphologic changes along the Colorado River were more difficult to discern as a result of previous debris flows that had altered channel forms and valley morphology prior to 1937 (Rubin, 2010). Deposition of up to 1-meter of gravel and sand occurred at the head of the wetland as a result of the 2003 event. Large amounts of sand and silt were transported through the wetland, with accumulations of fine sediment noted 43 kilometers downstream in Shadow Mountain Reservoir (Rathburn et al., 2013). Debris flows have historically been common along the headwaters of the Colorado River, but the ditch has increased the magnitude and frequency of debris flows on the west side of the valley (Grimsley, 2012). In addition to land use changes such as historic mining and deforestation in the area, increased debris flow magnitude has contributed to the six-fold increase in aggradation rates through the Lulu City wetland since Euro-American settlement in the region (Rubin et al., 2012). Rathburn et al. (2013) determined that the channel morphology of the Colorado River is currently outside of the historical range of variability for steep-gradient, pool-riffle channels because of episodic sediment supply from the tributary debris fan at the mouth of Lulu Creek.

1.3.3 Post-Debris Flow Monitoring and Channel Change

Following the initial 2003 debris flow, efforts were established to monitor the response and recovery of Lulu Creek and the Colorado River. The National Park Service plans to restore channels, riparian areas, and portions of the Lulu City wetland impacted by the 2003 debris flow. In order to develop a consistent suite of data to evaluate the trajectory of recovery and quantify the variability of fluvial processes, eight gages were installed throughout the site to monitor flow and sediment transport over time. Only two gages are referenced in this study, the locations of which are shown on Figure 2: Crooked Tree (CT) and Gravel Beach (GB). Additional information on the other gauges is provided in Rathburn et al. (2013). The CT and GB gages were equipped with continuous (15-minute) stage

recorders during the snowmelt seasons. Associated discharge rating curves were developed and are being updated annually (Rathburn et al., 2013). Additionally, bed-material transport was measured at these gages from direct, in-stream methods over several years and a range of discharges. Repeat cross-sections were conducted nearly annually at the gages and in various other locations throughout the site to identify site-specific planform changes since the initial breach. Lastly, multiple longitudinal profiles along Lulu Creek were surveyed to monitor step-pool adjustments following high flows.

Several years of low snowpack and associated snowmelt flows followed the 2003 debris flow (Figure 3). The first year in which bankfull flows occurred on the Colorado River following the debris flow was 2009, followed by two years of overbank flows in 2010 and 2011 (Rathburn et al., 2013). The 2011 snowmelt season was extreme, with overbank flows persisting for weeks and the peak discharge exceeding any flows within the 59-years of record at the downstream Baker Gulch gage. Extensive incision and degradation occurred on the Lulu Creek fan during runoff in 2011, adjusting the step-pool morphology of the creek and remobilizing stored sediment that was transported into and down the Colorado River. The Colorado River experienced substantial planform adjustments in addition to distinct locations of aggradation and degradation (Rathburn et al., 2013). Additional aggradation occurred in the wetland as sediment from upstream was remobilized and transported downstream. The morphologic alterations associated with the 2009-2011 high flows, especially the geomorphically significant flows of 2011, had once again destabilized the system.

Various site-specific controls on channel morphology along the upper Colorado River, such as the large sediment source at the Lulu Creek junction, varying valley confinement, in-stream wood, and proximity to footbridges, likely affect the common first-order response variables of grain size, bedforms, channel geometry, and stream gradient (Buffington, 2012). Below-average flows along the Upper Colorado River between 2004 and 2008 were followed by three years of high magnitude flows that drastically altered channel form and raised questions about the response of the site to future bankfull or higher flows. Variations in bed- and planform adjustments along the disturbed reach beginning in 2009

suggest a complex response (Schumm, 1973) is driving morphologic changes, with repeat surveys indicating simultaneous erosion and deposition at a cross-section or within a short river reach (Rathburn et al., 2013). Additionally, successive high flows mobilized and configured the slope and step-pool morphology of Lulu Creek into more stable and energy-efficient forms (Rathburn et al., 2013). However, the 2011 peak discharge on Lulu Creek disrupted step-height and spacing, and the recovery of that system (unpublished data, S. Rathburn, Colorado State University).

Bed-material transport within the study site, rather than the washload, exerts strong control over channel morphology (Rathburn et al., 2013). Pulsed sediment delivery from the Lulu Creek fan, and corresponding erosion and deposition along the Colorado River, have produced marked changes in channel morphology since the 2003 event. Traditional transport relationships do not adequately quantify bed-material transport at monitored cross-sections in the disturbed reach (unpublished data, S. Rathburn, Colorado State University) because conditions of the site violate the assumptions of constant sediment supply and steady, gradually-varied flow inherent in transport equations. Additionally, the initial debris flow within Lulu Creek incorporated material from within a hydrothermally altered region of rhyolite tuff, which disintegrates easily and is found weathering in situ throughout the study site. Therefore, abrasion may also have an influence on bed-material transport through this site.

1.3.4 Zones within Study Area

The areas affected by the 2003 overtopping of the Grand Ditch and subsequent debris flow into tributary Lulu Creek and the Colorado River headwaters form the basis of this study (Figure 2). Four distinct zones were affected by the 2003 ditch breach and subsequent debris flow. The uppermost zone is the debris flow scar exposed on a steep south-facing slope of Lulu Mountain, below the Grand Ditch (Figure 4A). This scar was the source for much of the material transported downstream, including large amounts of wood from fallen trees. The debris flow then entered Lulu Creek, which is composed mostly of boulders and cobbles, and has a large sediment fan that formed at the junction with the Colorado River

(Figure 4B). The third zone includes the Colorado River between the confluence with Lulu Creek and the Lulu City wetland (Figure 2). This is predominantly a gravel bed reach with a pool-riffle channel planform (Figure 4C) and varying valley morphology. The fourth and lowermost zone is the portion of the Lulu City wetland that received sediment deposition following the 2003 debris flow and subsequent high flows (Figure 4D). Due to the popularity of hiking in this portion of Rocky Mountain National Park, there are two footbridges (hereafter referred to as bridges) crossing the Colorado River in addition to one crossing Lulu Creek (Figure 2). This study will focus predominantly on the middle two zones – Lulu Creek and the Colorado River upstream of the wetland – because channel morphologic changes and the inverse method are most applicable to these areas of pronounced channel change detected by lidar.

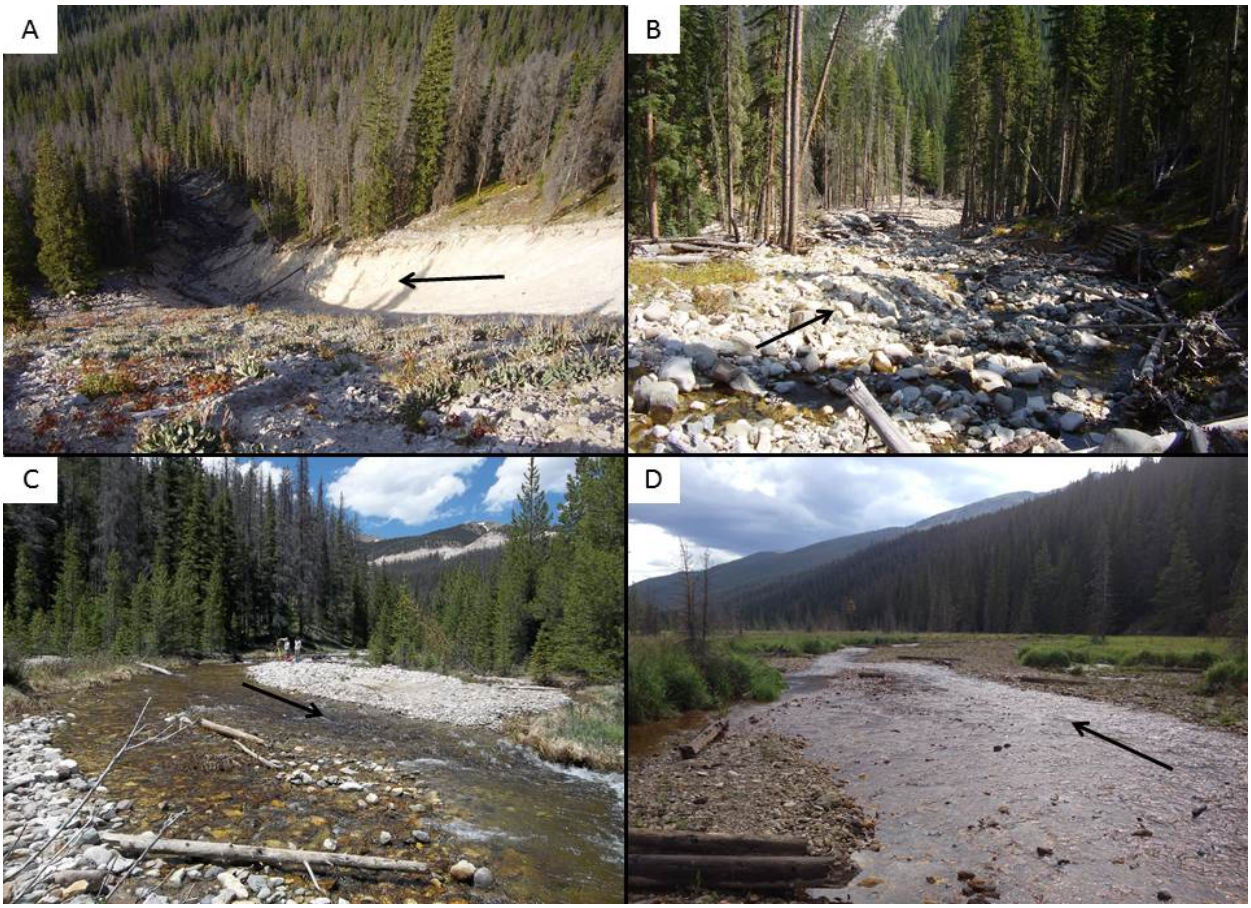

Figure 4: Representative photographs of the four zones affected by the Grand Ditch breach and subsequent debris flow, all taken summer 2013. Black arrows show direction of flow. A) The debris flow scar as seen from the Grand Ditch. B) Lulu Creek, looking downstream from near the bridge crossing lower Lulu Creek towards the debris fan at its confluence with the Colorado River. C) A pool-riffle portion of the Colorado River upstream of Gravel Beach gage – note the Grand Ditch and debris scar on the mountain side in the distance. D) Looking downstream where the Colorado River enters the Lulu City wetland.

2. METHODS

The majority of this project relied on remote sensing methods (lidar analysis and aerial photography interpretation) in addition to field-collected data during monitoring efforts over the past several years. All lidar processing and geomorphic analysis were performed in ArcGIS 10.1 in the NAD 83 UTM, Zone 10 projection and NAVD88 vertical datum. Field data collection included flow and sediment monitoring, channel surveys, and bed material analyses during summer 2013 to augment similar data collected since 2008.

2.1 Lidar Collection and Processing

The 2004 and 2012 airborne lidar surveys along Lulu Creek and the Upper Colorado River form the basis for this project. Similarity in post-processing procedures and alignment of the elevation datasets were important in reducing error in subsequent computations. Because of different acquisition companies and the eight years between flights (during which lidar technology quickly advanced), the original datasets were processed differently by their respective acquisition company and the resolution of the 2012 lidar survey is nearly twice that of the 2004 lidar survey.

The 2004 elevation data along the study reach were extracted from a larger flight of the entire upper Colorado River valley. This region of survey extended over seven kilometers south of the Lulu City wetland along the valley floor, and four kilometers northeast of the Lulu Creek confluence to where the Colorado River initiates at the Continental Divide. The 2004 flight extended one kilometer east and four kilometers west of the valley floor, encompassing the majority of the east flank of the Never Summer Mountains and the entirety of Grand Ditch. These 2004 flights occurred over the region on August 1 and August 9, 2004, but it is unspecified which day they flew over the study site. The horizontal accuracy of the laser shots was less than 0.5-meters, the vertical accuracy was less than 0.15-meters, and the average shot density for bare earth points was 0.7 points per square meter (Spectrum Mapping, LLC, 2004). Although the vertical accuracy was low, the vertical alignment to the true elevation datum was only

approximated for this survey. Adjustment of the 2004 dataset to true elevation is discussed later in this section. During the 2004 lidar flights, aerial photographs were also taken with a resolution of 0.152-meters per pixel.

The 2012 survey was flown over just the study reach on October 22, 2012. This survey included the debris scar, the disturbed portion of Lulu Creek, the Colorado River downstream of the Lulu Creek confluence, and the entirety of the Lulu City wetland (Figure 2). This flight only included the valley floor and a small portion of the valley walls. The horizontal accuracy of the laser shots was less than 0.5-meters, the vertical accuracy ($RMSE_{(z)}$) was 0.036-meters, and the average shot density for bare earth points was 1.4 points per square meter (Merrick and Company, 2013). Ground control points were placed and precisely surveyed throughout the reach for alignment of the lidar survey with the NAVD88 vertical datum. Aerial photographs with a resolution of 0.152-meters per pixel were taken within a few days following the 2012 surveys flights. It should be noted that a light dusting of snow occurred between the lidar flights and the aerial photography acquisition, hindering some visibility of features on the Colorado River floodplain but not interfering with the lidar collection.

Vertical adjustment of the 2004 elevation points was required for proper alignment with the NADV88 (Geoid03) datum, thus creating agreement with the 2012 elevation surface. To accomplish this, locations that were likely to have no vertical change between 2004 and 2012 were identified throughout the study reach. These typically included bare surfaces far from the active channel such as terraces, inactive fans flanking the valley edges, and large open spaces in the wetland. Twenty sets of neighboring lidar points from the two flights were identified and the differences in their elevations were calculated. The 2004 elevations were then adjusted by a constant value for all points until the minimum RMSE between the points was determined (RMSE of 0.144 meters when adjusted +10.868 meters; Appendix A). All 2004 lidar point elevations were then increased by 10.868 meters, placing the 2004 surface at its correct location in relation to the vertical datum and the 2012 elevation surface. The low RMSE value in the vertical adjustment measurements indicates a large offset yet small error between the surfaces.

Although elevation rasters were produced for each lidar flight by the different lidar providers, several issues warranted reprocessing of the raw lidar point clouds to create new elevation surfaces before conducting this analysis. First, it was important that the two surface rasters were created in similar manners to ensure agreement between datasets. The two surface rasters needed to be congruent (i.e., the raster grids between the two surveys are in alignment), a requirement for the Geomorphic Change Detection (http://gcd.joewheaton.org/) software used for lidar differencing. Additionally, careful initial observations of the raw point cloud data showed several extraneous data points that warranted removal. Specifically, there was variation in the selection and removal of points located in water bodies and the wetted channel. Points located in the water bodies were likely missed by the automated filter programs of the lidar acquisition companies, but it was worth spending the time to hand-remove extraneous points given the small size of the study area and the desire to be as accurate as possible in analyses. Water edges were digitized from aerial photographs at a scale of 1:500, and all points within the water polygons were removed. The water polygons were then used as breaklines when creating triangulated irregular network (TIN) surfaces from the point clouds. Lastly, Merrick and Company has a policy to exclude all survey points within 1.53-meters of the water boundaries to create a smooth transition between water and floodplain; this simplification of the 2012 land surface was detrimental to this type of analysis, given that the morphology near the water is a key component of this study. The final point cloud used for making the elevation surfaces included all ground points within the reach except those located within water.

The final elevation surfaces were produced by creating TINs from the final lidar point clouds. Hard break lines were applied to the TIN using the Colorado River water polygons and digitized Lulu Creek channel centerlines. The TINs were then hand-inspected for obvious topographic errors and adjusted if appropriate. The TINs were also converted to 1-meter resolution raster surfaces that were congruent with each other. Conversion to raster surfaces simplifies the topography in some cases, especially when making measurements on a small scale, so elevation values were typically extracted from

the TIN surfaces instead of the raster surfaces. Raster surfaces were required for the elevation differencing and height-above-water-surface analyses.

2.2 Geomorphic Change Detection

Locations of aggradation and degradation along Lulu Creek and the upper Colorado River were revealed by computing the difference between the 2004 and 2012 lidar surfaces. The resulting DEM of difference (DOD) showed the quantity of elevation change for each of the raster's 1-meter square pixels, which were then aggregated between each transect and for each reach. This method only shows the net change in elevation over the eight years between the collection of the elevation data in 2004 and 2012. The lack of geomorphically significant flows between 2004 and 2008 suggests that the majority of the vertical changes in the reach occurred during the bankfull flows of 2009 and 2010, and especially the high-magnitude, long duration flows of 2011. Collecting spatially extensive bathymetric surveys of the reach was outside the extent of this project; therefore, the change in elevation in locations where water exists in the lidar only shows change in relation to the water surface elevation. It is noteworthy that both lidar surveys were collected in fall during baseflow conditions (discharge less than 1-m^3/s). An average water depth of 0.25-meters was applied in later calculations (discussed below) to estimate reach-scale quantification of bed-material transport, but was not applied in the lidar differencing.

A fuzzy inference system (FIS) was applied in the elevation differencing to quantify and reduce the potential error during the differencing process (Wheaton et al., 2010). This method was warranted to distinguish real geomorphic change from the noise produced when processing DEMs of different quality. The Geomorphic Change Detection (GCD) version 5 plug-in for ArcGIS was used to apply the FIS in the DEM differencing process. The FIS used in this analysis included two input variables: slope and point density (Table 1, Figure 5). It was modified from a preexisting FIS stored in the GCD, with adjustments made to the point density input membership function to better represent the lower values of point density from the 2004 lidar survey (Appendix B). The 'error propagation' output method, which accounts for

error at each pixel and applies it to the DOD, was ultimately used for final analysis; the variability in form and location of deposits throughout the site was not conducive for the 'confidence interval' output method, which identifies spatially coherent, arc-shaped erosion and depositional units (i.e., distinct cut bank erosion and point bar migration) commonly seen in meandering rivers. The final vertical error or accuracy of elevation surfaces is less than 0.1-meter based on the careful method of data processing in combination with the FIS.

The final DOD still included distinct noise throughout the Colorado River floodplain, likely due to the low resolution of the 2004 lidar survey and dense, grassy vegetation of varying heights on the floodplain (unlike the bare sediment deposits). To distinguish the geomorphic change along the river system from the noise on the floodplain, a boundary of channel morphologic change was determined by creating a 1-meter buffer around all wetted channel edges and digitized bars from both years. This boundary was verified by hand to validate that all significant change was included within the bounds, with minor adjustments made where necessary. Boundaries of change detection along Lulu Creek were hand digitized by visually identifying distinct areas of change adjacent to the creek that were clearly related to in-channel bed-material transport caused by to high stream flows. Lastly, the aggradational deposits at the head of the Lulu City wetland were hand digitized in a similar method to Lulu Creek.

Table 1: Fuzzy inference system rules (inputs and outputs) applied to the geomorphic change detection analysis.

Rule	Inputs		Output
	Slope (%)	Point density (pts/m^2)	Elevation uncertainty (m)
1	Low	Low	High
2	Low	Medium	Medium
3	Low	High	Low
4	Medium	Low	High
5	Medium	Medium	Medium
6	Medium	High	Low
7	High	Low	Extreme
8	High	Medium	High
9	High	High	Medium

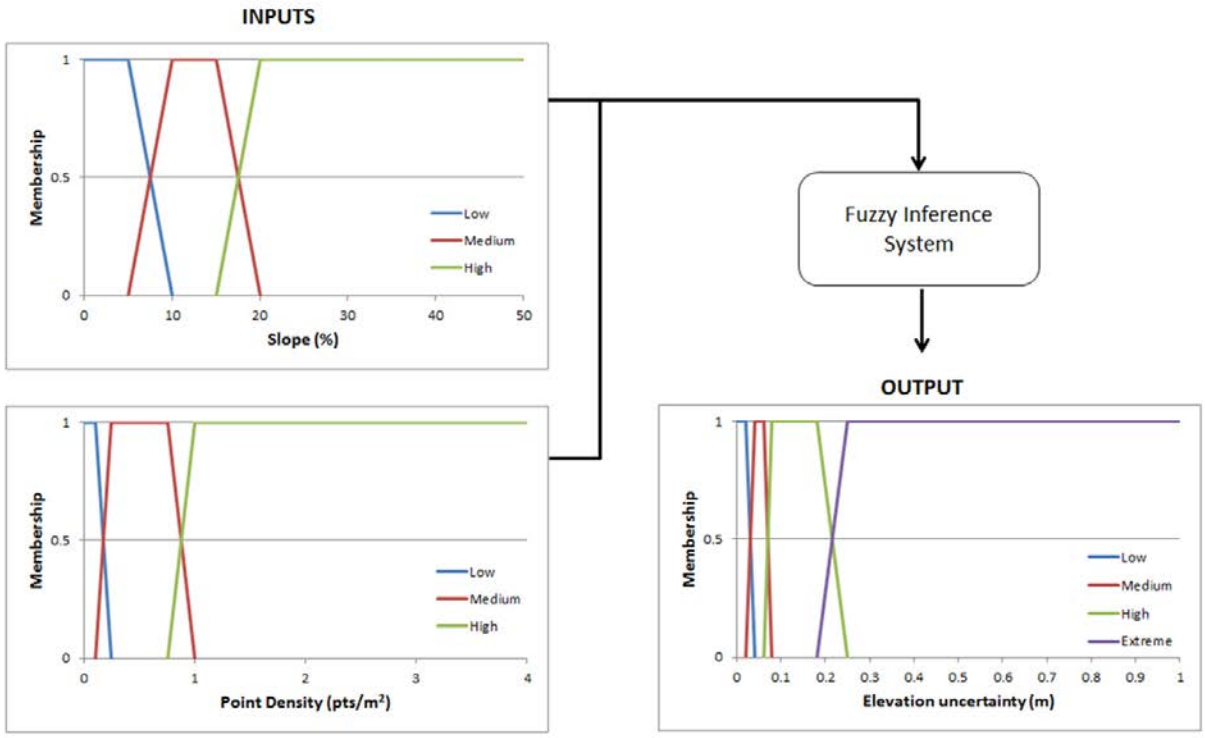

Figure 5: Input and output fuzzy inference system membership functions used for the geomorphic change detection analysis.

2.3 Channel and Valley Morphologic Metrics

Many morphologic metrics were extracted from the lidar-derived elevation surfaces. The general procedures for metric extraction are explained in this section.

2.3.1 Valley-spanning transects

Valley-spanning transects were automatically created at a 10-meter spacing perpendicular to a hand-digitized valley centerline. Separate sets of transects were created along the Colorado River and Lulu Creek. These transects form the basis for many of the calculated channel metrics, and provide a linear reference for the site based on valley location instead of distance along the river (which varies in time). Some channel metrics were measured at each transect and aggregated for each reach. The Colorado River transects begin at the south end of the wetland and extend just upstream of the Lulu Creek confluence. Although the transects include the entire wetland, most analyses were performed only on

transects along the fluvial reaches of the Colorado River upstream of the wetland. Transects are referenced as distance (in meters) along the valley axis downstream from the Lulu Creek confluence. The Lulu Creek transects begin at the confluence of Lulu Creek and the Colorado River and extend upstream 420 meters to the base of the debris flow scar. These transects are also referenced as distance (in meters) upstream from the Lulu Creek confluence with the Colorado River.

2.3.2 Water, bars, channel centerline, sinuosity, migration values, and braiding index

Several planform features were digitized from the high-resolution aerial photographs that accompanied both the 2004 and 2012 lidar surveys. As previously mentioned, the wetted channel edge was digitized at a scale of 1:500 along the Colorado River. The small size and step-pool morphology of Lulu Creek made it difficult to discern the exact extent of the water, so a wetted channel edge was not digitized along Lulu Creek. Gravel bars along the Colorado River were also digitized at a 1:500 scale from aerial photographs. This entailed differentiating areas of exposed sediment flanking the river from the vegetated floodplain surfaces, typically based on the lighter color of the sediment forming gravel bars. The elevation surfaces were used to differentiate exposed, light-colored cut banks from gravel deposits, although few distinct cut banks were noted within the site. Lastly, channel centerlines were digitized along both the Colorado River and Lulu Creek at a scale of 1:300. It should be emphasized that this is the center of the wetted channel and not the thalweg, which is indiscernible from aerial photos and lidar surveys. Channel centerlines were used to determine water surface slopes and reach-scale sinuosity values. Channel migration was determined along the Colorado River and Lulu Creek by measuring the change in centerline location between 2004 and 2012 at each of the valley-spanning transects. Along the Colorado River, a braiding index for each reach was calculated by determining the number of times each transect intersected the digitized water polygon.

2.3.3 Valley slope

Valley slope was determined along the Colorado River using an average valley floor elevation along each valley spanning transect. Valley floor was classified as any portion of the transect that was outside the bankfull channel and any adjacent gravel bars, and less than 1.5 meters above the water surface (see section on height-above-water-surface below). Points were constructed at 0.25-meter intervals along the valley spanning transects, and all points located within the wetted channel, adjacent sediment bars, or above 1.5 meters above the water surface were removed. Elevation values from the 2012 TIN were extracted to those points, and the average elevation from the remaining points along each transect was computed. The distance between transects was used to determine the slope. Small undulations and lateral variations in the floodplain necessitated using a running average of 10 and 20 transects to calculate slope rather than computing slope between two adjacent transects.

2.3.4 Channel cross-sections and bankfull measurements

Channel-spanning cross-sections along the Colorado River were derived from the valley-spanning transects (Appendix C). Elevation values were extracted at points spaced 0.20 meters along each transect from both the 2004 and 2012 TIN surfaces. Geomorphic bankfull width was measured at each of the cross-sections by discerning banks or other breaks in slope from the cross-section and cross-verifying them with the aerial photos. Resolution of and obvious irregularities on the lidar surfaces warranted ranking the cross-sections based on the quality of the width measurement (Table 2). Only bankfull cross-sections which received a rank of “1” or “2” (the highest of the four levels of ranking) were included in discerning trends in bankfull width along the river. Notebaert et al. (2008) note that widths extracted from lidar have a minimum error of 0.5-meters, so this error value was included on all measured bankfull values with larger values of error included where uncertainty was higher.

Table 2: Criteria for ranking lidar-derived cross-section confidence and appropriate error for the bankfull width analysis.

Rank	Criteria	Include	Error
1	Two distinct banks in cross-section with distinguishable floodplain behind, bank locations confirmed by air photo	Yes	0.5 m
1	One distinct bank in cross-section, very tall slope on other bank, bank location confirmed by air photo	Yes	0.5 m
2	Several breaks in slope in cross-section, one break in slope seems distinctly noticeable and can be confirmed in air photo	Yes	1 m
2	Distinct break in slope on one bank, undiscernibly break in slope on other bank but can be clearly identified in air photo	Yes	1 m
3	Several breaks in slope in cross-section, multiple banks seem possible, air photos don't help distinguish a bank	No	N/A
3	Distinct break in slope on one bank, undiscernibly break in slope on other bank and difficult to identify in air photo	No	N/A
4	Issues with TIN surface at cross-section, impossible to discern bank in air photos	No	N/A

2.3.5 Height-above-water-surface (HAWS) surface, confinement ratios, and valley power

A height-above-water-surface (HAWS) raster shows the height of the land surface perpendicular to the channel in relation to the water surface at the time of the survey (Jones, 2006). The HAWS surface delineates small-scale variations in elevation along the valley floor, defining confinement at a more detailed level than using the width of the entire valley floor, which may encompass more or less of the active floodplain. Two HAWS rasters were created from the 2012 elevation surveys and associated 2012 water surface; one each for the Colorado River and Lulu Creek. The Colorado River HAWS extended from the head of the wetland to upstream of the Lulu Creek confluence. Width measurements along the Colorado River were extracted at each transect for HAWS elevations at 0.25-meter intervals. The Lulu Creek HAWS extended from the confluence of Lulu Creek and the Colorado River to the base of the debris flow scar. Along Lulu Creek, the HAWS elevation interval was only 0.50-meters due to the thick, coarse deposits and lower confidence in the lidar surface in the steep, narrow valley of Lulu Creek.

Although HAWS surfaces from the 2004 lidar were created, the low resolution of the 2004 lidar in comparison to the 2012 HAWS rendered them less reliable for analysis. The HAWS surfaces and associated width transects were used to help define valley confinement and indicate potential for floodplain connectivity through the site.

Valley confinement was calculated at each transect by taking the ratio of the width of the floodplain to bankfull width at various height intervals above the water surface. Unconfined reaches were described at those with confinement ratios below two, partially confined were between two and ten, and unconfined were greater than ten. Confinement ratios were computed at each transect along the Colorado River where a confident bankfull width was computed from the 2012 lidar survey. These bankfull widths were compared to the width at each HAWS level to show variability in confinement at different heights above the water surface, although the highest HAWS value (1.5 meters) is the most representative of the total valley width.

Lastly, the HAWS was used to determine a proxy for a "valley power," or the potential of the valley to transport bed-material given the valley slope and valley width. Valley power was determined for the 0.75-meter and 1.50-meter HAWS levels in 2012 along the Colorado River valley and valley slope determined at a 100-meter running length.

2.3.6 Lulu Creek longitudinal profiles

Long profiles along Lulu Creek were extracted from the lidar surfaces in both 2004 and 2012, from approximately the Lulu Creek (LC) gage to the foot bridge that crosses Lulu Creek (Figure 2). The lidar-derived long profiles were compared to field surveys performed in 2010 (the earliest measured survey) and 2013, respectively. Although individual step characteristics were not discernible from the lidar profiles, local and reach scale variations were compared between the lidar profiles and field profiles.

2.4 Estimate of Bed-material Transport using the Morphologic Inverse Method

Bed-material transport rates were estimated along the Colorado River using the morphologic inverse approach that incorporates changes in planform geometry (and therefore sediment storage) as an indicator of sediment transport (Ashmore and Church, 1998). This method relies on the continuity approach, incorporating bed material inputs, outputs, and changes in storage in a defined reach such that:

$$\boldsymbol{S_o = S_i - \Delta S} \quad (1)$$

where S_o is the bed material output, S_i is the bed material input, and ΔS is the change in storage through the reach. When extended over a period of time, the equation adjusts to:

$$\boldsymbol{Q_o = Q_i - (1 - p)(\Delta S/\Delta t)} \quad (2)$$

where Q_o is the volumetric transport out of a reach over the period of time, Q_i is the volumetric transport into a reach over the period of time, and p is the porosity of the sediment. When several adjoining reaches are evaluated using the inverse method, the sediment flux leaving one reach becomes the incoming flux to the next reach downstream. In addition to the changes in sediment storage through each reach, this approach requires that at least one additional variable is known, either an input or output bed-material flux for the entire system (Q_i or Q_o).

Changes in sediment storage along the site were obtained from the lidar differencing. Net change was determined as a reach sum of vertical change for each of the response reaches later identified. Lidar differencing in this study excluded changes occurring below the water surface. If reach-scale water surface area had remained constant between surveys, a reasonable assumption could have been made that in-channel sediment changes were relatively small in comparison to the substantial changes seen above the water surface. Substantial reductions in water surface area due to a decrease in sinuosity were noted in some reaches, indicating likely additional in-channel sediment storage in those reaches. To accommodate for the change in underwater volume, an estimated average water depth of 0.25-meters was applied to the entire wetted channel through each reach for each year and changes in that volume per reach were

incorporated in the final sediment budget. It is assumed that the small tributaries along the reach provide negligible input of bed material.

Two approaches were used to determine an end member sediment flux (either input or output) for the system, and results of each were then compared. The first approach used the Lulu City wetland as a local bed-material sink, with the assumption that all bed material was deposited as a fan at the head of the wetland (Figure 2), and zero bed-material transported past the wetland. This approach is similar to previous studies that used the gravel-sand transition in a river as a location of zero bed-material transport (Surian and Cisotto, 2007; Martin and Church, 1995). A second approach used the total volume of sediment removed from the Lulu Creek fan (Figure 2) as an input flux into the system. Some uncertainty exists in both these approaches because the aerial extent of both the wetland fan and Lulu Creek fan was subjectively determined from the lidar differencing and aerial photographs. The commonly used approximated value for porosity of 0.25 for cobble- to gravel-sized bed material was also applied to this study because measuring porosity of bed-material in the field is difficult (Martin and Church, 1995).

Output from the morphological inverse method is a rate of transport over the time between surveys, or eight years in this study. The low flows of 2004-2008 and 2012 suggest that the majority of the bed-material transport in those eight years occurred during the high flows of 2009-2011, but obtaining yearly rates proved difficult. An attempt was made to constrain the total transport rate to annual rates by relating reach-scale changes in sediment volume to changes in cross-sectional area at repeat cross-sections. The yearly change in cross-section area at each cross-section was compared to the net change in area between 2004 and 2012 (or, in most cases, between 2009 and 2011). Unfortunately, repeat cross-sections with adequate records only existed in two of the five reaches, both showing similar responses to the high flows. Therefore, the added benefit of results of the cross section resurveys is low and little extra analysis was conducted.

Previous work at this site has shown that field-measured bed-material transport rates and transport rates estimated from existing transport equations show differences of two to four orders of magnitude (unpublished data, S. Rathburn, Colorado State University, 2014). Results of the morphologic inverse method were compared to field measured rates of bed-material transport at the existing Gravel Beach gage. Measured rates of bed-material transport at Gravel Beach from 2004-2005 and 2008-2010 were regressed in relation to discharge at the time of sampling to create a sediment rating curve at Gravel Beach. This sediment rating curve was then applied to mean daily flows over the entire snowmelt hydrograph at the site for the years 2008-2012. Bed-material flux for years of 2005-2007 was estimated by comparing the shape of the annual hydrograph to the 2008 and 2012 hydrographs, all of which were low flow years.

Continuous discharge measurements were taken at Gravel Beach over the summers of 2008-2010 and 2012, but all gage equipment was destroyed in the high flows of 2011. To estimate the 2011 discharge hydrograph at Gravel Beach, the mean daily discharge at Gravel Beach was regressed by the mean daily discharge at Baker Gulch for all measured Gravel Beach discharge measurements from 2008-2010. This relationship was then applied to the mean daily discharge at Baker Gulch over the 2011 snowmelt hydrographs to obtain discharge estimates at Gravel Beach for that summer. Simplifications in this process are acknowledged, including the lack of hysteresis between the rising and falling limbs of the hydrograph, the assumption that the initial high stream flow in 2009 mobilized a greater amount of stored sediment compared to subsequent years, or the lack of bed-material transport rates at extremely high flow conditions. Combining all bed-material transport rates over the years was justified by the low number of measurements taken annually, the varying magnitude of discharges each year, and the strong correlation of the final regression. Although strong relationships in the sediment rating curve give confidence to annual estimates of bed-material flux at Gravel Beach, a sensitivity analysis in the relationship between the Baker Gulch and Gravel Beach gage discharges was applied in the final results.

Attrition during bed-material transport was considered in the sediment budget because breakdown of larger clasts can affect sediment loads and, hence, transport capacity. The material abraded from a large clast is presumed to be fine-grained material that is transported in the suspended or washload, and therefore transported rapidly out of the reach or deposited as sheets undetectable within the vertical error of the lidar differencing. Attrition was applied at several levels in the final sediment budget, following Sternberg (1875) in the form of:

$$\boldsymbol{W_x = W_0 * e^{(-\alpha x)}} \quad (3)$$

where W_x is the mass (in grams) of sediment after traveling a distance of x (km), W_0 is the initial mass of sediment (grams;), and α is the mass loss coefficient (km^{-1}). Attrition was applied at the reach scale, where W_0 is equivalent to Q_i in equation 2 and x is the length of the reach.

The effect of clast attrition was tested at several levels of the mass loss coefficient (α) in the sediment budget to determine its possible effect on reducing bed-material transport through the site. Attrition rates from α=0.01-km^{-1} to α=1.0-km^{-1} were applied to the sediment budget. The lower attrition rates (α=0.01-km^{-1}) agree with rates determined for Tertiary andesite and basalt from the Oregon Cascades, while the higher rates (α=0.5-km^{-1} to α=1.0-km^{-1}) are representative of weak sedimentary rocks from the Coast Range of Oregon and northern California (O'Connor et al, 2014; Sutherland et al., 2002). Although the 2003 debris flow material is volcanic in origin, the hydrothermal alteration and micro-fractures from the initial debris flow cause the rhyolite tuff to exhibit field conditions more similar to the sedimentary lithologies mentioned in O'Connor et al. (2014).

3. RESULTS

Lidar differencing and changes in channel planform reveal reaches of varying geomorphic response to high flows following a sedimentation event along Lulu Creek and the Colorado River. Six distinct response reaches were identified through the study site, one on Lulu Creek (LC) and five along the Colorado River (CR1-CR5), based primarily on locations of aggradation and degradation between 2004 and 2012. Additionally, the portion of the wetland that aggraded between 2004 and 2012 was treated as a reach (WL) for the morphologic inverse method calculations. Table 3 summarizes the morphologic metrics and changes identified in each response reach, and the individual reaches have been highlighted in figures showing morphologic metrics throughout this section. Only the portion of Lulu Creek within 260-meters upstream from the Colorado River, where extensive aggradation begins and lidar surfaces were confidently created, will be classified as the LC response reach (although some figures show morphologic trends all the way upstream to the debris scar).

This chapter begins by presenting variations in morphologic metrics within the study area, followed by a section that identifies distinct trends in morphologic metrics by revisiting the hypotheses pertaining to geomorphologic change. It concludes with results of the bedload estimates using the inverse method and revisiting the sediment transport hypothesis.

3.1 Locations of Aggradation and Degradation

Locations of aggradation and degradation identified by lidar differencing showed distinct zones of change along the Colorado River and Lulu Creek between 2004 and 2012 (Figure 6 and Figure 7). By incorporating the FIS to compute error in the DOD process, reductions in areal and volumetric changes were most noticeable in areas where the vertical change was near zero or negative (Figure 8). Lulu Creek (reach LC) showed nearly uniform degradation, with incision into the Lulu Creek debris fan deposited during the initial 2003 breach. Net degradation of Lulu Creek fan obtained by lidar differencing (1556-m^3) was similar to the 1650-m^3 estimate in Rathburn et al. (2013) based on field resurveys across the fan.

Table 3: Summary table of morphologic metrics and changes for each response reach.

Reach	LC	CR1	CR2	CR3	CR4	CR5	WL
River	Lulu Cr.	Colorado R.	Colorado R.	Colorado R.	Colorado R.	Colorado R.	Colorado R.
Reach boundaries							
Upstream end	270	0	220	420	620	740	980
Downstream end	0	220	420	620	740	980	--
Valley length (m)	270	220	200	200	120	240	--
Channel length (m)							
2004	316.2	252.3	189.2	247.2	128.5	281.0	--
2012	321.8	251.2	190.1	228.7	134.9	246.5	--
Sinuosity							
2004	1.17	1.10	1.00	1.18	1.07	1.22	--
2012	1.19	1.09	1.00	1.09	1.12	1.07	--
Change	Minor	Minor	Constant	Decrease	Minor	Decrease	--
Water surface slope							
2004-2012 change	No change	No change	No change	Decreased	No change	Decreased	--
Elevation changes							
Aggradation (m^3)	--	193	0	627	42	679	--
Degradation (m^3)	--	-1360	-604	-186	-250	-72	--
Net change (m^3)	-1556	-1167	-604	441	-208	607	638
Level	Degradation	Degradation	Degradation	Aggradation	Degradation	Aggradation	
Migration							
Average (m)	4.5	7.0	0.7	3.5	2.5	4.3	--
Max (m)	14.6	13.8	1.8	13.5	8.2	13.3	--
Level	High	High	Minimal	High	Moderate	High	--
Braiding Index							
2004	--	1.05	1.00	1.19	1.50	1.42	--
2012	--	1.00	1.00	1.10	1.00	1.38	--
Change	--	Minor	No change	Decrease	Decrease	Minor	--
Confinement							
Level	--	Unconfined	Confined	Unconfined	Unconfined	Unconfined	--
2012 Valley Slope							
Reach-length change	--	Decreasing	Increasing	Constant	Decreasing	Constant	--
Bar area (m^2)							
2004	--	2494	168	1165	1112	1925	--
2012	--	2802	101	2045	1093	2097	--
Change	--	Increase	Decrease	Increase	Constant	Increase	--
Water area (m^2)							
2004	--	948	659	1208	585	1488	--
2012	--	8801	582	833	426	1289	--
Change	--	Increase	Decrease	Decrease	Decrease	Decrease	--
2004 to 2012 bankfull width							
# transects increased	--	5	3	4	5	5	--
# transects decreased	--	7	2	7	1	4	--
# transects no change	--	2	12	2	1	9	--
Average change (m)	--	-0.53	1.52	1.75	1.63	0.82	--

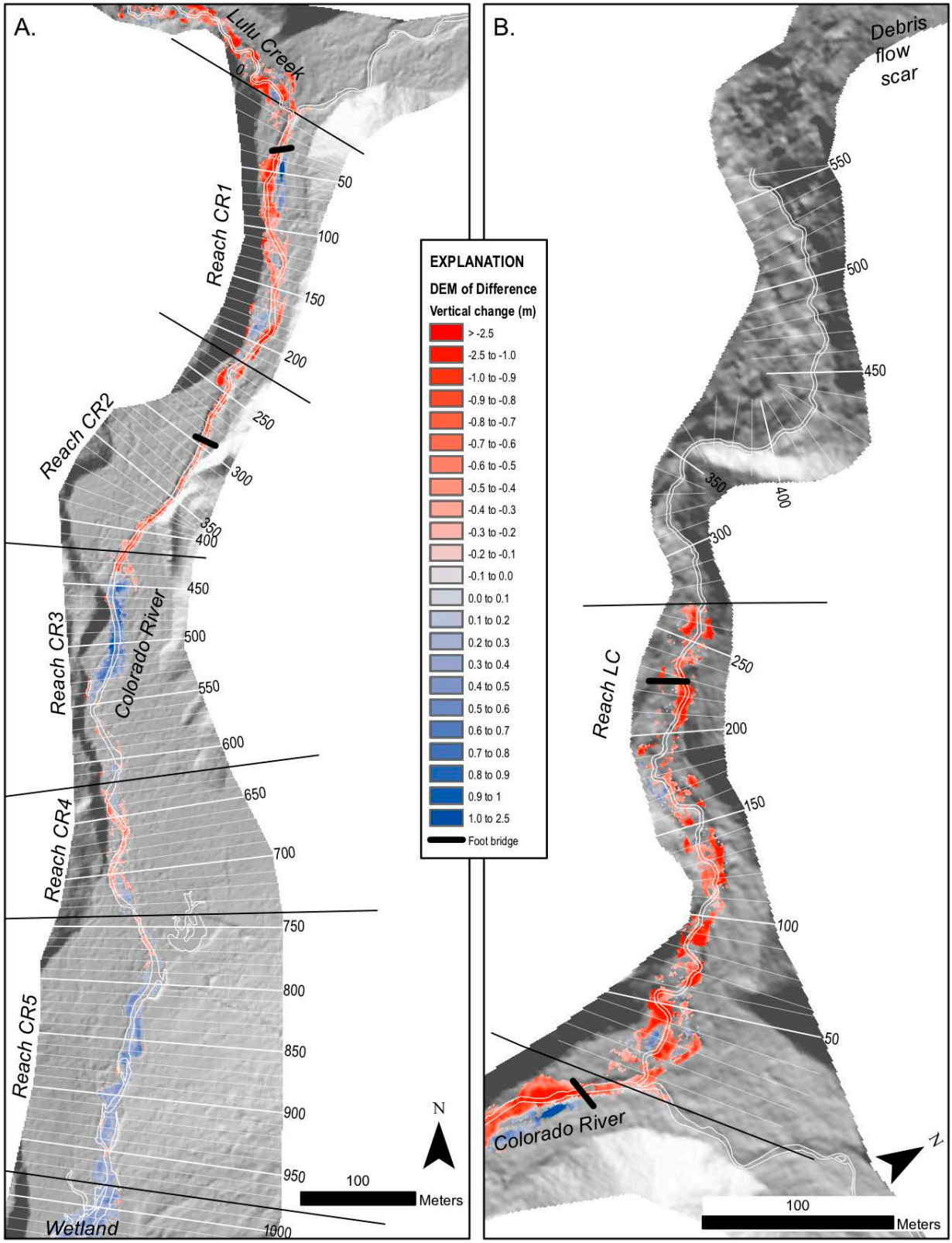

Figure 6: Spatial extent of aggradation and degradation along A) the Colorado River and B) Lulu Creek. Water along the Colorado River and Lulu Creek shown by white outlines (Lulu Creek width approximated). Transects labeled as distance (meters) from the Colorado River/Lulu Creek confluence.

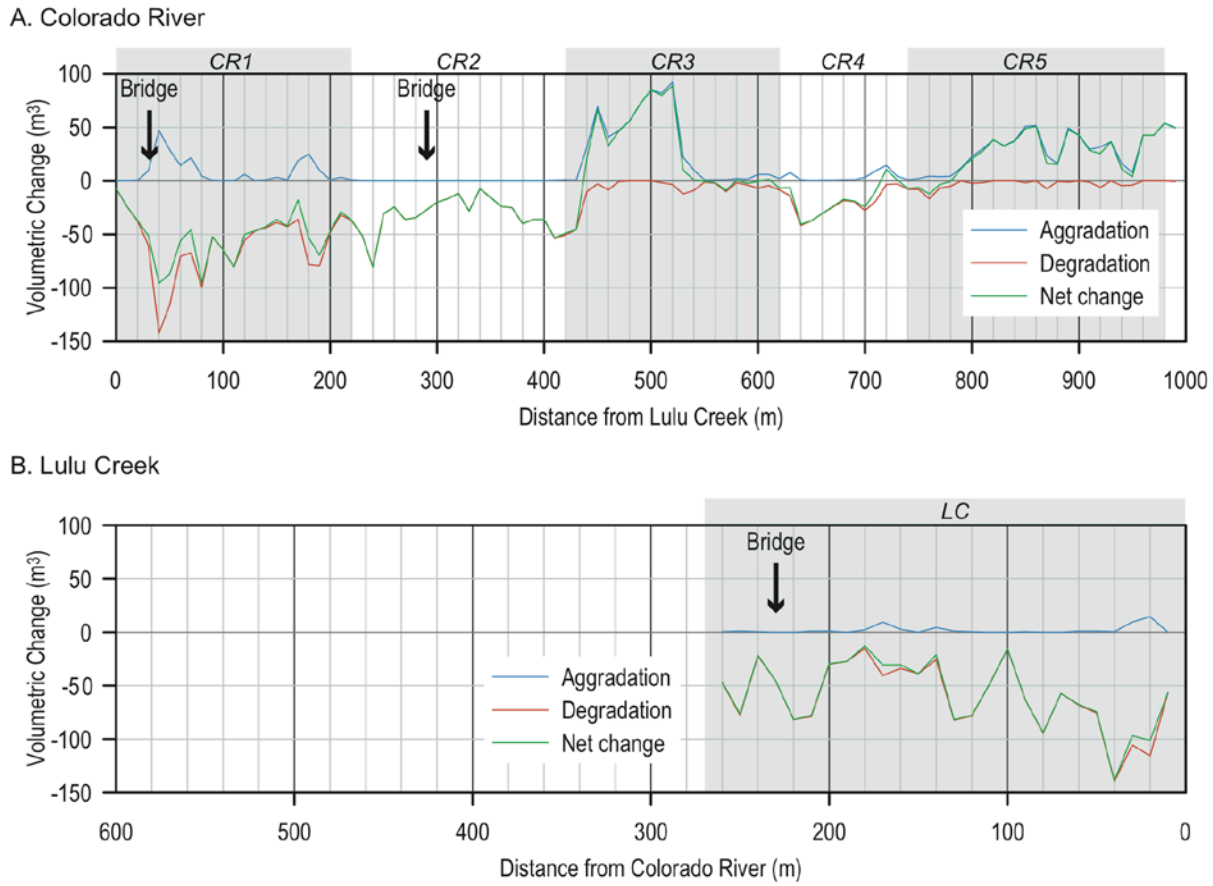

Figure 7: Volume of aggradation and degradation at each transect along A) the Colorado River and B) Lulu Creek based on lidar differencing between 2004 and 2012. See Figure 6 for spatial extend of changes.

Degradation was also prominent in reaches CR1, CR2, and CR4, yet the style of degradation varied. CR1 and CR4 both showed net degradation, but also areas of aggradation as the channel adjusted position. CR1, the reach adjacent to the Lulu Creek fan, had the largest total volumetric change of all the reaches along the Colorado River, and included areas of aggradation as well as degradation. Reach CR2 experienced solely degradation, but vertical changes were related to a drop in water surface elevation (and therefore assumed to be a drop in the river bed) because the channel did not adjust position except at the very upstream end of the reach. Some degradation in CR2 may in part be due to variations in the water surface elevation and issues with creation of the elevation surface along an incised channel from a low-resolution lidar survey in 2004. Abundant aggradation occurred within reaches CR3 and CR5 between 2004 and 2012. Aggradation in reach CR3 was concentrated more at the upstream end of the reach where

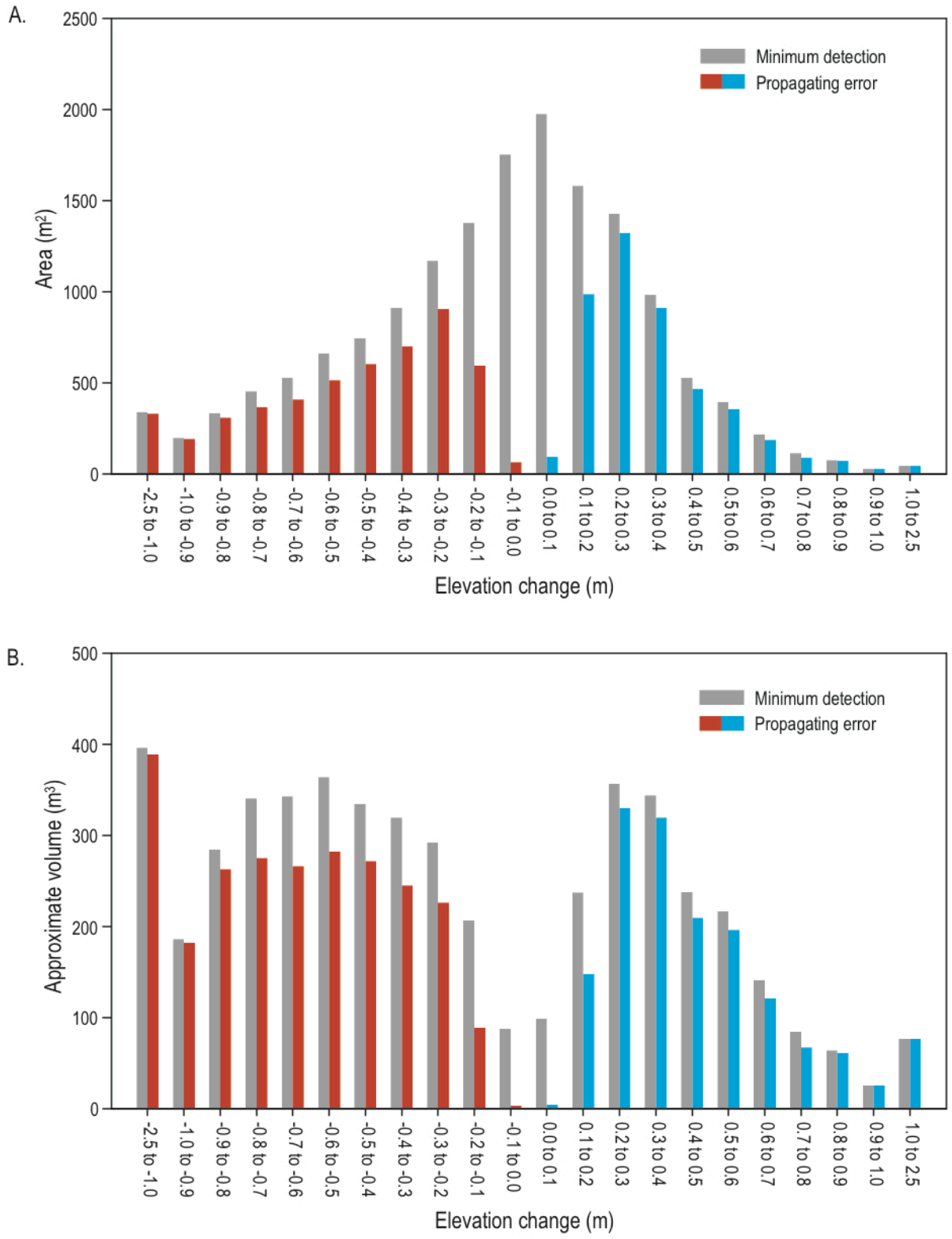

Figure 8: Differences in areal and volumetric changes along the Colorado River using different methods in the geomorphic change detection program. This study relied on the 'propagating error' method, which accounts for error at the pixel-scale. The minimum detection method does not account for any error. Blue bars represent aggradation while red bars represent degradation.

the Colorado River exits the confined reach CR2, whereas aggradation is more evenly spread through reach CR5.

Hereafter, reaches CR1 and CR4 will be referred to as degradational reaches, and reaches CR3 and CR5 as aggradational reaches. Although reach CR2 is degradational, it will be treated separate from reaches CR1 and CR4 due to its unusually high valley confinement.

3.2 Planform Geometry Metrics and Changes

3.2.1 Water surface slope

Water surface profiles along the Colorado River show a gradual decrease in slope when moving downstream (Figure 9A and Figure 10). The 2004 water surface profiles exhibit more variability in comparison to the 2012 profile, likely a result of the lower resolution of the 2004 lidar survey. Water surface slope values, commonly used in various hydraulic equations, indicate large variation when calculated by lidar at 20-meter intervals, but variation is reduced substantially when a 100-meter length is used (Figure 10). Variation in water surface slope at 20-meter intervals is likely a combination of noise from uneven TIN surfaces crossing the water surface and local variations in slope along the channel. A distinct decrease in water surface slope between 2004 and 2012 occurred in the degradational reaches (CR3 and CR5), while water surface slope remained more constant in reaches CR1, CR2, and CR4. Water surface slope along Lulu Creek was more consistent except for a slight decrease in both years at the Lulu Creek fan near the confluence with the Colorado River (Figure 9B). Differences between valley elevation and water surface elevation (Figure 9) could be used as one indicator of floodplain connectivity, but a different approach was used in this study (discussed below).

3.2.2 Valley slope

Valley slope varies along the Colorado River through the study site, with a general decrease in the downstream direction (Figure 11). Most noticeable is the increase in valley slope in reach CR2, where

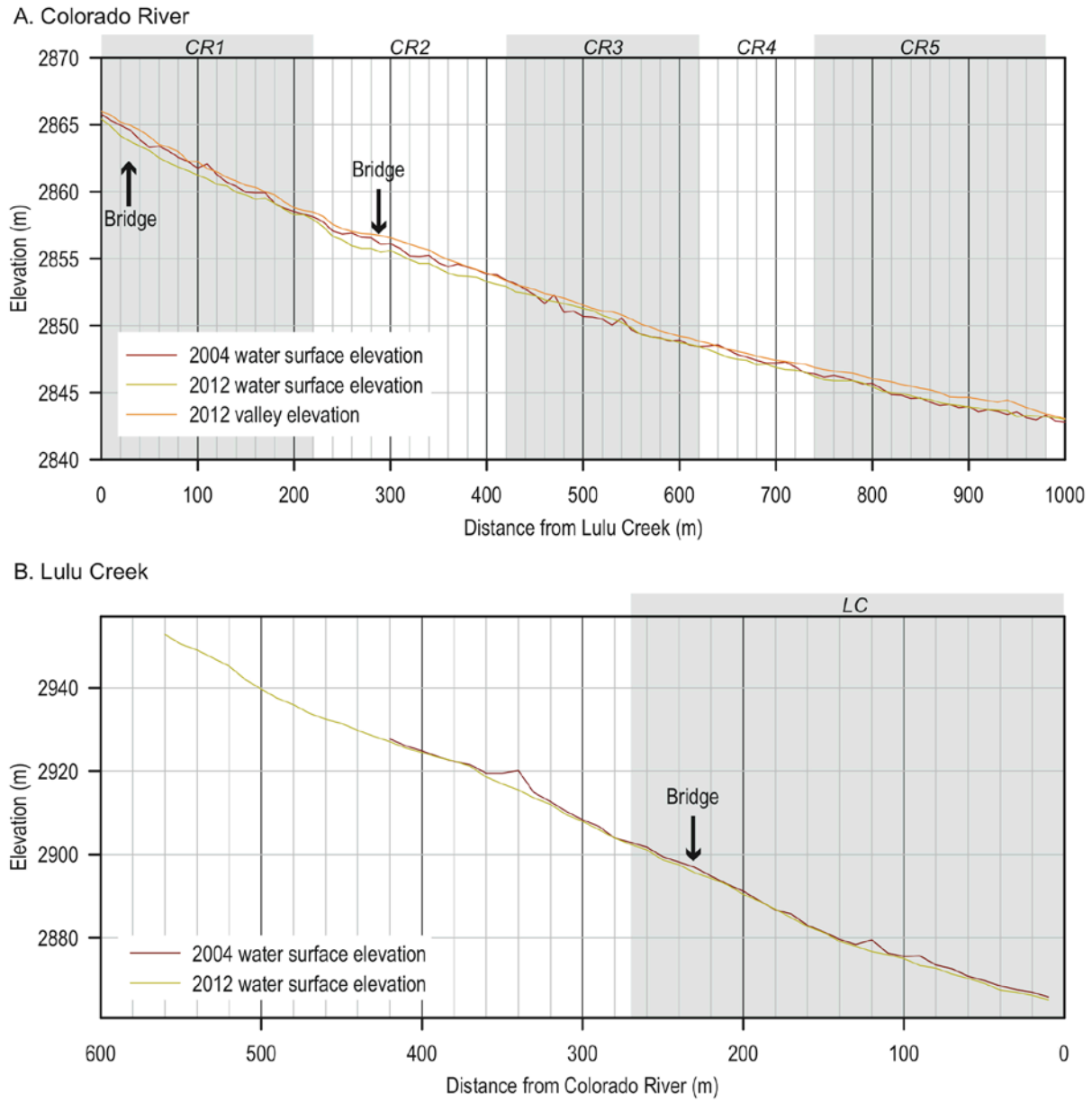

Figure 9: Water surface and valley elevations along A) the Colorado River and B) Lulu Creek (only water surface elevations for Lulu Creek). See Figure 10 and Figure 11 for variations in water surface and valley slope values along the Colorado River.

the Colorado River flows adjacent to older debris flow deposits near the Sawmill Creek confluence (Grimsley, 2012). This increase in valley slope is prominent when using a 100-meter running length for computing slope, but smoothed away when using a 200-meter length. Degradational reaches (CR1 and

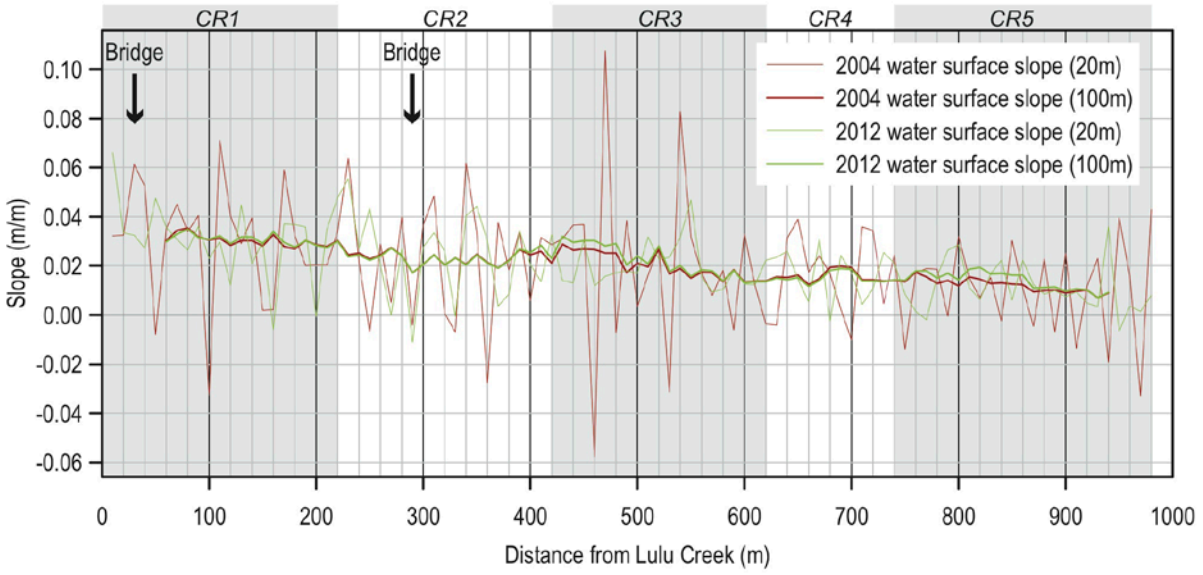

Figure 10: Water surface slope along the Colorado River. Abundant variation is noticeable when using a 20-meter length for calculating slope (one transect upstream to one transect downstream), but variation is greatly reduced when using a 100-meter length.

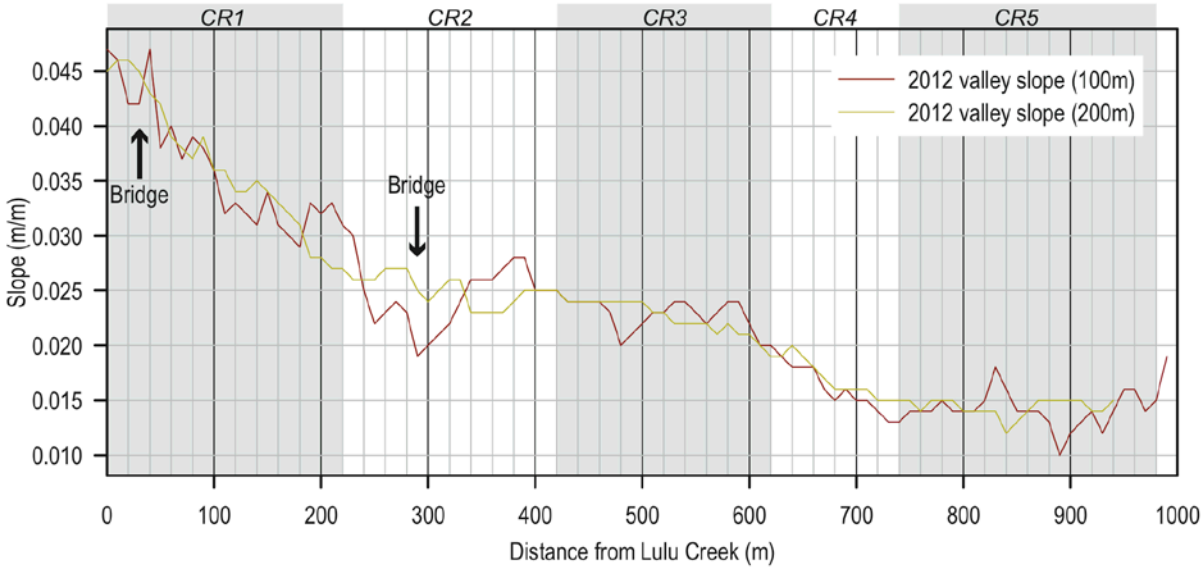

Figure 11: Valley slope along the Colorado River valley.

CR4) occur in areas with a distinct decrease in valley slope, whereas aggradational reaches (CR3 and CR5) occur in locations where valley slope is more constant.

3.2.3 Channel migration, braiding index, and sinuosity

Channel migration between 2004 and 2012 was common along both the Colorado River and Lulu Creek (Figure 12). Only one distinct reach (CR2) shows minimal channel migration, while lateral migration of over 8 meters (and commonly greater than 12 meters) was seen in all other reaches (Figure 13 and Table 3). Migration along the Colorado River was associated with river meanders flipping position between 2004 and 2012 or decreases in sinuosity, whereas migration on Lulu Creek was associated with adjustments in thalweg location as the Lulu Creek fan was substantially degraded. Although channel migration was common in most reaches, reach-scale sinuosity only decreased in the aggradational reaches (Table 3). Braiding index along the Colorado River decreased in all reaches except CR2 as the planform switched from a multi-thread to single thread channel. Reach CR4 showed a substantial decrease in braiding index as a result of a left-side channel aggrading between 2004 and 2012 (Table 3; Figure 12).

3.2.4 Bankfull width

Changes in bankfull width between 2004 and 2012 along the Colorado River showed within-reach variations in channel adjustment (Figure 14). Portions of both CR2 and CR5 showed locations of minimal change in bankfull width. Reach CR2 was confined both years with minor lateral channel adjustment, yet reach CR5 had substantial lateral change but all change remained within the defined bankfull area in the middle portion of the reach. A distinct pattern of channel narrowing followed by channel widening occurred in reaches CR1 and CR3 (Figure 14A). Additionally, transects closest to Lulu Creek experienced a greater degree of change in bankfull width than reaches more distant from Lulu Creek, except within the confined reach CR2 (Figure 14B).

3.2.5 Valley confinement

Variations in width at different height above water surface (HAWS) levels is a way to represent confinement along the Colorado River and Lulu Creek (Figure 15). Along the Colorado River, the width of the 1.25- and 1.50-meter HAWS levels generally indicates the valley edge that would be discernible

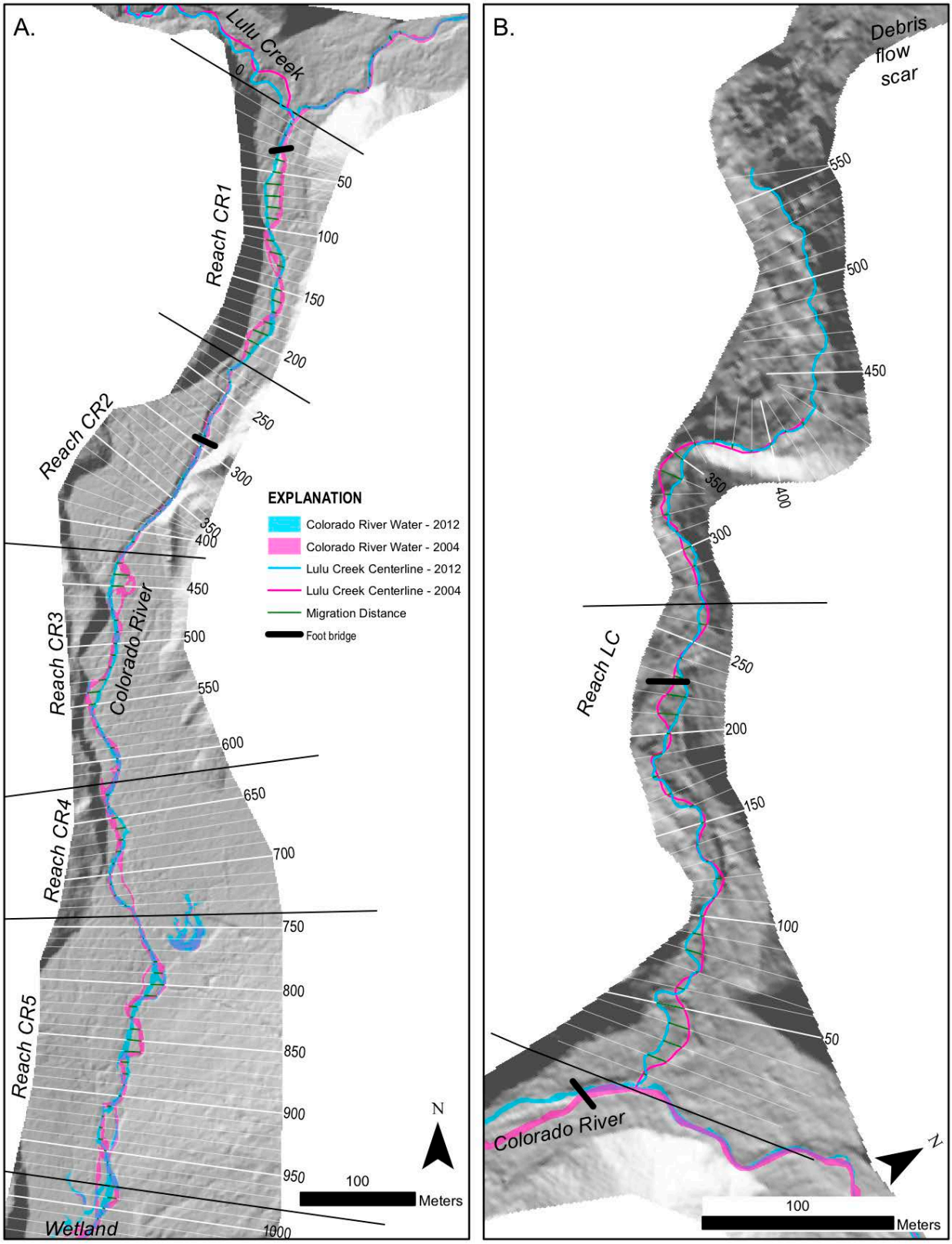

Figure 12: Locations of the 2004 and 2012 channel along A) the Colorado River and B) Lulu Creek. Transects labeled as distance (meters) from the Colorado River/Lulu Creek confluence. Dense vegetation in the 2004 aerial photographs made it difficult to identify the 2004 channel beyond 420-meters up Lulu Creek.

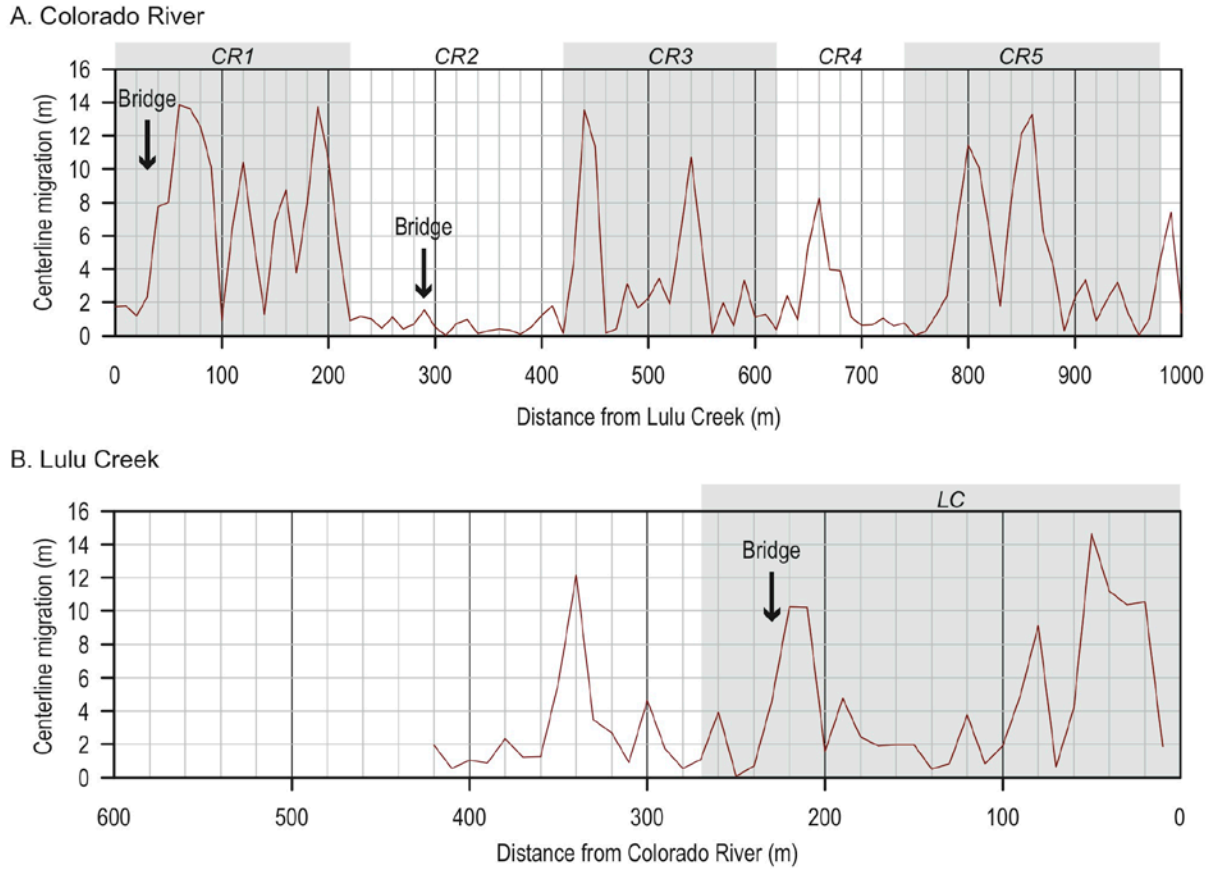

Figure 13: Channel migration along A) the Colorado River and B) Lulu Creek. Migration is calculated as the distance between the 2012 and 2004 channel centerlines at each transect.

from sources other than lidar (i.e., 10-meter DEMs or aerial photographs). In reaches CR2 and CR5, where old debris fans constrict the floodplain yet abrupt elevation changes do not exist, the HAWS helps define the width of the valley (1.50-meter HAWS level) in relation to other reaches. In general, the HAWS widths are smaller in the upper reaches of the Colorado River and increase in the lower reaches (Figure 16). Although reach CR1 is on average the most narrow reach for the higher HAWS levels, the Colorado River passes through a distinct constriction at the entrance of reach CR2 that remains narrow through the entire reach up to the 0.75-meter HAWS level. Reach CR4 is the widest in terms of the entire valley width, but CR3 shows multiple locations where the 0.50-meter HAWS level is the widest along the river, except where the Colorado River enters the wetland in reach CR5. Reach CR5 shows a distinct downstream narrowing of the higher HAWS levels where the lower HAWS levels widen. Along Lulu

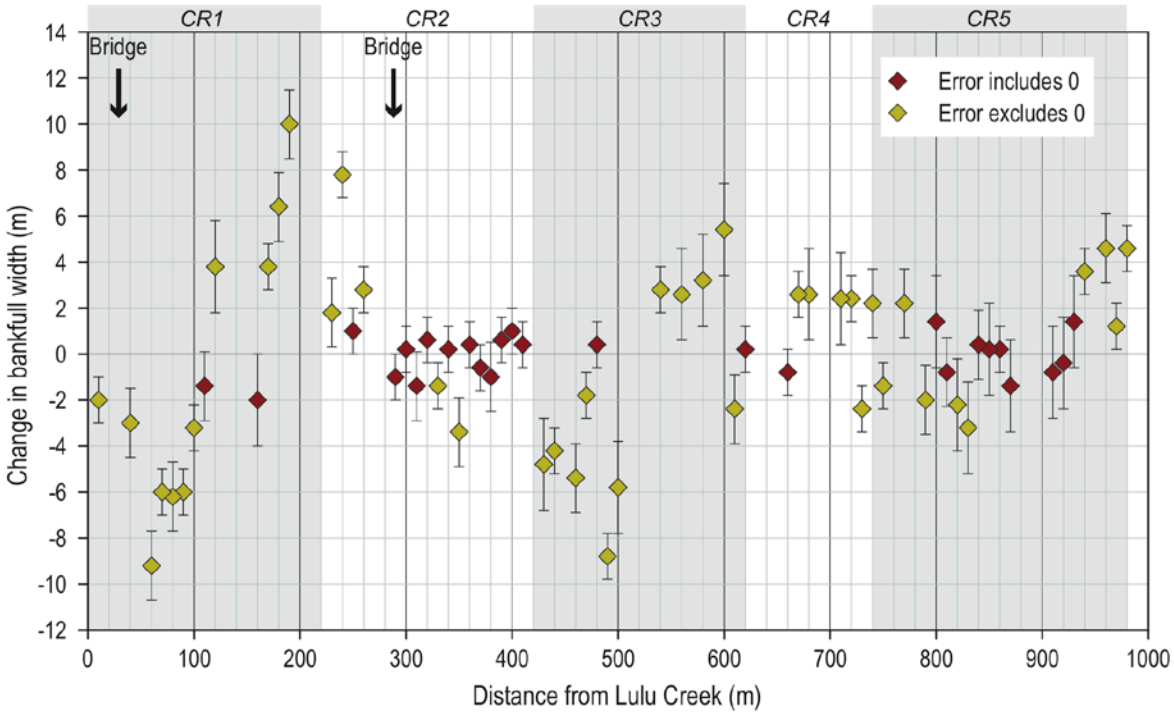

Figure 14: Total change in bankfull width between 2004 and 2012 along the Colorado River, with positive values indicating increased bankfull width and negative values indicating narrowing between 2004 and 2012. Different colors indicate values that include or exclude zero within the error of calculating changes in width.

Creek, the HAWS widths are moderately wide where the debris flow scar intersects Lulu Creek, but narrow as the creek passes through a short bedrock gorge (~370-meters from the Colorado River) (Figure 16B). The Lulu Creek valley then slowly widens before substantially widening at the Lulu Creek debris fan (70-meters from the Colorado River). Lower HAWS levels support less variation in width along Lulu Creek than the Colorado River, not an unexpected result due to the narrow width of the valley, the incised nature of Lulu Creek, and the larger HAWS interval used.

The majority of the Colorado River valley is classified as partially confined by the confinement ratios at the 1.5-meter HAWS, although abundant variation existed within each reach (Figure 17). At the boundary between reaches CR1 and CR2, the valley does briefly fall into the confined category. Results of this confinement method are questionable because field evidence indicates that the river never flowed

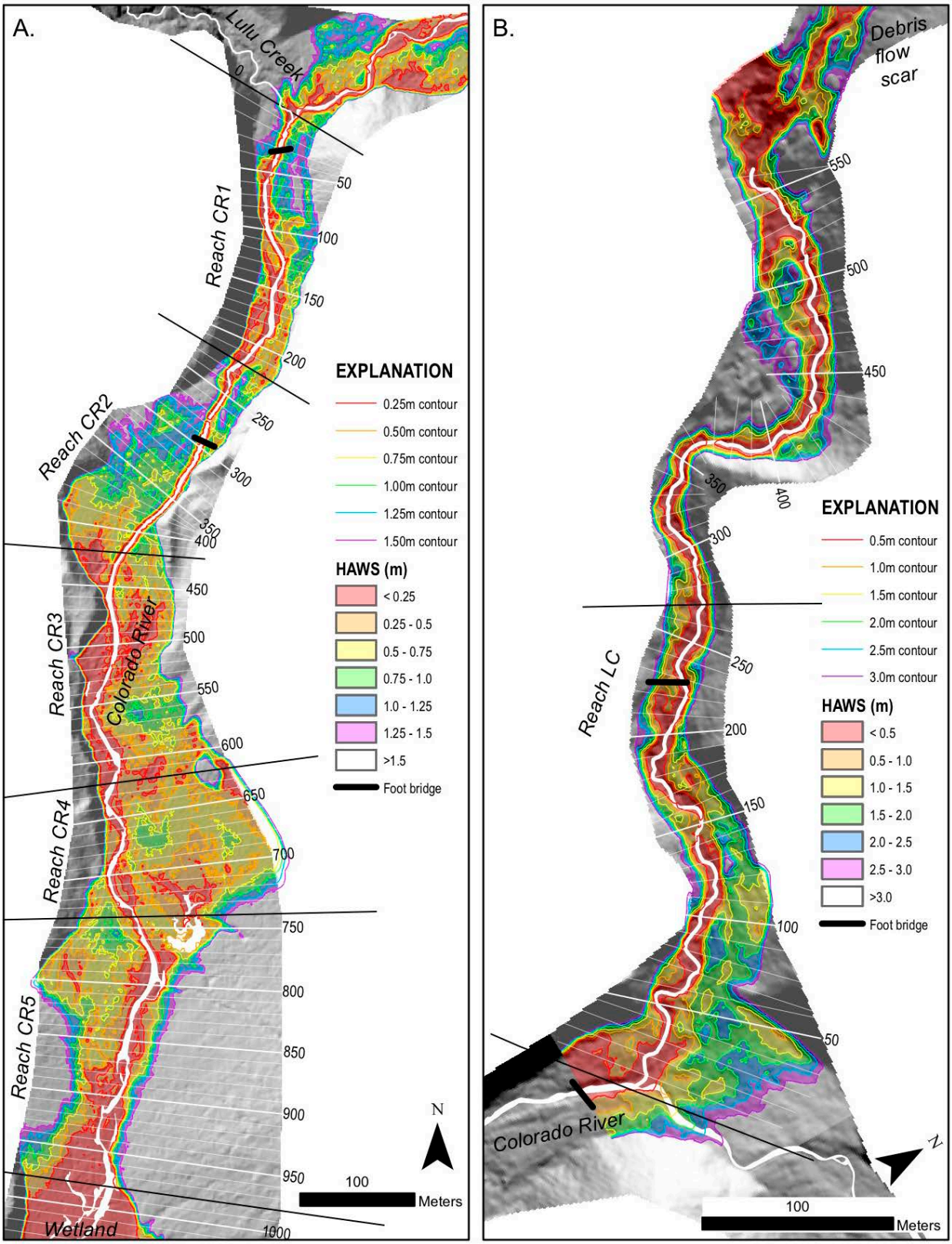

Figure 15: Height above water surface (HAWS) raster for 2012, overlaying the lidar topography along A) the Colorado River and B) Lulu Creek. Water along the Colorado River and Lulu Creek is shown in white (Lulu Creek width approximated). Transects labeled as distance (meters) from the Colorado River/Lulu Creek confluence.

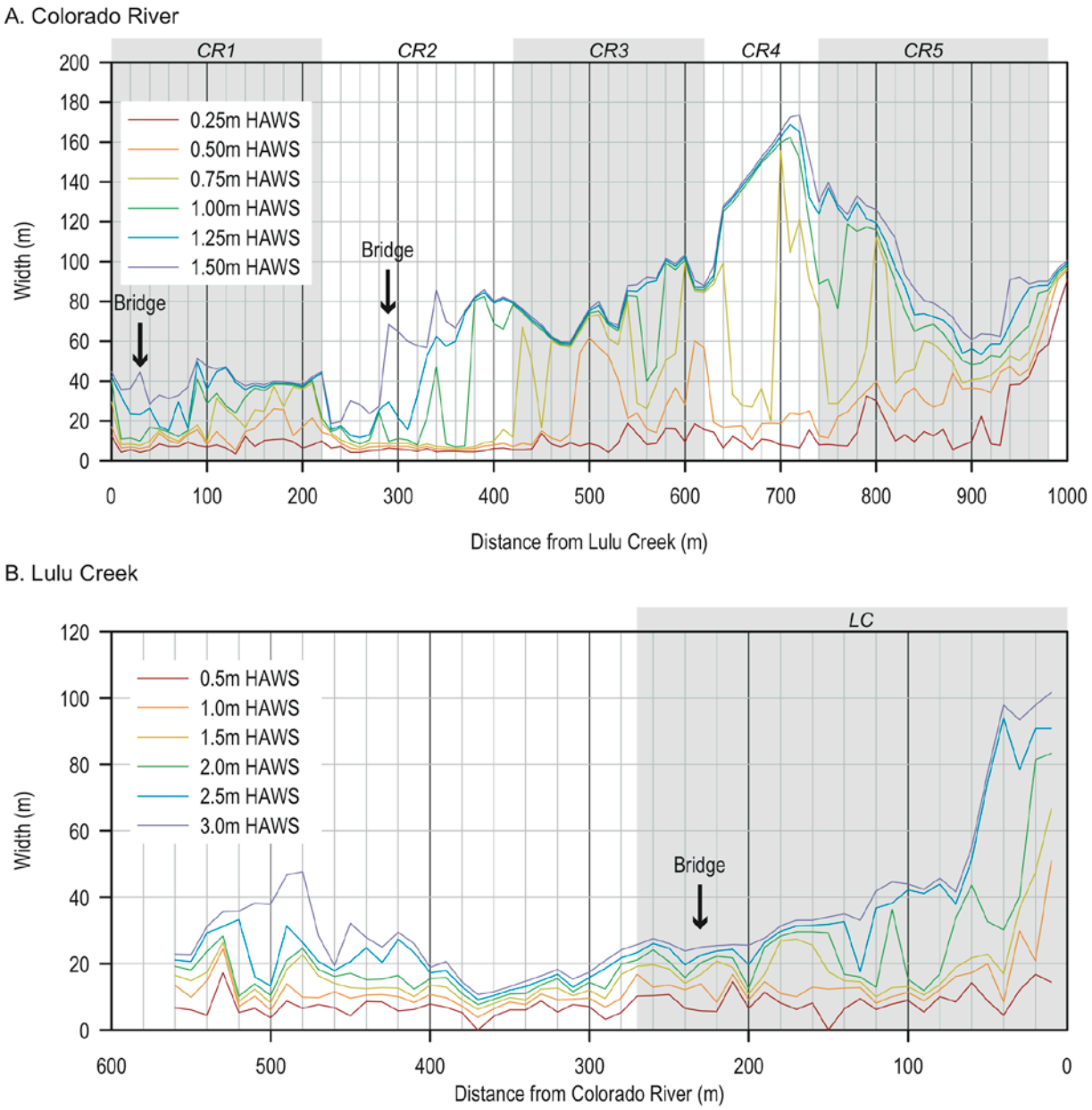

Figure 16: Width of the valley floor at various heights above the water surface along A) the Colorado River and B) Lulu Creek. HAWS = height above water surface. See Figure 15 for spatial extend of HAWS surface.

over its bank in reach CR2 during any of the high flow years, yet reach CR2 shows some of the highest values for confinement (Figure 17). The lack of planform changes between 2004 and 2012 in reach CR2 also suggests that flow did not overtop the channel and, therefore, it is inaccurate to define the valley along that reach as active floodplain. This sheds light on the uncertainty associated with using lidar to identify active floodplain along a channel. Confinement could be determined using a HAWS level less than 1.5-meters to represent floodplain width, but the recent and future aggradation and degradation

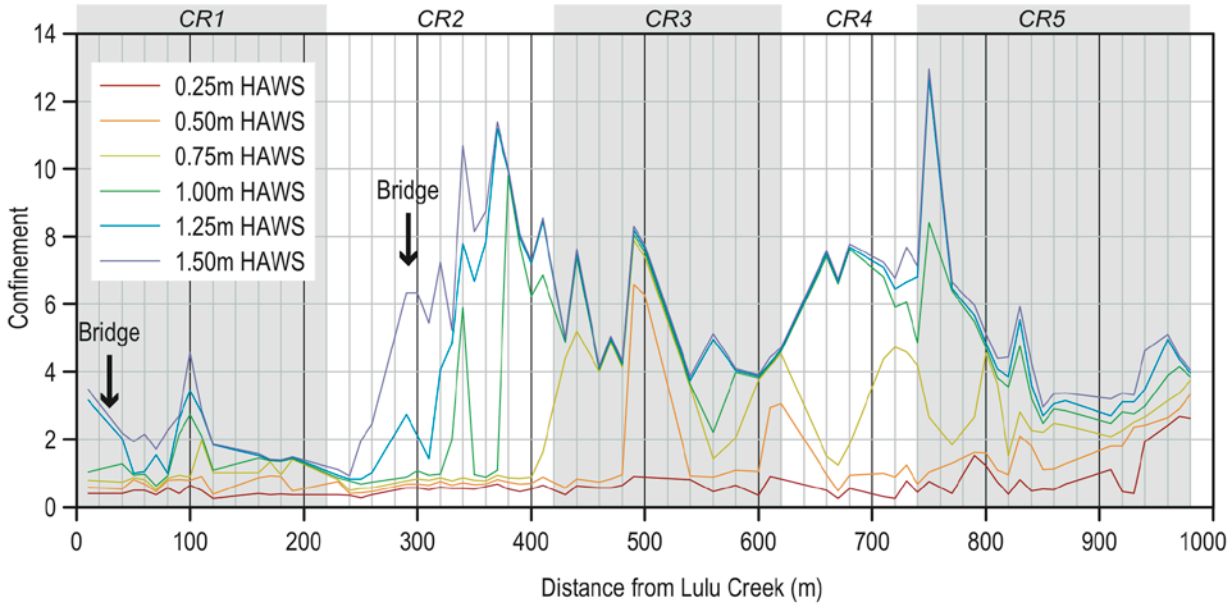

Figure 17: Confinement ratios along the Colorado River using various HAWS levels as the valley width. The 1.5-meter HAWs typically align with the base of the main valley walls, but not necessarily representative of the active floodplain.

through the site creates variability in channel elevation in relation to the floodplain that would cause much uncertainty in choosing an appropriate HAWS level. Due to the inability to confidently determine confinement values from lidar, reach CR2 will be referred to as confined, while all other reaches will be considered unconfined based on field observations. Confinement ratios could not be calculated along Lulu Creek because no bankfull width measurements were taken on Lulu Creek.

3.2.6 Valley power

The proxy for valley power, using valley slope and valley width at various HAWS levels, shows the variability in the potential for bed-material transport through the Colorado River valley during extreme flows (Figure 18). The 1.50-meter HAWS level best represents the width of the entire valley floor, whereas the 0.75-meter HAWS level best identifies the confinement along reach CR2 but may not accurately represent fluctuations in valley width in the other reaches. It is clear that reach CR1 has relatively high valley power at both HAWS levels when compared to reaches CR3, CR4, and CR5. The relative level of valley power in reach CR2 varies depending on which HAWS level is used. When using

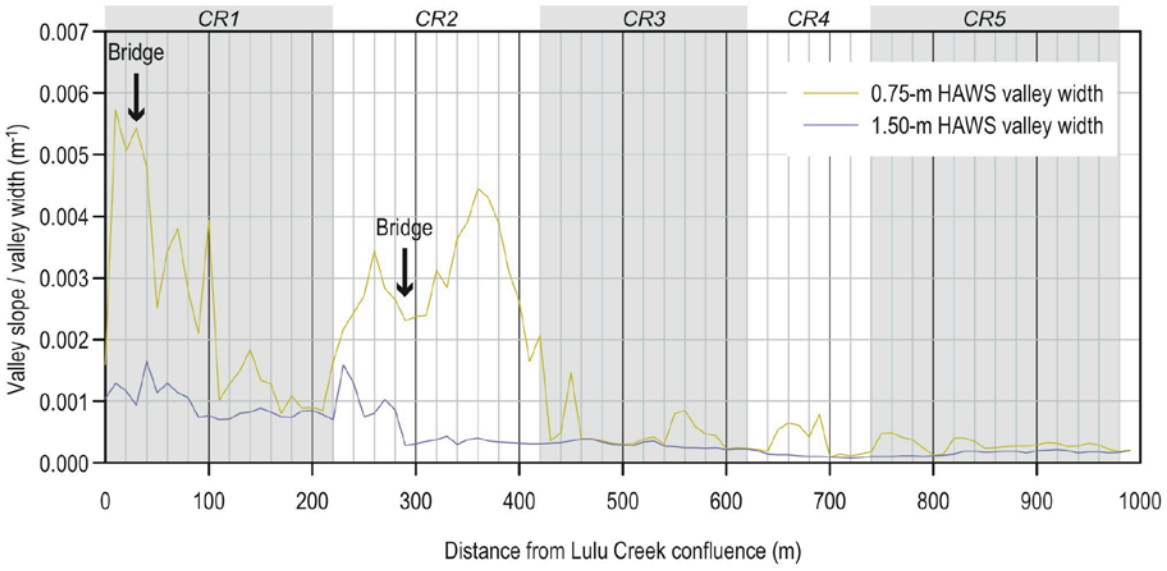

Figure 18: Valley power (valley slope/valley width) along the Colorado River valley for two HAWS levels used for valley width in Figure 16.

the 1.50-meter HAWS level, valley power is high at the upstream end of reach CR2 but substantially decreases halfway through the reach. Valley power stays high through the entire reach at the 0.75-meter HAWS level. Reaches CR3, CR4, and CR5 show minimal relative reach scale variability in valley power. No trend existed between the proxy for valley power and locations of aggradation and degradation.

3.2.7 Lulu Creek longitudinal profiles

The high resolution lidar profile from 2012 shows a strong match with local-scale variations in slope from the 2013 field survey, but misses details of bedform geometry (Figure 19A). Less of a comparison can be made between the 2004 lidar and 2010 field profiles, even though the 2010 field profile exhibits less-defined step characteristics than the 2013 field profile (Figure 19B) because the 2010 field survey was before the high intensity, long duration stream flows of 2011 that drastically adjusted step-pool bedforms along Lulu Creek.

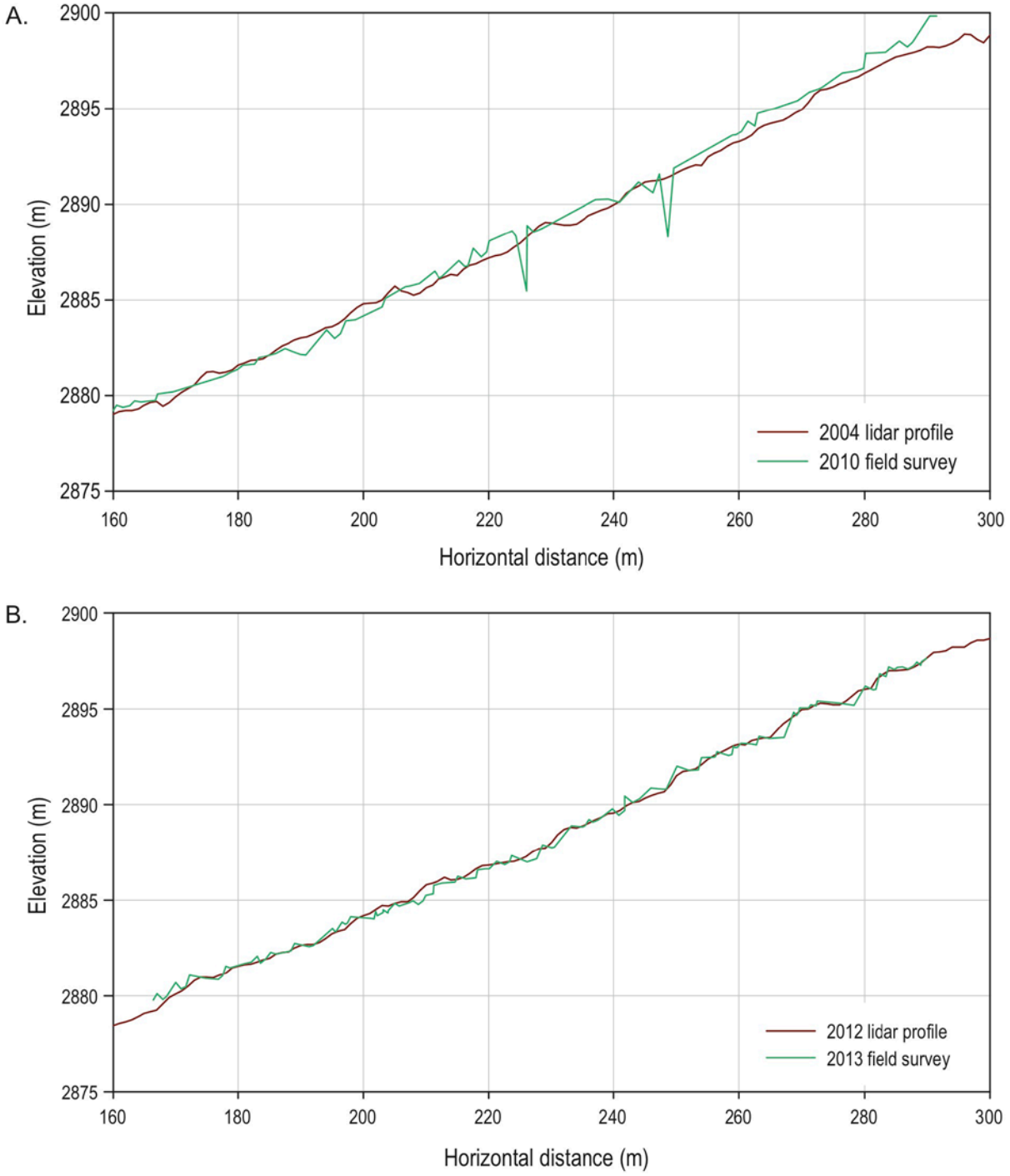

Figure 19: Long profiles along Lulu Creek from lidar and field surveys. A) 2004 lidar profile overlaying the 2010 field survey. B) 2012 lidar profile overlaying the 2013 lidar survey.

3.3 Trends in Morphologic Metrics (Revisiting Morphologic Metric Hypotheses)

3.3.1 Revisiting Hypothesis 1

Hypothesis 1 predicted that aggradational response reaches within the study site between 2004 and 2012 correspond to low valley confinement and low valley slope, whereas erosional reaches correspond to high valley confinement and high valley slope. The one confined reach (determined from field evidence instead of lidar) experienced minor bed degradation, whereas the other confined reaches were a mix of aggradation and degradation. Valley slope continuously decreases along the Colorado River valley, while locations of aggradation and degradation vary downstream, yet aggradational reaches clearly occur in locations where the valley slope was constant as opposed to changing. The data, therefore, partially support hypothesis 1.

3.3.2 Revisiting Hypothesis 2

Hypothesis 2 predicted that locations of avulsions, channel migration, and changes in sinuosity within pool-riffle reaches would most closely correspond to reaches with low valley confinement. Channel migration and a reduction in braiding index occurred in all reaches except for the confined reach CR2. Reach scale sinuosity only decreased in aggradational reaches, which were confined and had constant valley slope. Therefore, the data fully support hypothesis 2.

3.3.3 Revisiting Hypothesis 3

Hypothesis 3 predicted that bankfull width changes within pool-riffle reaches following high stream flows are related to distance from a sediment source. Although there is no clear trend in the direction of change with distance from the Lulu Creek fan along the entire reach, it is clear that a greater magnitude of bankfull width change have occurred closer to the fan, with less pronounced change farther from the fan. Additionally, local controls such as foot bridges and valley confinement likely influence local changes in bankfull width. Overall, the data support hypothesis 3.

3.4 Sediment Budget from Morphologic Inverse Method

Estimating sediment transport rates along the Colorado River using the morphologic inverse method involved developing a sediment budget between 2004 and 2012 from the lidar differencing. The response reaches designated above were the same reaches used for the sediment budget, with four reaches showing a net decrease in sediment and three reaches showing a net increase (Table 3).

One requirement of the inverse method is a location of known sediment transport rates. For this analysis, two methods were used to estimate a known sediment flux. The first assumed that bed material is not transported past the wetland; therefore, a transport rate of zero was applied at the downstream end of the wetland fan and volumetric changes in each reach are incorporated, working upstream. Using this method, a transport rate of approximately zero is predicted at the confluence of the Colorado River and Lulu Creek (Figure 20). Results from this approach seem unreasonable, based on the large amounts of

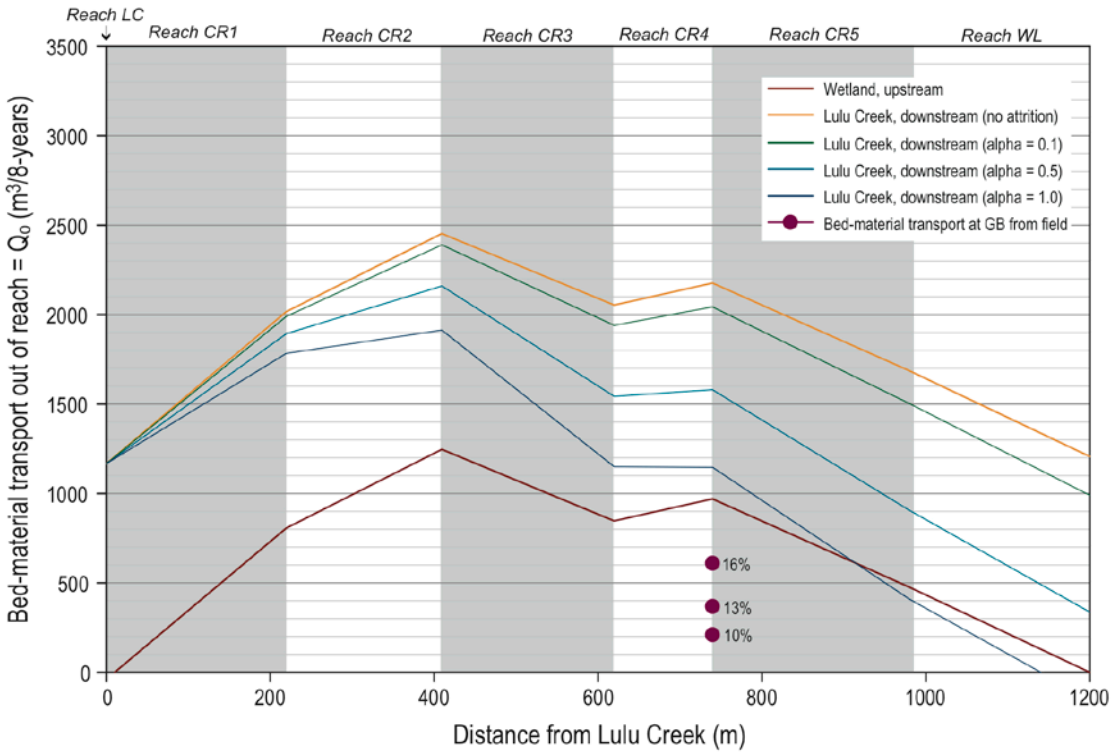

Figure 20: Sediment budget along the Colorado River created using the morphologic inverse method. Bedload from Gravel Beach (GB) gage measurements labeled as the percent applied between the Baker Gulch and Gravel Beach gage discharge measurements for 2011 and 2012. See text for explanations of the different directions and abrasion rates shown above. Plots of the attrition rate α=0.01 plots directly on the 'Lulu Creek down' line, and therefore is not shown.

debris flow material along Lulu Creek that were mobilized and transported into the Colorado River between 2004 and 2012. The second approach treated all material degraded from the Lulu Creek fan (1,556 m^3 from lidar; 1,650 m^3 field measurements) as an input of sediment to the Colorado River and incorporated volumetric changes in the downstream direction. Using this method, the volume of sediment transported beyond the wetland over eight years is predicted to be greater than 1,200 m^3 – approximately the volume of material eroded from the Lulu Creek fan (top orange line, Figure 20).

Accounting for clast attrition reduces the calculated volume of bed material passing the wetland closer to the expected value of zero. An attrition rate of α=0.01-km^{-1} had virtually no effect on reducing bedload over the 1.2-kilometer reach (Appendix D). At α=0.1-km^{-1}, the bed-material transport past the wetland was reduced over 200-m^3, or more than 15% of the originally predicted volume (Figure 20). At α=0.5-km^{-1}, which is the mean value of the sedimentary lithologies from O'Connor et al. (2014), bed-material transport past the wetland was reduced nearly 875-m^3, or more than 70% of the originally predicted volume (Figure 20). At α=0.01-km^{-1}, bed material was reduced to a rate below zero at the wetland.

3.4.1 Comparison to Transport Rates at Gravel Beach Gage

Total bed-material transport over the eight-year period was determined at the Gravel Beach (GB) gage so that comparisons could be made between field-derived transport rates and rates determined from the morphologic inverse method. Both the bed-material rating curve at GB (Figure 21) and the regression analysis between the mean daily discharge at Baker Gulch and GB (Figure 22) show strong relationships, but integrating the sediment transport rates over the snowmelt hydrograph proved sensitive to discharge. A sensitivity analysis between the GB and Baker Gulch gages indicates that slight variations in the relationship between GB and Baker Gulch had a large effect on estimates of bed-material transport at the GB gage (Table 4). Additionally, the exponent value in the sediment rating curve (2.86; Figure 21) is low compared to values of bedload rating curves in other Colorado Rivers, although previous studies occurred

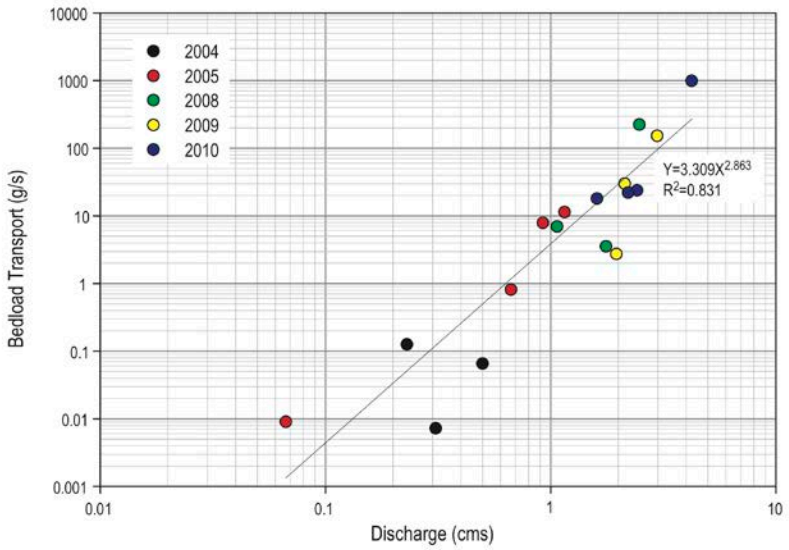

Figure 21: Sediment rating curve at the Gravel Beach gage. Bed-material rates are an accumulation of measurements between 2004-2005 and 2008-2010. (After Rathburn, unpublished data)

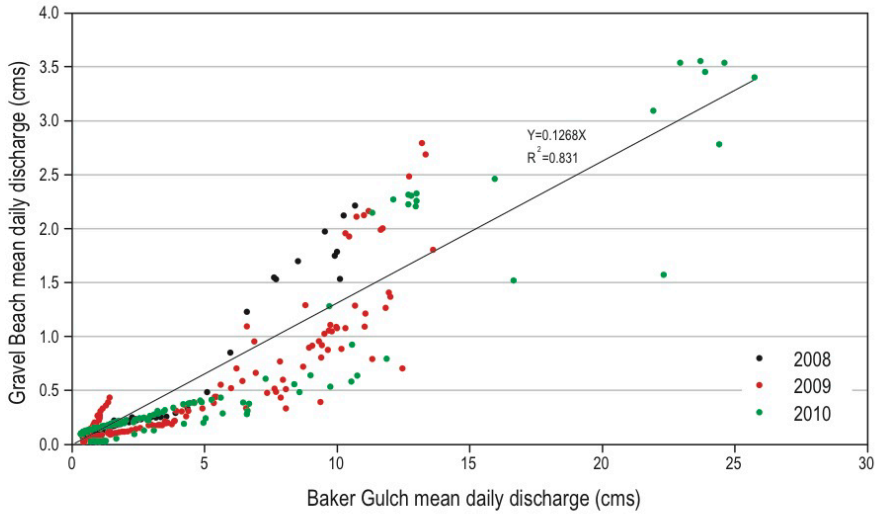

Figure 22: Relationship between the Baker Gulch gage and Gravel Beach gage for all continuous gage measurements at Gravel Beach between 2008-2010.

in larger and wider river systems than this study (Bunte et al., 2004). All estimates of total bed-material transport at the BG gage from field-derived transport rates are less than the values predicted by the inverse method (solid dots, Figure 20), but are within an order of magnitude of the most reasonable estimate (α=0.5).

Table 4: Sensitivity of sediment transport estimates at the Gravel Beach (GB) gage to the relationship between mean daily discharge at the Baker Gulch gage and GB gage. Variations in transport only exist in 2011 as that is the year that lacked continuous gage data and therefore relied on the regressed relationship with the Baker Gulch gage. Bedload transport in 2005 through 2008 were approximated based on visual similarities between snowmelt hydrographs from 2008 or 2012.

	Bedload Transport (m^3)		
	(GB gage discharge as percent of Baker Gulch)		
Year	16%	13%	10%
2005	5.8	5.8	5.8
2006	5.8	5.8	5.8
2007	0.7	0.7	0.7
2008	5.8	5.8	5.8
2009	15.5	15.5	15.5
2010	35.9	35.9	35.9
2011	541.8	299.0	141.1
2012	0.7	0.7	0.7
Total	612.0	369.2	211.2

3.4.2 Estimating Annual Rates from Repeat Cross-sections

Constraining bed-material transport rates to an annual rate using repeat channel cross-sections was only possible at two locations – at the Gravel Beach and Crooked Tree gage sites. These two cross-sections have annual surveys that encompass the two years of major geomorphic change, while all other cross sections lacked annual changes from 2009 to 2011. Annual rates extrapolated from the repeat cross-sections and the morphologic inverse method are still much higher than rates calculated by extrapolating the sediment transport relationship over the entire hydrograph at Gravel Beach (Table 5). The use of one cross-section to determine reach scale changes is unreasonable because changes in cross-sectional area at one location may be far from representative for the entire reach.

3.4.3 Revisiting Hypothesis 4

Hypothesis 4 predicted that bed-material transport quantified by the morphologic inverse method will more closely approximate field measurements of bed-material transport relative to calculated transport rates using applicable transport laws. Although bed-material transport rates predicted by the

Table 5: Changes in cross-sectional area at repeat cross-sections. The percentage of change was used to estimate annual rates of bed-material transport using the morphologic inverse method. In this analysis, it is assumed that all geomorphic changes occurred between 2009-2011. Locations of the Gravel Beach (GB) and Crooked Tree (CT) gages are shown on Figure 2.

Site	Reach	Years	Change in cross-section area	Percent of total change	Inverse Method (no attrition)	Inverse Method (α=0.01)	Inverse Method (α=0.50)
Gravel Beach	CR4	2009-2011	-2.31 m^2	100%	2179 m^3	2043 m^3	1580 m^3
		2009-2010	-0.91 m^2	40%	872 m^3	817 m^3	632 m^3
		2010-2011	-1.40 m^2	60%	1307 m^3	1226 m^3	948 m^3
Crooked Tree	CR1	2009-2011	-0.88 m^2	100%	2454 m^3	2391 m^3	2160 m^3
		2009-2010	-0.12 m^2	13%	319 m^3	311 m^3	281 m^3
		2010-2011	-0.77 m^2	87%	2135 m^3	2080 m^3	1879 m^3

inverse method were higher than field measurements, they are within a similar order of magnitude. Additionally, determining the influence of attrition on bed-material flux along the Colorado River, as well as identifying other possibilities that cause the inverse method to over-predict transport at the wetland, could reduce the difference between field- and inversely-measured rates. Therefore, the data support hypothesis 4.

4. DISCUSSION

4.1 Channel Morphologic Changes

Repeat lidar datasets along the headwaters of the Colorado River following a large sediment input and multiple geomorphically significant flows, including the highest flow on the 59-year record, show that variations exist in local channel response. Heterogeneity in valley morphology, local channel constrictions, and distance from the sediment source strongly influence channel morphologic changes.

4.1.1 Valley Confinement and Local Channel Constrictions

The wide, expansive valley along the upper Colorado River promoted planform changes following an abrupt increase in sediment except within one short, confined reach. Had the entire valley been more confined, the introduced bed-material would likely have been transported downstream, with channel adjustments being less pronounced (Montgomery and Buffington, 1997). The portion of the Colorado River examined in this study shows that only minor morphologic changes occurred in the confined reach CR2, which acted as a transport reach following the initial 2003 debris flow and during the 2009-2011 high flows. Downstream transitions from transport to response reaches commonly define locations where impacts from increased sediment supply may be both pronounced and persistent (Montgomery and Buffington, 1997). Madej and Ozaki (1996) demonstrated that aggradation was highest immediately downstream of an abrupt increase in channel width. This is confirmed along the upper Colorado River, where the first location of abundant aggradation downstream of the sediment source occurs in reach CR3, where increased valley width promotes low transport capacity and room for the river to adjust channel location. Sklar et al. (2009) point out that “dispersion is favored over translation in particular when pulse volumes are large relative to the channel dimensions.” This held true along the unconfined reaches of the Colorado River; the small channel in combination with the large sediment input from upstream promoted aggradation and degradation, as well as channel migration and reductions in braiding index along much of the channel.

In addition to reach-scale valley confinement, local channel constrictions can strongly influence the morphology of a river channel. Pitlick (1993) demonstrated that even a single meander cut-off can be a local control, with abundant sediment deposition upstream of the cut-off and no deposition occurring downstream. Widespread channel changes in reach CR1 were in large part induced by the bridge along the Colorado River, which set up a local control on processes of water and sediment transport and hence created pronounced morphologic changes. In CR2, the existence of another footbridge did not exert a local control on channel processes because the bridge fully spans a confined reach. Locations of resistant or vegetated channel banks can also act as local controls. Studies by Pitlick (1993) and Sutherland et al. (2002) both describe resistant banks that prevented changes in bankfull width. The wide valley floors along most reaches of the Colorado River, in combination with the coarse deposits lining portions of the floodplain from historic debris flows, permitted extensive lateral adjustments to the channel, including changes in bankfull width. Near the Gravel Beach gage, however, a short portion of the channel is flanked by stable, well-vegetated banks that prevented channel adjustments between 2004 and 2012, including the highest discharge of record in 2011.

Introduced in-stream wood enhances channel complexity following a sedimentation event (Bigelow et al., 2007; Andrews, 2010). Vast amounts of wood were introduced from the initial debris flow, and much of that wood still exists within upper portions of Lulu Creek or within the Lulu Creek fan. Transport of that wood into the Colorado River during high flows may promote additional planform changes unless the wood can be adequately transported downstream. Local channel constrictions such as footbridges and cohesive banks may hinder the transport of wood, enhancing the effects of local channel constrictions on planform changes.

4.1.2 Proximity to Sediment Source

Madej and Ozaki (1996) saw greater planform changes closer to a sediment source, with less pronounced changes farther downstream. Changes in bankfull width along the Colorado River were only

distinguishable in unconfined reaches, but greater magnitude of change occurred in reaches closer to the sediment source and less magnitude farther from the source. Additionally, the magnitude of volumetric changes was greatest in reach CR1, the reach closest to the fan.

4.1.3 Continued Sediment Inputs and Timing of Recovery

Rathburn et al. (2013) suggest that the increased frequency of debris flows along the upper Colorado River due to anthropogenic activity will reduce the relaxation time between significant events. Geomorphically significant flows are important for remobilizing and transporting the introduced bed material from the debris flow and returning the channel to a more stable form. Pitlick (1993) notes that the "time it takes for a new equilibrium to be established appears to be quite variable, but it clearly depends on the rate that processes within the watershed continue to supply sediment, and on the types of flows that can move sediment." As time between sedimentation events decreases, the likelihood that a geomorphically significant flow will occur between events is reduced, and cumulative effects from multiple events can persist (Montgomery and Buffington, 1997). Madej and Ozaki (1996) demonstrated that the timing of the sediment pulse along Redwood Creek was slower than other studies, likely because peak flows were low during their twenty years of monitoring. The upper reaches of the Fall River returned to nearly background sediment loads within five years of a catastrophic flood because the system lacked a continued sediment source (most of the original outburst flood deposits were too coarse to be transported by typical snowmelt flows) and higher than average snowmelt occurred the year following the flood (Pitlick, 1993). Along the Colorado River, five years of low stream flows immediately followed the initial debris flow prior to the three geomorphically significant flows, including the highest flow in the 59-year record. Minor channel adjustments occurred during the low flow years, but degradation and entrainment of the stored debris in the Lulu Creek fan during the geomorphically significant flows promoted extensive channel migration and locations of aggradation and degradation in the unconfined reaches. Introduced material from debris flows is commonly coarser than the ambient bed material (Sutherland et al., 2002; Madej and Ozaki,1996), making the geomorphically significant flows key for

transporting the introduced bed material. The continued input of sediment as the Lulu Creek fan degrades in subsequent high flows will continue to promote downstream channel adjustments.

4.1.4 Complex Response

A complex response at the site was clearly discernible from previous repeat channel cross-sections (Rathburn et al., 2013; Appendix E), yet this process was not initially evident from repeat lidar surveys. Frequent repeat cross-sections in Pitlick (1993) showed extensive aggradation followed by degradation along the Colorado River. The lidar surveys along the Colorado only expose planform morphology at two points in time. Multiple high flows occurred between the two lidar surveys, but the 2012 survey only captures the remnant morphology of the 2011 long duration, high intensity flows. It is possible that stream flows in 2009 and 2010 caused incision in reaches that were aggradational in 2003, but those reaches then experienced aggradation again in 2011.

4.2 Bed-material Transport

The geomorphic inverse method is a useful, potentially accurate way to estimate bed-material transport in gravel-bed rivers (Martina and Church, 1995; Ham and Church, 2000; Surian and Cisotto, 2007). As with all bed-material transport estimates, transport estimated using the inverse method includes a degree of uncertainty as a result of multiple factors. Surian and Cisotto (2007) noticed gaps between inputs and outputs in their sediment budget along an Italian gravel-bed river, but attributed those gaps to the large distance between cross-sections and a lack of data regarding in-channel gravel extraction over the last several decades. Fuller et al. (2003) proved that the use of DEMs creates much more constrained transport rates than the cross-section approach. Additionally, the DEM approach shows specific patterns of erosion and deposition, something that is not possible with the cross-section surveys without very closely-spaced cross-sections (Fuller et al., 2003). This study shows that lidar-derived DEMs may be used as a tool in the geomorphic inverse method, yet higher resolution of the lidar is key to constraining error between repeat surveys. Multiple cross-sections per reach or other types of high-resolution repeat surveys

(i.e., terrestrial laser scanning surveys) would have been necessary to extend the interpretation to estimates of annual bed-material flux. Overall, bed-material transport rates obtained by the morphologic inverse method using lidar show greater promise than widely spaced cross sectional surveys.

High levels of attrition may be associated with debris flow material, thereby reducing bed-material transport as the sediment wave moves downstream (Lisle, 2010). Sutherland et al. (2002) noticed that attrition rates of introduced sediment were an order of magnitude higher than the ambient bed material in the river. O'Connor et al. (2014) showed that sedimentary rocks of the Oregon and California Coast Range, where the Sutherland et al. (2002) landslide occurred, have drastically higher attrition rates than all adjacent geologic provinces. In this study, the field-confirmed weakness of the introduced bed material suggests that attrition rates would be high, although tumbler experiments are necessary to constrain the level of attrition. Overall, accounting for the local lithology of debris flow material is important when incorporating attrition into sediment budgets.

4.3 Additional Applications of the Lidar Differencing

Analysis using lidar differencing and the morphologic inverse method could be extended to other geomorphologic applications besides those associated with large sedimentation events. This approach is best suited for areas that experience moderate- to large-scale morphologic changes over both short and long time periods. Investigations of small-scale or very local changes may be better suited for higher-resolution survey equipment such as TLS. In riverine environments, additional uses of the morphologic method may include evaluating channel morphologic adjustments caused by large floods or adjustments in the flow or sediment regimes caused by changing dam operations upstream. Advances in "green" lidar will additionally benefit lidar applications in river research, revealing changes in bedform geometry in addition to planform changes. One underlying difficulty in using lidar differencing in assessing sudden hazards is a likely lack of pre-disturbance topographic data. Some states within the U.S. have recently acknowledged the need for baseline topography by surveying the entire state for use in future analyses.

4.4 Limitations of Lidar

4.4.1 Resolution

The use of lidar in quantitative measurement of channel morphologic change has its limitations. In this study, the resolution of the lidar surveys had a large influence on parts of the analysis. The 2004 lidar survey had half the resolution of the 2012 surface, creating error in the survey that reduced confidence in determining the 2004 water surface slope, HAWS surface, and bankfull widths in several locations. A fuzzy inference system that included point density was applied in the lidar differencing to reduce error when determining vertical changes between surveys, but irregularities in the final DOD surface likely still exist. The steep slope and coarse material along Lulu Creek also made surface formation and metric extraction unreliable. In combination with dense vegetation, all confidence was lost when creating the elevation surface and computing respective morphologic measurements in the disturbed areas farther up Lulu Creek. High-resolution repeat survey options, such as terrestrial laser scanning, may be more appropriate for future work on steep channels such as Lulu Creek, although access to remote sites must be considered. Lastly, higher resolution lidar surveys should be encouraged in reaches were quantitative measurements are desired near a small river or in narrow valleys. Although the vertical resolution of the surveys was adequate, the point density of the 2012 lidar was considered too low for determining sub-meter changes (e.g., an error of 0.5-meter in determining bankfull width measurements is substantial when the channel is only a few meters wide). High-resolution lidar comes at a cost, but acquisition should become easier as technology advances over time.

4.4.2 Field Familiarity

Although the use of lidar formed the basis of this study, field familiarity with the site proved essential in verifying several results of this study. Confidently determining the active floodplain along the Colorado River proved difficult, but this may be more promising on larger channels where distinct slope breaks can be discerned from lidar. This influences the ability to determine if a reach is truly confined.

Grain size distribution, commonly analyzed in studies related to extreme sedimentation events (Miller and Benda, 2000; Madej et al., 2009; Hoffman and Gabet, 2007), also cannot be determined by lidar. Site visits would be required to acquire data on sediment grain size distributions. Knowledge of the characteristics of the debris sediment, such as the hydrothermal alteration that causes in situ disintegration along the Colorado River, is also difficult to predict without field observations or detailed geologic mapping of the source area. Lastly, local channel constrictions caused by footbridges or stable, vegetative banks were difficult to detect from lidar, although they are a major control on channel morphologic changes in this study.

4.5 Future Work

Flow and sediment transport monitoring of the Upper Colorado River should be continued to determine additional channel adjustments following high flows. Repeat cross-section surveys should continue to record elevation changes at previously established locations, especially at locations where channel avulsions occurred at existing gages, creating new channel geometry relationships. Monitoring cross-sections in additional locations along the Colorado River, especially areas that experience major channel adjustments such as reaches CR1 and CR3, could be beneficial in detecting continued complex response. Although acquiring an additional lidar survey in the future is unlikely, other survey methods such as TLS may be combined with the 2012 lidar to detect future spatial patterns in morphologic adjustments. These surveys would also be beneficial for providing baseline conditions prior to restoration efforts. Continued monitoring of the site following restoration efforts will be essential to determine the success of the restoration practices.

5. CONCLUSIONS

This study used airborne lidar surveys to capture channel morphologic conditions immediately following a large debris flow within a mountainous headwater stream to determine controls on geomorphic response and constrain bed-material transport rates during geomorphically significant flows. Along the upper Colorado River, local and reach-scale variations in valley morphology influence locations of aggradation and degradation. Aggradational reaches occurred in locations where the valley was unconfined, yet a degradational reach existed where the valley bottom was the widest and confinement was similar to adjacent aggradational reaches. This suggests local variations in morphology, and the distance from the sediment source, may influence the balance of transport supply and capacity and, therefore, locations of aggradation and degradation. Additionally, a complex response initially seen in repeat cross-sections is broadly supported by lidar differencing, although the differencing captures only the net change over eight years. This complex response is occurring as a result of multiple high flows that occurred between airborne lidar surveys and the presence of a continued sediment source upstream. Channel avulsions, migration, and changes in sinuosity were common in all reaches (both aggradational and degradational) except for a very confined, incised reach. Bankfull width showed greater changes in unconfined reaches closer to the sediment source and smaller changes farther downstream, and in both aggradational and degradational reaches. Although confidence was low in lidar-derived elevation surface on the steep, coarse step-pool channel of Lulu Creek, longitudinal profiles from the higher resolution surface showed local variations in channel slope that mimicked field surveys. Airborne lidar is shown to be a useful tool for extracting metrics of morphologic change, but higher spatial resolution is crucial for stronger confidence in measurements along small, headwater channels.

A sediment budget for the upper Colorado River using lidar differencing identified variation in location and volume of bed-material transport in the eight years between surveys. An initial budget that incorporates reach-scale volumes of aggradation and degradation identifies a net system loss of bed-

material, yet this prediction disagrees with assumptions of transport at the upstream and downstream end of the system. It is assumed that all bed-material input to the system came from the degrading Lulu Creek fan, and that all bed-material output was deposited in the downstream wetland. By accounting for a moderate level of attrition of the weak debris flow material, gaps between expected inputs and outputs were minimized. Bed-material estimates using the geomorphic inverse method were greater than field-measured transport estimates, but the two were within an order of magnitude. This morphologic inverse method approach appears promising, especially if lidar resolution were more similar between sequential surveys. Through the geomorphic inverse method, restoration planners will be able to better understand spatial patterns of bed-material flux and ensure channel designs adequately transport the delivered sediment load, and accommodate processes of aggradation and degradation.

Lidar differencing is a useful tool to assess morphologic changes and bed-material transport following a large sediment flux, especially to help guide future restoration plans that will accommodate the aggradational, degradational and complex response of the upper Colorado River. The differencing, however, relies on field measurements of controlling processes over time. Efforts to use field measurements without lidar will miss the larger spatial and temporal complexities of morphologic adjustments following sediment loading, and applying lidar differencing without field verification may lose sight of local controls on valley and channel geometry.

6. WORKS CITED

Adler, R.W., 2007, Restoring Colorado River ecosystems: a troubled sense of immensity: Washington, D.C., Island Press, 311 p.

Andrews, C., 2010, A stream in transition: Short term morphodynamics of Fishtrap Creek following wildfire [MS thesis]: Vancouver, The University of British Columbia, 142p.

Ashmore, P.E., 1991, Channel morphology and bedload pulses in braided, gravel-bed streams: Geografiska Annaler, v. 73A, no. 1, p. 37-52.

Ashmore, P. E., and Church, M.A., 1998, Sediment transport and river morphology: A paradigm for study *in* Klingeman, P.C., Beschta, R.L., Komar, P.D., and Bradley, J.B., eds., Gravel-bed rivers in the environment: Highlands Ranch, Colorado, Water Resources Publications, p. 115-148.

Benda, L., and Dune, T., 1997, Stochastic forcing of sediment supply to channel networks from landsliding and debrs flow: Water Resources Research, v. 33, p. 2865-2880.

Bigelow, P.E., Benda, L.E., Miller, D.J., and Burnett, K.M., 2007, On debris flows, river networks, and the spatial structure of channel morphology: Forest Science, v. 52, no. 2, p. 220-238.

Brasington, J., Langham, J., and Rumsby, B., 2002, Methodological sensitivity of morphometric estimates of coarse fluvial sediment transport: Geomorphology, v. 53, p. 299-316.

Brewer, P.A., and Passmore, D.G., 2002, Sediment budgeting techniques in gravel-bed rivers *in* Jones, S.J., and Frostick, L.E., eds., Sediment Flux to Basins: Causes, Controls, and Consequences: London, UK, Geological Society of London, p. 97-113.

Buffington, J.M., 2012, Changes in channel morphology over human time scales *in* Church, M., Biron, P.M., and Roy, A.G., eds., Gravel-bed rivers: Processes, tools, environments: Chichester, UK, John Wiley & Sons, Ltd., p. 435-463.

Bunte, K., Abt, S.R., Potyondy, J.P., and Ryan, S.E., 2004, Measurement of course gravel and cobble transport using portable bedload traps: Journal of Hydraulic Engineering, v. 130, no. 9, p. 879-893.

Capesius, J.P., and Stephens, V.C., 2010, Regional regression equations for estimation of natural streamflow statistics in Colorado: U.S. Geological Survey Scientific Investigations Report 2009-5136, 46 p.

Cavalli, M., Trevisani, S., Comiti, F., and Marchi, L., 2013, Geomorphometric assessment of spatial sediment connectivity in small Alpine catchments: Geomorphology, vol. 188, p. 31-41.

Cavalli, M., Tarolli, P., Marchi, L., and Dalla Fontana, G., 2008, The effectiveness of airborne LiDAR data in the recognition of channel-bed morphology: Catena, v. 73, p. 249-260.

Church, M., 2006, Bed material transport and the morphology of alluvial river channels: Annual Review of Earth and Planetary Sciences, v. 34, p. 325-354.

Clayton, J.A., and Westbrook, C.J., 2008, The effect of the Grand Ditch on the abundance of benthic invertebrates in the Colorado River, Rocky Mountain National Park: River Research and Applications, v. 24, p. 975-987.

Cole, J.C., and Braddock, W.A., 2009, Geologic map of the Estes Park 30' x 60' quadrangle, north-central Colorado: U.S. Geological Survey Scientific Investigations Map 3039, 1 sheet, scale 1:100,000, 56 p. text.

Costa, J.E. and O'Connor, J.E., 1995, Geomorphically effective floods *in* Costa, J.E., Miller, A.J., Potter, K.W., and Wilcock, P.R., eds., Natural and anthropogenic influence in fluvial geomorphology: Washington, D.C., American Geophysical Union Geophysical Monograph, v. 89, p. 45-56.

Elliott, J.G., and Capesius, J.P., 2009, Geomorphic changes resulting from floods in reconfigured gravel-bed channels in Colorado, USA, *In* Management and Restoration of Fluvial Systems with Broad Historical Changes and Human Impacts, James, A.J., Rathburn, S.L., and Whittecar, G.R., eds., Geological Society of American Special Paper, 451, p. 173-198.

Fitzpatrick, F.A., Knox, J.A., and Schubauer-Berigan, J.P., 2009, Channel, floodplain, and wetland responses to floods and overbank sedimentation, 1846-2006, Halfway Creek Marsh, Upper Mississippi Valley, Wisconsin, *In* Management and Restoration of Fluvial Systems with Broad Historical Changes and Human Impacts, James, A.J., Rathburn, S.L., and Whittecar, G.R., eds., Geological Society of American Special Paper, 451, p. 23-42.

French, J.R., 2002, Airborne LiDAR in support of geomorphological and hydraulic modeling: Earth Surface Processes and Landforms, v. 28, p. 321-335.

Fuller, I.C., Large, A.R.G., Charlton, M.E., Heritage, G.L., and Milan, D.J., 2003, Reach-scale sediment transfers: an evaluation of two morphological budgeting approaches: Earth Surface Processes and Landforms, v. 28, p. 889-903.

Gaeuman, D.A., and Schmidt, J.C., 2003, Evaluation of in-channel gravel storage with morphology-based gravel budgets developed from planimetric data: Journal of Geophysical Research, v. 108, no. F1.

Graf, W.L., 2001, Damage control: Restoring the physical integrity of American's Rivers: Annals of the Associate of American Geographers, v. 91, no. 1, p. 1-27.

Grimsley, K.J., 2012, A debris flow chronology and analysis of controls on debris flow occurrence in the Upper Colorado River valley, Rocky Mountain National Park, CO [MS thesis]: Fort Collins, Colorado State University, 97 p.

Ham, D.G., and Church, M., 2000, Bed-material transport estimated from channel morphodynamics: Chilliwack River, British Columbia: Earth Surface Processes and Landforms, v. 25, p. 1123-1142.

Hoffman, D.F., and Gabet, E.J., 2007, Effects of sediment pulses on channel morphology in a gravel-bed river: Geological Society of America Bulletin, v. 119, no. 1/2, p. 116-125.

Humpries, R., Vendetti, J.G., Sklar, L.S., and Wooster, J.K., 2012, Experimental evidence for the effect of hydrographs on sediment pulse dynamics in gravel-bedded rivers: Water Resources Research, v. 48, W01533, 15 p.

James, L.A., Watson, D.G., and Hansen, W.F., 2007, Using LiDAR data to map gullies and headwater streams under forest canopy: South Carolina, USA: Catena, v. 71, p. 132-144.

James, L.A., Hodgson, M.E., Ghoshal, S., and Latiolias, M.M., 2011, Geomorphic change detection using historic maps and DEM differencing: The temporal dimension of geospatial analysis: Geomorphology, vol. 137, p. 181-198.

Jones, J.L., 2006, Side channel mapping and fish habitat suitability analysis using lidar topography and orthophotography: Photogrammetric Engineering and Remote Sensing, p. 1202-1206.

Jones, A.F., Brewer, P.A., Johnstone, E., and Macklin, M.G., 2007, High-resolution interpretive geomorphological mapping of river valley environments using airborne LiDAR data: Earth Surface Processes and Landforms, v. 32, p. 1574-1592.

Jones, K.L., Poole, G.C., O'Daniel, S.J., Mertes, L.A.K., and Stanford, J.A., 2008, Surface hydrology of low-relief landscapes: Assessing surface water flow impendence using LiDAR-derived digital elevation models: Remote Sensing of Environment, v. 112, p. 4148-4158.

Kondolf, G.M., Boulton, A.J., O'Daniel, S., Poole, G.C., Rahel, F.J., Stanley, E.H., Wohl, E., Bång, A., Carlstrom, J., Cristoni, C., Huber, H., Koljonen, S., Louhi, P., and Nakamura, K., 2006, Process-based ecological river restoration: visualizing three-dimensional connectivity and dynamic vectors to recover lost linkages: Ecology and Society, v. 11, no. 2, art. 5, [online] URL: http://www.ecologyandsociety.org/vol11/iss2/art5/

Knighton, D.K., 1998, Fluvial Forms and Processes: A New Perspective: London, Arnold, 383 p.

Lane, S.N., 2000, The measurement of river channel morphology using digital photogrammetry: Photogrammetric Record, v. 16, no. 96, p. 937-961.

Lisle, T.E., 2010, The evolution of sediment waves influenced by varying transport capacity in heterogeneous rivers, *in* Gravel-bed Rivers VI: From Process Understanding to River Restoration, Habersack, H., Piegay, H., and Rinaldi, M., eds., Elsevier, p. 443-469.

Madej, M.A., 2001, Development of channel organization and roughness following sediment pulses in single-thread, gravel bed rivers: Water Resources Research, v. 37, no. 8, p. 2259-2272.

Madej, M.A., and Ozaki, V., 1996, Channel response to sediment wave propagation and movement, Redwood Creek, California, USA: Earth Surface Processes and Landforms, v. 21, p. 911-927.

Madej, M.A., Sutherland, D.G., Lisle, T.E., and Pryor, B., 2009, Channel responses to varying sediment input: A flume experiment modeled after Redwood Creek, California: Geomorphology, v. 103, p. 507-509.

Marcus, W.A., and Fonstad, M.A., 2010, Remote sensing of rivers: the emergence of a subdiscipline in the river sciences: Earth Surface Processes and Landforms, v. 35, p. 1867-1872.

Marks, K., and Bates, P., 2000, Integration of high-resolution topographic data with floodplain flow models: Hydrologic Processes, v. 14, p. 2109-2122.

Martin, Y., and Church, M., 1995, Bed-material transport estimated from channel surveys, Vedder River, British Columbia: Earth Surface Processes and Landforms, v. 20, p. 347-361.

Megahan, W.F., Platts, W.S., and Kulesza, B., 1980, Riverbed improves over time: South Fork Salmon River *in* Symposium on Watershed Management, Boise ID, 21-23 July: American Society of Civil Engineers, New York, p. 380-395.

Merrick and Company, 2013, CSU RMNP, Grand Ditch area of Rocky Mountain National Park, Colorado, LiDAR mapping report: Merrick and Company Job number 65217542, Aurora, CO.

Milan, D.J., Heritage, G.L., Large, A.R.G., and Fuller, I.C., 2011, Filtering spatial error from DEMs: Implications for morphological change estimation: Geomorphology, v. 125, p. 160-171.

Miller, D.J., and Benda, L.E., 2000, Effects of punctuated sediment supply on valley-floor landforms and sediment transport: Geological Society of American Bulliten, v. 112, p. 1814-1824.

Montgomery, D.R., and Buffington, J.M., 1997, Channel-reach morphology in mountain drainage basins: Geological Society of America Bulletin, v. 109, no. 5, p. 596-611.

Notebaert, B., Verstraeten, G., Govers, G., and Poesen, J., 2008, Qualitative and quantitative applications of LiDAR imagery in fluvial geomorphology: Earth Surface Processes and Landforms, v. 34, p 217-231.

O'Connor, J.E., Mangano, J.F., Anderson, S.W., Wallick, J.R., Jones, K.L., and Keith, M.K., 2014, Geologic and physiographic controls on bed-material yield, transport, and channel morphology for alluvial and bedrock rivers, western Oregon: Geological Society of America Bulletin, v. 126, no. 3/4, p. 377-397.

Picco, L., Mao, L., Cavalli, M., Buzzi, E., Rainato, R., and Lenzi, M.A., 2013, Evaluating short-term morphologic changes in a gravel-bed braided river using terrestrial laser scanner: Geomorphology, v. 201, p. 323-334.

Pitlick, J., 1993, Response and recovery of a subalpine stream following a catastrophic flood: Geological Society of America Bulletin, v. 105, p.657-670.

Poff, N.L., Allan, J.D., Bain, M.B., Karr, J.R., Prestegaard, K.L., Richter, B.D., Sparks, R.E., and Stromberg, J.C., 1997, The natural flow regime: BioScience, v. 47, no. 11, p 769-784.

Rathburn, S.L., and Wohl, E.E., 2003, Predicting fine sediment dynamics along a pool-riffle mountain channel: Geomorphology, v. 55, p. 111-124.

Rathburn, S.L., Rubin, Z.K., and Wohl, E.E., 2013, Evaluating channel response to an extreme sedimentation event in the context of historical range of variability: Upper Colorado River, USA: Earth Surface Processes and Landforms, v. 38, p. 391-406.

Rubin, Z.K., 2010, Post-glacial valley evolution and post-disturbance channel response as a context for restoration, upper Colorado River, Rocky Mountain National Park [MS thesis]: Fort Collins, Colorado State University, 101 p.

Rubin, Z.K., Rathburn, S.L., Wohl, E.E., and Harry, D.H., 2012, Historic range of variability in geomorphic processes as a context for restoration: Rocky Mountain National Park, Colorado, USA: Earth Surface Processes and Lanforms, v. 37, p. 209-222.

Rumsby, B.T., Brasington, J., Langham, J.S., McLelland, S.J., Middleton, R., and Rollinson, G., 2008, Monitoring and modeling particle and reach-scale morphological change in gravel-bed rivers: Applications and challenges: Geomorphology, v. 93, p. 40-54.

Scheidl, C., Rickenmann, D., and Chiari, M., 2008, The use of airborne LiDAR data for the analysis of debris flow events in Switzerland: Natural Hazards and Earth System Sciences, v. 8, p. 1113-1127.

Schumm, S.A., 1973, Geomorphic thresholds and complex response of drainage systems *in* Morisawa, M., ed., Fluvial geomorphology: SUNY Binghamton Publications in Geomorphology, 299-310.

Sklar, L.S., Fadde, J., Venditti, J.G., Nelson, P., Wydzga, M.A., Cui, Y., and Dietrich, W.E., 2009, Translation and dispersion of sediment pulses in flume experiment simularing gravel augmentation below dams: Water Resources Research, v. 45, W08439, 14 p.

Smith, M.J., and Pain, C.F., 2009, Applications of remote sensing in geomorphology: Progress in Physical Geography, v. 34, no. 4, p. 568-582.

Snyder, N.P., 2009, Studying stream morphology with airborne laser elevation data: EOS, v. 90, no. 6, p. 45-46.

Spectrum Mapping, LLC, 2004, Rocky Mountain National Park Project Report: for contract 14040033, Denver, CO.

Sternberg, H., 1875, Untersuchungen uber Langen-und Querprofil geschienbefuhrender Flusse: Zeitschrift für Bauwesen, v. 25, p. 483-506.

Surian, N., and Cisotto, A., 2007, Channel adjustments, bedload transport and sediment sources in a gravel-bed river, Brenta River, Italy: Earth Surface Processes and Landforms, v. 32, p. 1641-1656.

Sutherland, D.G., Hansler, M.E., Hilton, S., Lisle, T.E., 2002, Evolution of a landslide-induced sediment wave in the Navarro River, California: Geological Society of American Bulliten, v. 114, p. 1036-1048.

Wheaton, J.M., Brasington, J., Darby, S.E., and Sear, D.A., 2010, Accounting for uncertainty in DEMs from repeat topographic surveys: improved sediment budgets: Earth Surface Processes and Landforms, v. 35, p. 136-156.

Wilson, J.P., 2011, Digital terrain modeling: Geomorphology, v. 137, p. 107-122.

Wohl, E.E., 2011, What should these rivers look like? Historical range of variability and human impacts in the Colorado Front Range, USA: Earth Surface Processes and Landforms, v. 36, p. 1378-1390.

Wohl, E.E., 2014, Rivers in the Landscape: Chichester, UK, Wiley Blackwell.

Wohl, E.E., and Cenderelli, D.A., 2000, Sediment deposition and transport patters following a reservoir sediment release: Water Resources Research, v. 36, p. 319-333.

Wohl, E.E., Angermeier, P.L., Bledsoe, B., Kondolf, G.M., MacDonnell, L., Merritt, D.M., Palmer, M.A., Poff, N.L., and Tarboton, D., 2005, River restoration: Water Resources Research, v. 42, W10301.

Woods, S.W., 2000, Hydrologic effects of the Grand Ditch on streams and wetlands in Rocky Mountain National Park, Colorado [MS thesis]: Fort Collins, Colorado State University, 219 p.

APPENDIX A: VERTICAL ADJUSTMENT OF LIDAR

RMSE FOR VERTICAL ADJUSTMENT OF 2004 LIDAR SURFACE

					10.8676	<-- 2004 Z_adjust			
Polygon ID	Latitude (m)	Longitude (m)	Z_2004	Z_2012	2004_new	2012-2004	abs(2012-2004)	$(2012-2004)^2$	
1	4478593.8	428053.8	2880.578	2891.188	2891.4456	-0.2576	0.2576	0.06636	
2	4478576.0	428155.6	2866.756	2877.368	2877.6236	-0.2556	0.2556	0.06533	
3	4478421.6	428186.4	2853.439	2864.137	2864.3066	-0.1696	0.1696	0.02876	
4	4477553.4	427970.3	2832.793	2843.524	2843.6606	-0.1366	0.1366	0.01866	
5	4478568.0	428218.7	2859.733	2870.486	2870.6006	-0.1146	0.1146	0.01313	
6	4478050.7	428012.0	2851.086	2861.841	2861.9536	-0.1126	0.1126	0.01268	
7	4477321.0	428105.0	2829.421	2840.199	2840.2886	-0.0896	0.0896	0.00803	
8	4477104.0	427868.1	2825.976	2836.766	2836.8436	-0.0776	0.0776	0.00602	
9	4477793.7	428161.6	2837.314	2848.126	2848.1816	-0.0556	0.0556	0.00309	
10	4477728.5	428013.8	2835.27	2846.134	2846.1376	-0.0036	0.0036	0.00001	
11	4477873.2	428085.3	2837.302	2848.226	2848.1696	0.0564	0.0564	0.00318	
12	4478229.3	428066.8	2845.933	2856.887	2856.8006	0.0864	0.0864	0.00746	
13	4477988.4	428090.2	2840.812	2851.773	2851.6796	0.0934	0.0934	0.00872	
14	4478075.7	428064.7	2841.975	2852.936	2852.8426	0.0934	0.0934	0.00872	
15	4477666.1	428121.9	2840.975	2851.938	2851.8426	0.0954	0.0954	0.00910	
16	4477569.1	428166.5	2848.34	2859.309	2859.2076	0.1014	0.1014	0.01028	
17	4476971.1	427947.8	2828.948	2839.959	2839.8156	0.1434	0.1434	0.02056	
18	4477532.2	428057.0	2834.612	2845.637	2845.4796	0.1574	0.1574	0.02477	
19	4476893.1	427738.5	2824.754	2835.832	2835.6216	0.2104	0.2104	0.04427	
20	4476788.6	427795.3	2823.148	2834.251	2834.0156	0.2354	0.2354	0.05541	
								0.41457	Sum
						-1.50931E-10	0.1273	0.02073	Average
								0.14397	RMSE

APPENDIX B: FUZZY INFERENCE SYSTEM CODE

Final fuzzy inference system script used in geomorphic change detection software.

```
[System]
Name='TS_2Input_PD_SLP'
Type='mamdani'
Version=2.0
NumInputs=2
NumOutputs=1
NumRules=9
AndMethod='min'
OrMethod='max'
ImpMethod='min'
AggMethod='max'
DefuzzMethod='centroid'

[Input1]
Name='Slope'
Range=[0 10000]
NumMFs=3
MF1='Low':'trapmf',[0 0 5 10]
MF2='Medium':'trapmf',[5 10 15 20]
MF3='High':'trapmf',[15 20 10000 10000]

[Input2]
Name='PointDensity'
Range=[0 100]
NumMFs=3
MF1='Low':'trapmf',[0 0 0.1 0.25]
MF2='Medium':'trapmf',[0.1 0.25 0.75 1]
MF3='High':'trapmf',[0.75 1 100 100]

[Output1]
Name='ElevUncertainty'
Range=[0 1.5]
NumMFs=4
MF1='Low':'trapmf',[0 0 0.02 0.04]
MF2='Average':'trapmf',[0.02 0.04 0.06 0.08]
MF3='High':'trapmf',[0.06 0.08 0.18 0.25]
MF4='Extreme':'trapmf',[0.18 0.25 1.5 1.5]

[Rules]
1 1, 3 (1) : 1
1 2, 2 (1) : 1
1 3, 1 (1) : 1
2 1, 3 (1) : 1
2 2, 2 (1) : 1
2 3, 1 (1) : 1
3 1, 4 (1) : 1
3 2, 3 (1) : 1
3 3, 2 (1) : 1
```

APPENDIX C: BANKFULL WIDTH DATA AND REPRESENTATIVE CROSS-SECTIONS

BANKFULL WIDTH ANALYSIS DATA

TransectID	Distance from Lulu	Reach	2004RB	2004LB	2004Rank	2004Error	2004Max	2004Width	2004Min	2012RB	2012LB	2012Rank	2012Error	2012Max	2012Width	2012Min	2012-2004	abs(2012-2004)	Error Sum	Error less than difference 1=yes, 0=no
--	(m)	--	(Units of 0.2m)		--	(m)	(m)	(m)	(m)	(Units of 0.2m)		--	(m)	(m)	(m)	(m)	(m)	(m)	(m)	
95	980	5	181	93	1	0.5	18.1	17.6	17.1	198	87	1	0.5	22.7	22.2	21.7	4.6	4.6	1	1
96	970	5	357	282	1	0.5	19.5	19	18.5	388	267	1	0.5	20.7	20.2	19.7	1.2	1.2	1	1
97	960	5	510	446	2	1	13.8	12.8	11.8	529	442	1	0.5	17.9	17.4	16.9	4.6	4.6	1.5	1
99	940	5	838	758	1	0.5	16.5	16	15.5	845	747	1	0.5	20.1	19.6	19.1	3.6	3.6	1	1
100	930	5	980	893	2	1	18.4	17.4	16.4	995	891	2	1	19.8	18.8	17.8	1.4	1.4	2	0
101	920	5	1135	1039	2	1	20.2	19.2	18.2	1135	1041	2	1	19.8	18.8	17.8	-0.4	0.4	2	0
102	910	5	1320	1217	2	1	21.6	20.6	19.6	1309	1210	2	1	20.8	19.8	18.8	-0.8	0.8	2	0
106	870	5	1938	1819	2	1	24.8	23.8	22.8	1943	1831	2	1	23.4	22.4	21.4	-1.4	1.4	2	0
107	860	5	2123	2006	1	0.5	23.9	23.4	22.9	2124	2006	1	0.5	24.1	23.6	23.1	0.2	0.2	1	0
108	850	5	2330	2165	2	1	28	27	26	2333	2197	2	1	28.2	27.2	26.2	0.2	0.2	2	0
109	840	5	2508	2409	2	1	20.8	19.8	18.8	2507	2406	1	0.5	20.7	20.2	19.7	0.4	0.4	1.5	0
110	830	5	2721	2626	2	1	20	19	18	2709	2630	2	1	16.8	15.8	14.8	-3.2	3.2	2	1
111	820	5	2943	2806	2	1	28.4	27.4	26.4	2938	2812	2	1	26.2	25.2	24.2	-2.2	2.2	2	1
112	810	5	3146	3007	1	0.5	28.3	27.8	27.3	3144	3009	2	1	28	27	26	-0.8	0.8	1.5	0
113	800	5	3305	3189	2	1	24.2	23.2	22.2	3307	3184	2	1	25.6	24.6	23.6	1.4	1.4	2	0
114	790	5	3475	3358	1	0.5	23.9	23.4	22.9	3470	3363	2	1	22.4	21.4	20.4	-2	2	1.5	1
116	770	5	3706	3624	1	0.5	16.9	16.4	15.9	3710	3617	2	1	19.6	18.6	17.6	2.2	2.2	1.5	1
118	750	5	3979	3918	1	0.5	12.7	12.2	11.7	3974	3920	1	0.5	11.3	10.8	10.3	-1.4	1.4	1	1
119	740	4	4107	4027	2	1	17	16	15	4116	4025	1	0.5	18.7	18.2	17.7	2.2	2.2	1.5	1
120	730	4	4254	4143	1	0.5	22.7	22.2	21.7	4240	4141	1	0.5	20.3	19.8	19.3	-2.4	2.4	1	1
121	720	4	4408	4292	1	0.5	23.7	23.2	22.7	4409	4281	1	0.5	26.1	25.6	25.1	2.4	2.4	1	1
122	710	4	4554	4447	2	1	22.4	21.4	20.4	4560	4441	2	1	24.8	23.8	22.8	2.4	2.4	2	1
125	680	4	4950	4865	2	1	18	17	16	4950	4852	2	1	20.6	19.6	18.6	2.6	2.6	2	1
126	670	4	5080	4985	1	0.5	19.5	19	18.5	5081	4973	1	0.5	22.1	21.6	21.1	2.6	2.6	1	1
127	660	4	5209	5113	1	0.5	19.7	19.2	18.7	5208	5116	1	0.5	18.9	18.4	17.9	-0.8	0.8	1	0
131	620	3	5694	5602	1	0.5	18.9	18.4	17.9	5697	5604	1	0.5	19.1	18.6	18.1	0.2	0.2	1	0
132	610	3	5836	5722	1	0.5	23.3	22.8	22.3	5842	5740	2	1	21.4	20.4	19.4	-2.4	2.4	1.5	1
133	600	3	5985	5880	2	1	22	21	20	5986	5853	2	1	27.4	26.4	25.4	5.4	5.4	2	1
135	580	3	6215	6107	2	1	22.6	21.6	20.6	6215	6091	2	1	25.8	24.8	23.8	3.2	3.2	2	1
137	560	3	6439	6362	2	1	16.4	15.4	14.4	6450	6360	2	1	19	18	17	2.6	2.6	2	1
139	540	3	6694	6564	1	0.5	20.5	20	19.5	6703	6589	1	0.5	23.3	22.8	22.3	2.8	2.8	1	1
143	500	3	7225	7147	2	1	16.6	15.6	14.6	7203	7154	2	1	10.8	9.8	8.8	-5.8	5.8	2	1
144	490	3	7334	7249	1	0.5	17.5	17	16.5	7316	7275	1	0.5	8.7	8.2	7.7	-8.8	8.8	1	1
145	480	3	7435	7368	1	0.5	13.9	13.4	12.9	7440	7371	1	0.5	14.3	13.8	13.3	0.4	0.4	1	0
146	470	3	7547	7479	1	0.5	14.1	13.6	13.1	7561	7502	1	0.5	12.3	11.8	11.3	-1.8	1.8	1	1
147	460	3	7727	7625	2	1	21.4	20.4	19.4	7730	7655	1	0.5	15.5	15	14.5	-5.4	5.4	1.5	1
149	440	3	8037	7969	1	0.5	14.1	13.6	13.1	8062	8045	1	0.5	9.9	9.4	8.9	-4.2	4.2	1	1
150	430	3	8236	8139	2	1	21	20	19	8245	8169	2	1	16.2	15.2	14.2	-4.8	4.8	2	1
152	410	2	8480	8434	1	0.5	9.7	9.2	8.7	8484	8436	1	0.5	10.1	9.6	9.1	0.4	0.4	1	0
153	400	2	8579	8529	1	0.5	10.5	10	9.5	8587	8532	1	0.5	11.5	11	10.5	1	1	1	0
154	390	2	8672	8622	1	0.5	10.5	10	9.5	8689	8616	1	0.5	11.1	10.6	10.1	0.6	0.6	1	0
155	380	2	8743	8667	2	1	10.2	9.2	8.2	8740	8669	1	0.5	8.7	8.2	7.7	-1	1	1.5	0
156	370	2	8804	8768	1	0.5	7.7	7.2	6.7	8803	8770	1	0.5	7.1	6.6	6.1	-0.6	0.6	1	0
157	360	2	8870	8834	1	0.5	7.7	7.2	6.7	8874	8836	1	0.5	8.1	7.6	7.1	0.4	0.4	1	0
158	350	2	8855	8865	2	1	13	12	11	8938	8895	1	0.5	9.1	8.6	8.1	-3.4	3.4	1.5	1
159	340	2	9001	8962	1	0.5	8.3	7.8	7.3	9002	8962	1	0.5	8.5	8	7.5	0.2	0.2	1	0
160	330	2	9093	9032	1	0.5	12.7	12.2	11.7	9090	9036	1	0.5	11.3	10.8	10.3	-1.4	1.4	1	1
161	320	2	9140	9103	1	0.5	7.9	7.4	6.9	9142	9102	1	0.5	8.5	8	7.5	0.6	0.6	1	0
162	310	2	9222	9160	2	1	13.4	12.4	11.4	9217	9162	1	0.5	11.5	11	10.5	-1.4	1.4	1.5	0

BANKFULL WIDTH ANALYSIS DATA (CONT.)

TransectID	Distance from Lulu	Reach	2004RB	2004LB	2004Rank	2004Error	2004Max	2004Width	2004Min	2012RB	2012LB	2012Rank	2012Error	2012Max	2012Width	2012Min	2012-2004	abs(2012-2004)	Error Sum	Error less than difference
--	(m)	--	(Units of 0.2m)		--	(m)	(m)	(m)	(m)	(Units of 0.2m)		--	(m)	(m)	(m)	(m)	(m)	(m)	(m)	1=yes, 0=no
163	300	2	9291	9241	1	0.5	10.5	10	9.5	9296	9245	1	0.5	10.7	10.2	9.7	0.2	0.2	1	0
164	290	2	9372	9313	1	0.5	12.3	11.8	11.3	9375	9321	1	0.5	11.3	10.8	10.3	-1	1	1	0
167	260	2	9609	9566	1	0.5	9.1	8.6	8.1	9615	9558	1	0.5	11.9	11.4	10.9	2.8	2.8	1	1
168	250	2	9710	9639	1	0.5	14.7	14.2	13.7	9706	9630	1	0.5	15.7	15.2	14.7	1	1	1	0
169	240	2	9802	9736	1	0.5	13.7	13.2	12.7	9835	9730	1	0.5	21.5	21	20.5	7.8	7.8	1	1
170	230	2	9924	9850	1	0.5	15.3	14.8	14.3	9931	9848	2	1	17.6	16.6	15.6	1.8	1.8	1.5	1
174	190	1	10422	10341	2	1	17.2	16.2	15.2	10423	10292	1	0.5	26.7	26.2	25.7	10	10	1.5	1
175	180	1	10574	10465	2	1	22.8	21.8	20.8	10579	10438	1	0.5	28.7	28.2	27.7	6.4	6.4	1.5	1
176	170	1	10737	10616	1	0.5	24.7	24.2	23.7	10740	10600	1	0.5	28.5	28	27.5	3.8	3.8	1	1
177	160	1	10890	10760	2	1	27	26	25	10891	10771	2	1	25	24	23	-2	2	2	0
181	120	1	11531	11424	2	1	22.4	21.4	20.4	11537	11411	2	1	26.2	25.2	24.2	3.8	3.8	2	1
182	110	1	11629	11542	2	1	18.4	17.4	16.4	11648	11568	1	0.5	16.5	16	15.5	-1.4	1.4	1.5	0
183	100	1	11764	11696	1	0.5	14.1	13.6	13.1	11766	11714	1	0.5	10.9	10.4	9.9	-3.2	3.2	1	1
184	90	1	11923	11798	1	0.5	25.5	25	24.5	11925	11830	1	0.5	19.5	19	18.5	-6	6	1	1
185	80	1	12098	11986	2	1	23.4	22.4	21.4	12105	12024	1	0.5	16.7	16.2	15.7	-6.2	6.2	1.5	1
186	70	1	12281	12155	1	0.5	25.7	25.2	24.7	12286	12190	1	0.5	19.7	19.2	18.7	-6	6	1	1
187	60	1	12449	12331	1	0.5	24.1	23.6	23.1	12460	12388	2	1	15.4	14.4	13.4	-9.2	9.2	1.5	1
188	50	1	12547	12488	1	0.5	12.3	11.8	11.3	12620	12535	2	1	18	17	16	5.2	5.2	1.5	1
189	40	1	12667	12587	1	0.5	16.5	16	15.5	12690	12625	2	1	14	13	12	-3	3	1.5	1
192	10	1	12930	12869	1	0.5	12.7	12.2	11.7	12930	12879	1	0.5	10.7	10.2	9.7	-2	2	1	1

Representative lidar-derived cross-section plots

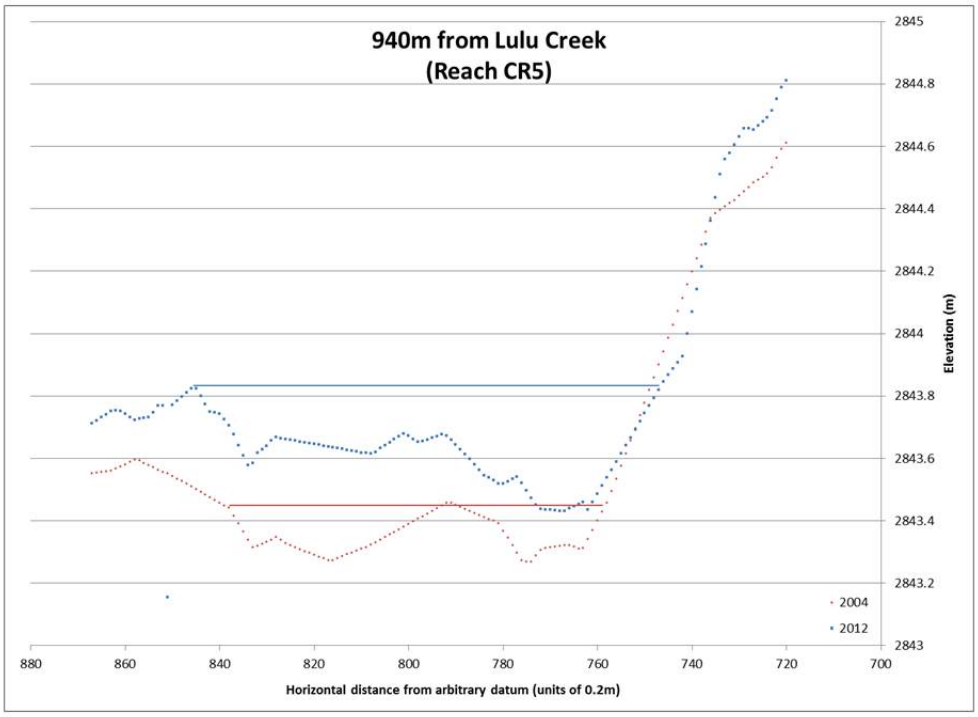

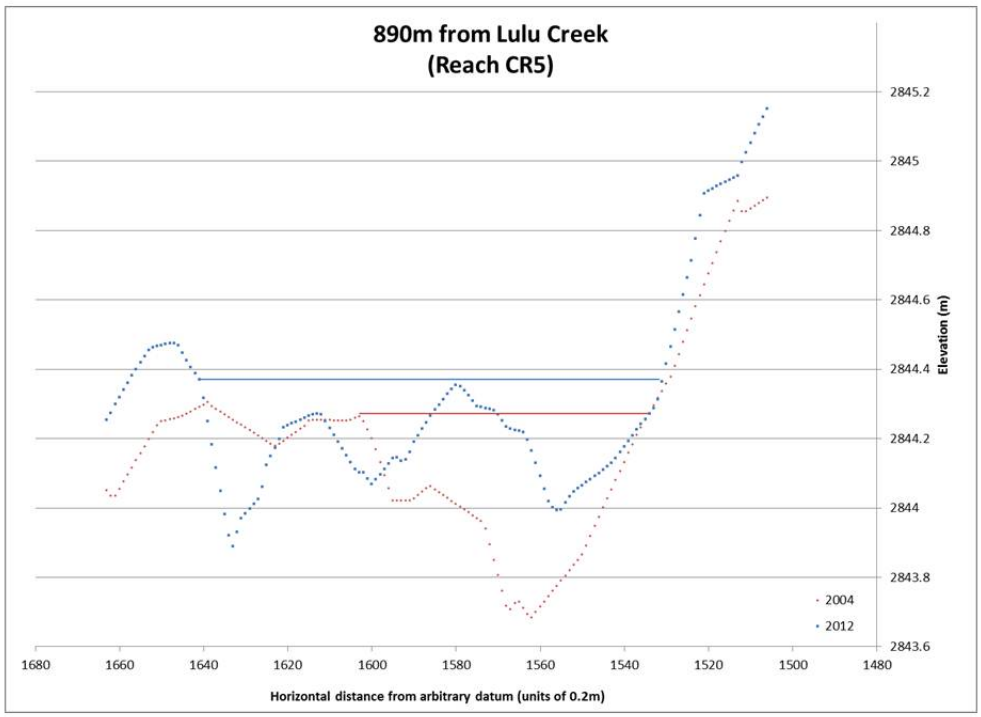

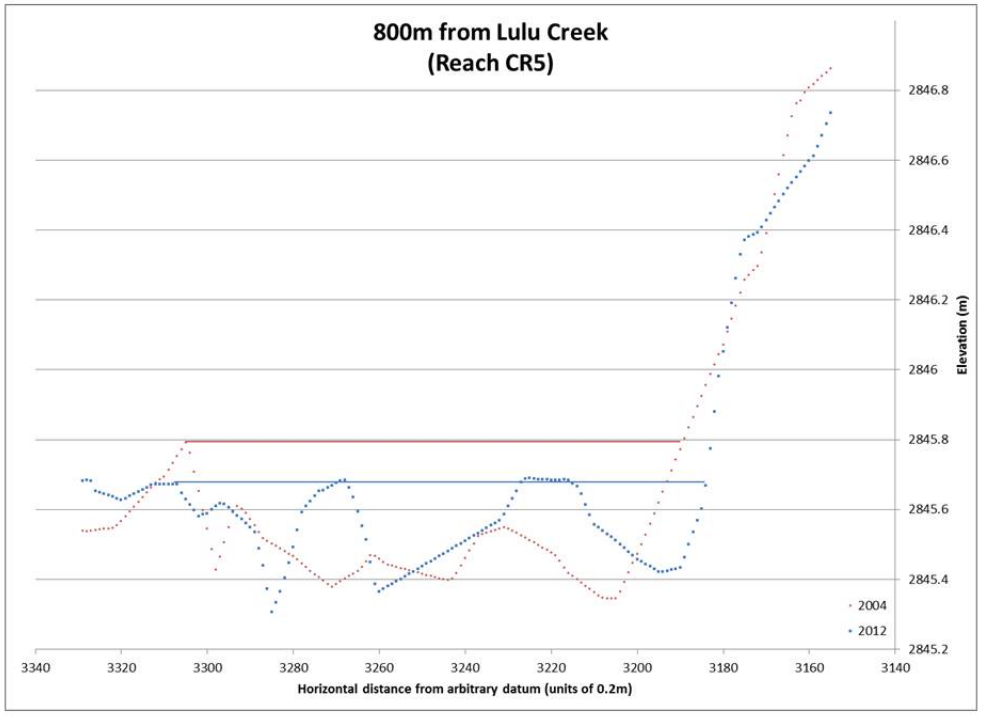
800m from Lulu Creek
(Reach CR5)
2846.8
2846.6
2846.4
2846.2
2846
2845.8
2845.6
2845.4
2845.2
Elevation (m)
2004
2012
3340
3320
3300
3280
3260
3240
3220
3200
3180
3160
3140
Horizontal distance from arbitrary datum (units of 0.2m)

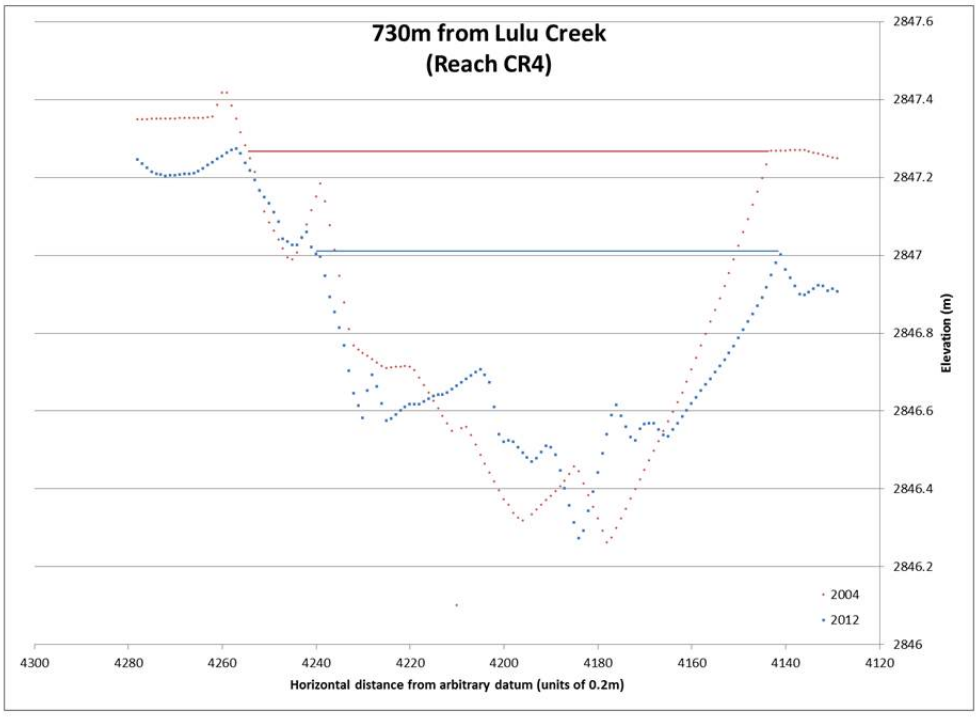
730m from Lulu Creek
(Reach CR4)
2847.6
2847.4
2847.2
2847
2846.8
2846.6
2846.4
2846.2
2846
Elevation (m)
2004
2012
4300
4280
4260
4240
4220
4200
4180
4160
4140
4120
Horizontal distance from arbitrary datum (units of 0.2m)

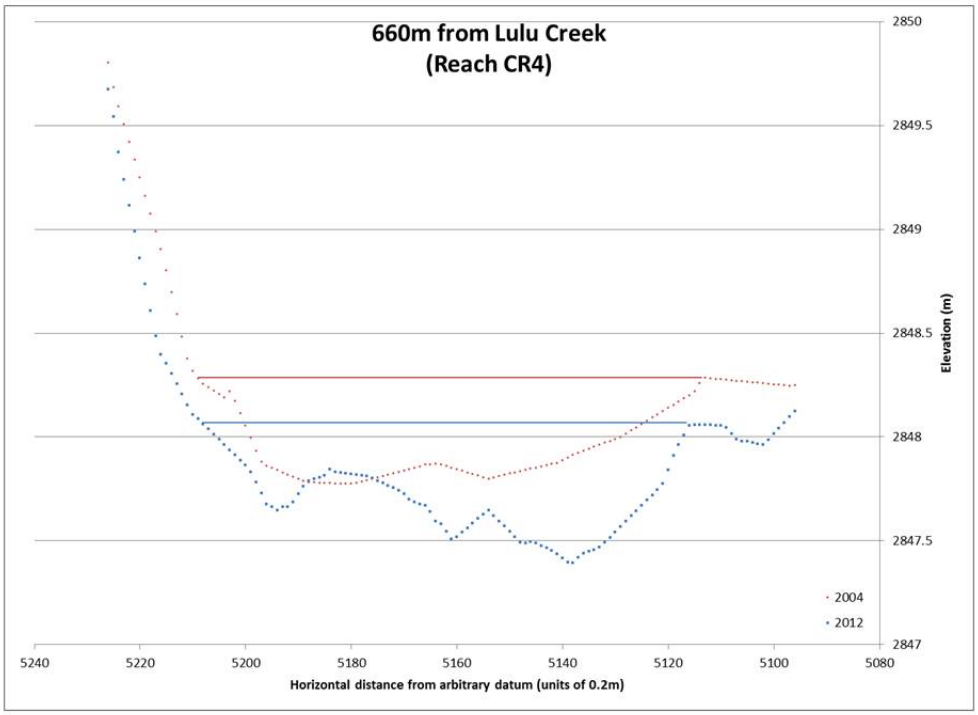
660m from Lulu Creek
(Reach CR4)
2850
2849.5
2849
2848.5
2848
2847.5
2847
Elevation (m)
2004
2012
5240
5220
5200
5180
5160
5140
5120
5100
5080
Horizontal distance from arbitrary datum (units of 0.2m)

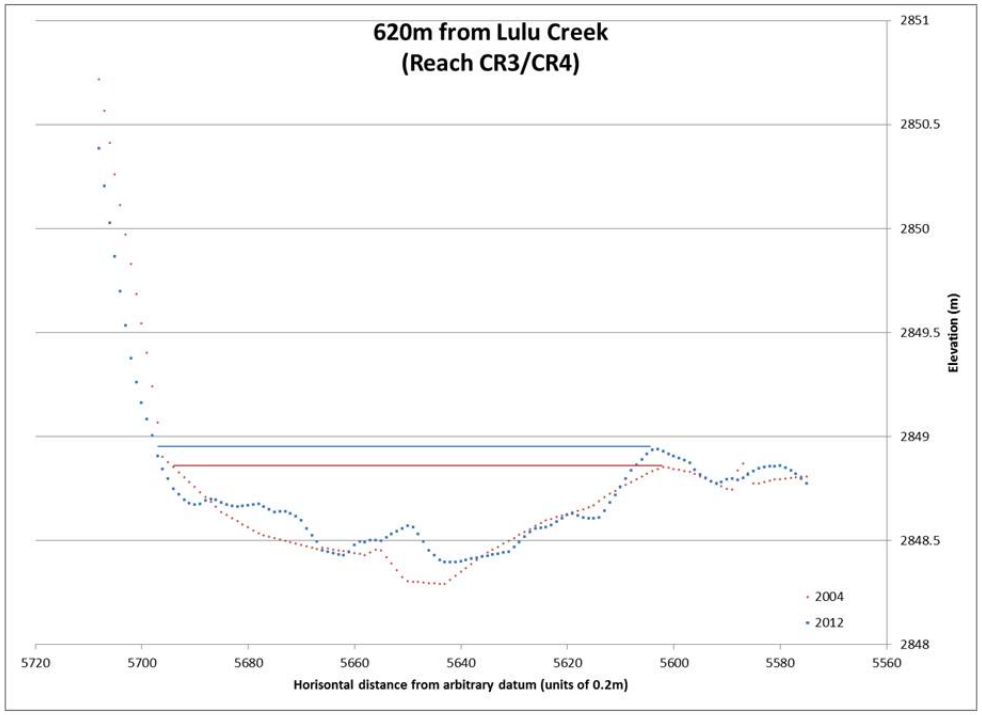
620m from Lulu Creek
(Reach CR3/CR4)
2851
2850.5
2850
2849.5
2849
2848.5
2848
Elevation (m)
2004
2012
5720
5700
5680
5660
5640
5620
5600
5580
5560
Horisontal distance from arbitrary datum (units of 0.2m)

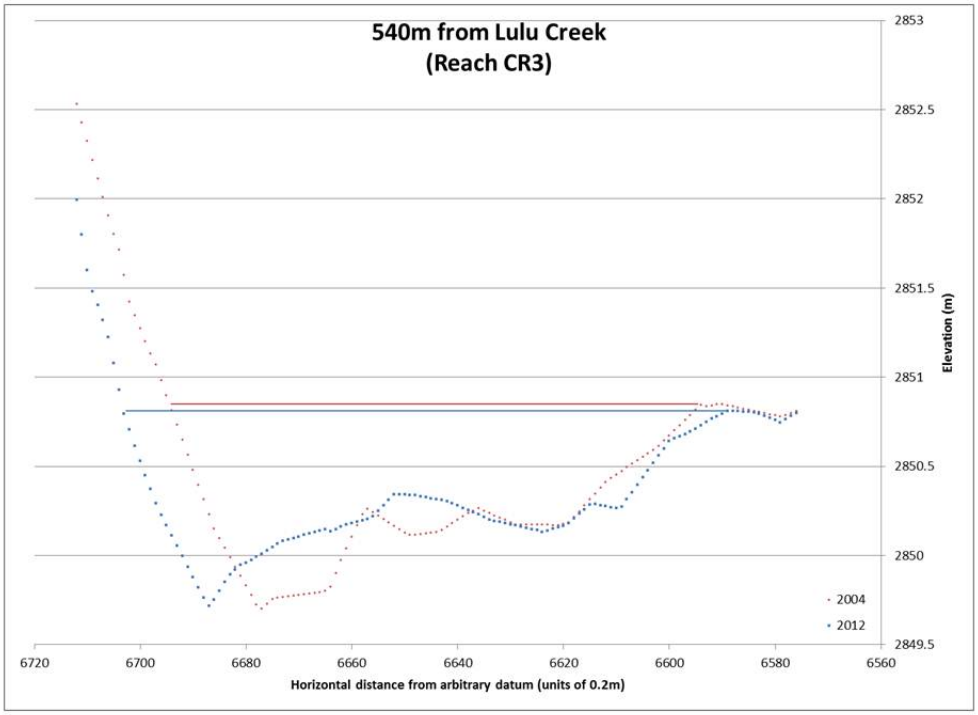
540m from Lulu Creek
(Reach CR3)
2853
2852.5
2852
2851.5
2851
2850.5
2850
2849.5
Elevation (m)
2004
2012
6720
6700
6680
6660
6640
6620
6600
6580
6560
Horizontal distance from arbitrary datum (units of 0.2m)

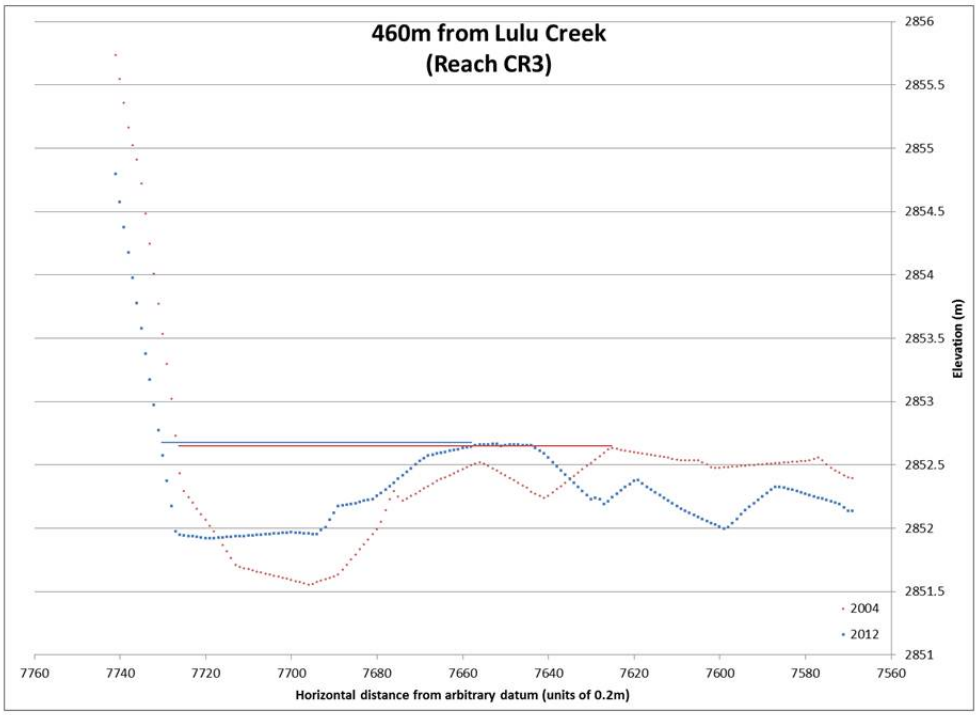
460m from Lulu Creek
(Reach CR3)
2856
2855.5
2855
2854.5
2854
2853.5
2853
2852.5
2852
2851.5
2851
Elevation (m)
2004
2012
7760
7740
7720
7700
7680
7660
7640
7620
7600
7580
7560
Horizontal distance from arbitrary datum (units of 0.2m)

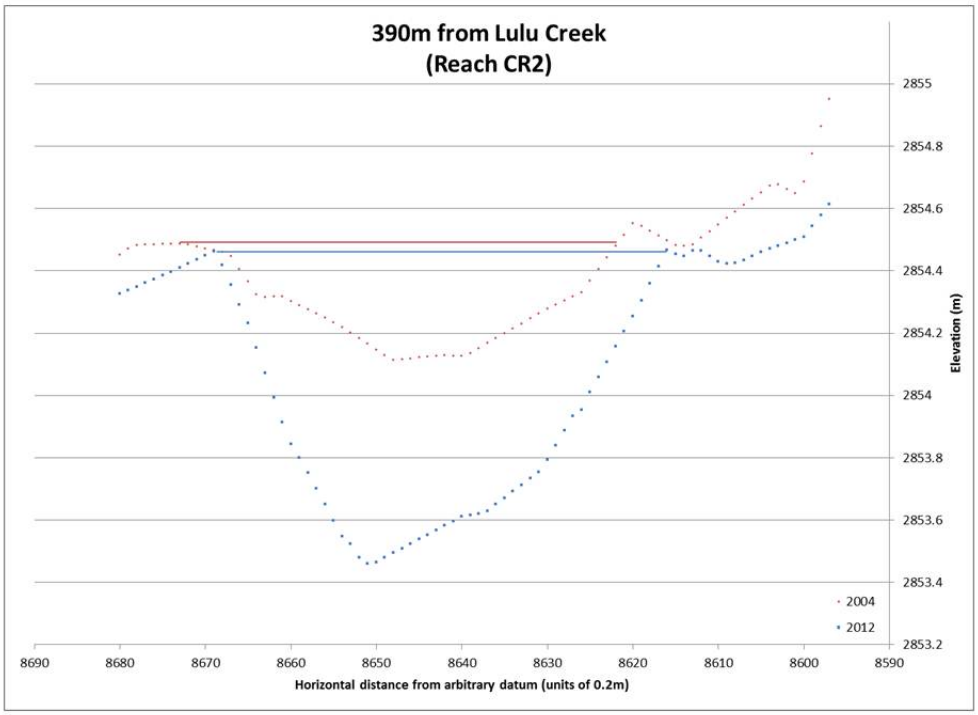
390m from Lulu Creek
(Reach CR2)
2855
2854.8
2854.6
2854.4
2854.2
2854
2853.8
2853.6
2853.4
2853.2
Elevation (m)
2004
2012
8690
8680
8670
8660
8650
8640
8630
8620
8610
8600
8590
Horizontal distance from arbitrary datum (units of 0.2m)

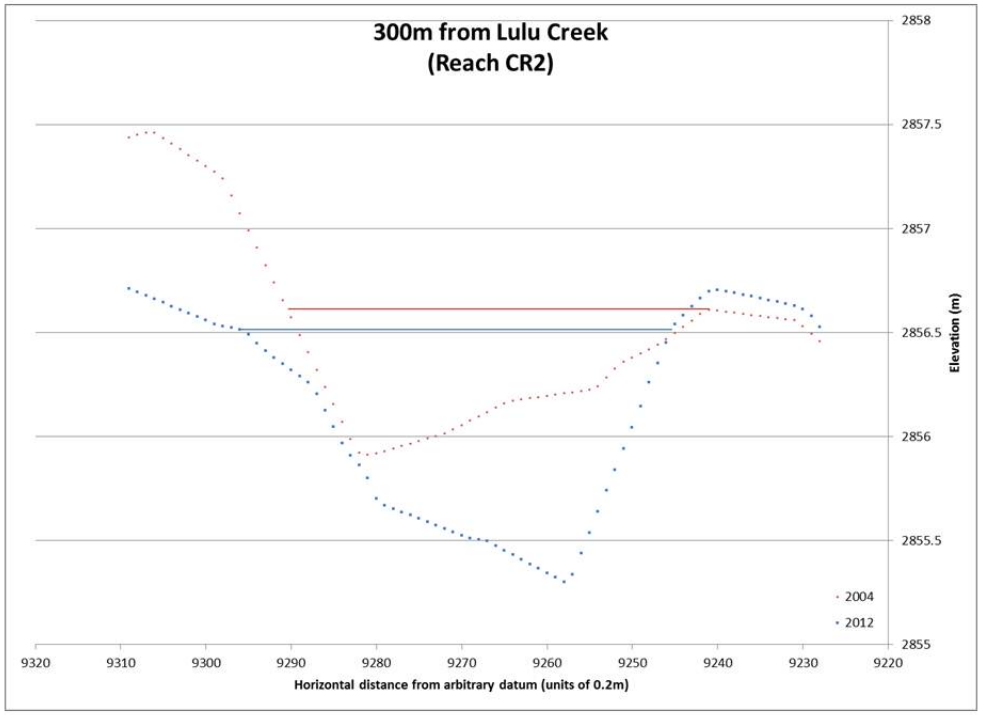
300m from Lulu Creek
(Reach CR2)
2858
2857.5
2857
2856.5
2856
2855.5
2855
Elevation (m)
2004
2012
9320
9310
9300
9290
9280
9270
9260
9250
9240
9230
9220
Horizontal distance from arbitrary datum (units of 0.2m)

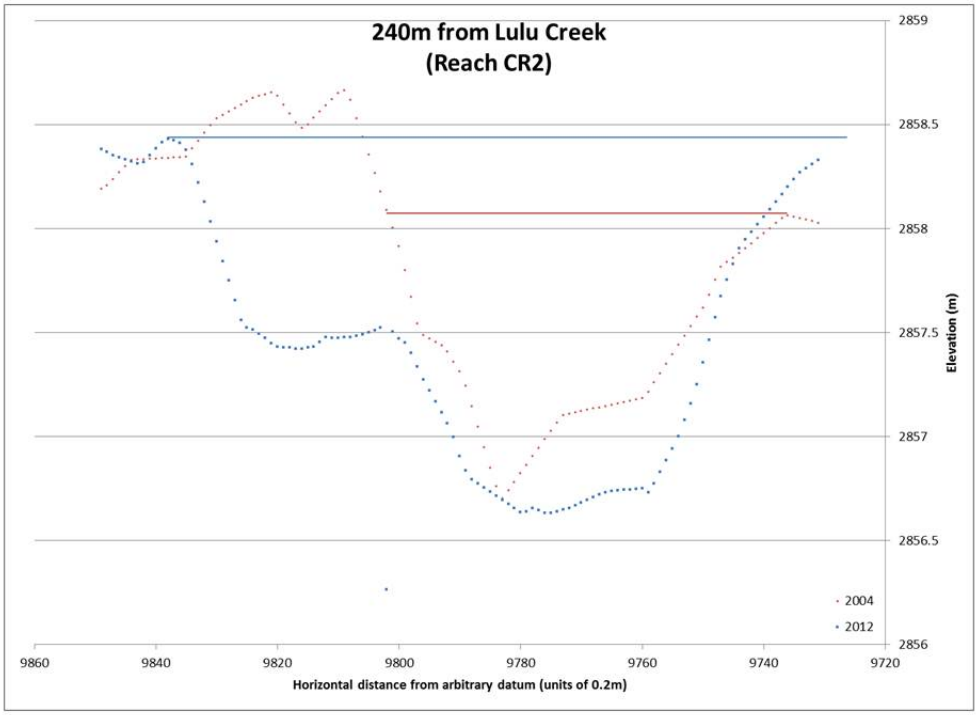
240m from Lulu Creek
(Reach CR2)
2859
2858.5
2858
2857.5
2857
2856.5
2856
Elevation (m)
2004
2012
9860
9840
9820
9800
9780
9760
9740
9720
Horizontal distance from arbitrary datum (units of 0.2m)

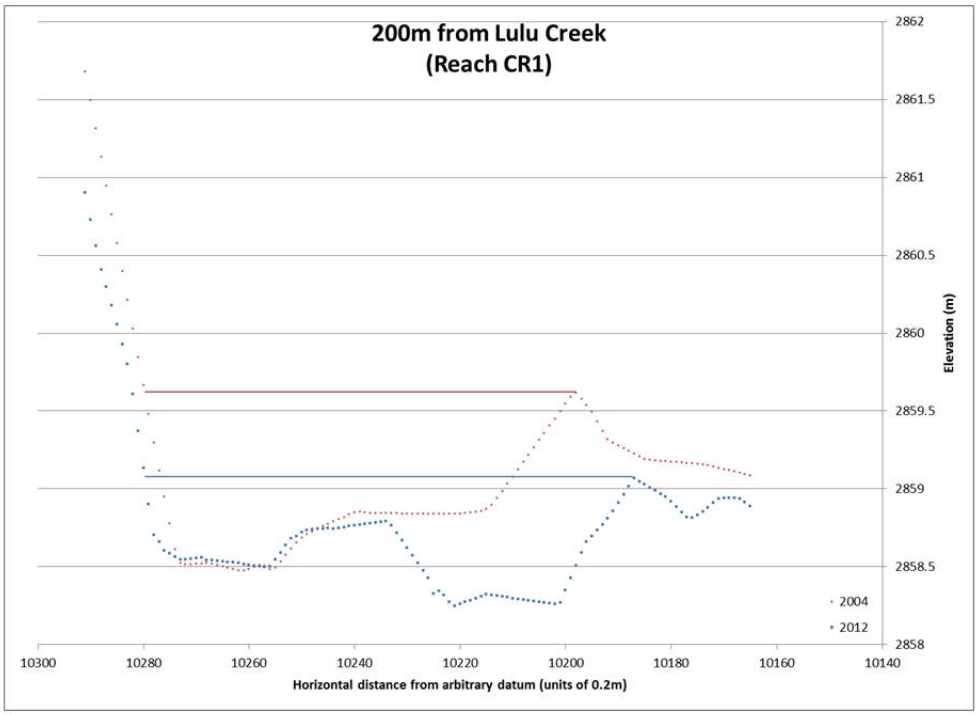
200m from Lulu Creek
(Reach CR1)
2862
2861.5
2861
2860.5
2860
2859.5
2859
2858.5
2858
Elevation (m)
2004
2012
10300
10280
10260
10240
10220
10200
10180
10160
10140
Horizontal distance from arbitrary datum (units of 0.2m)

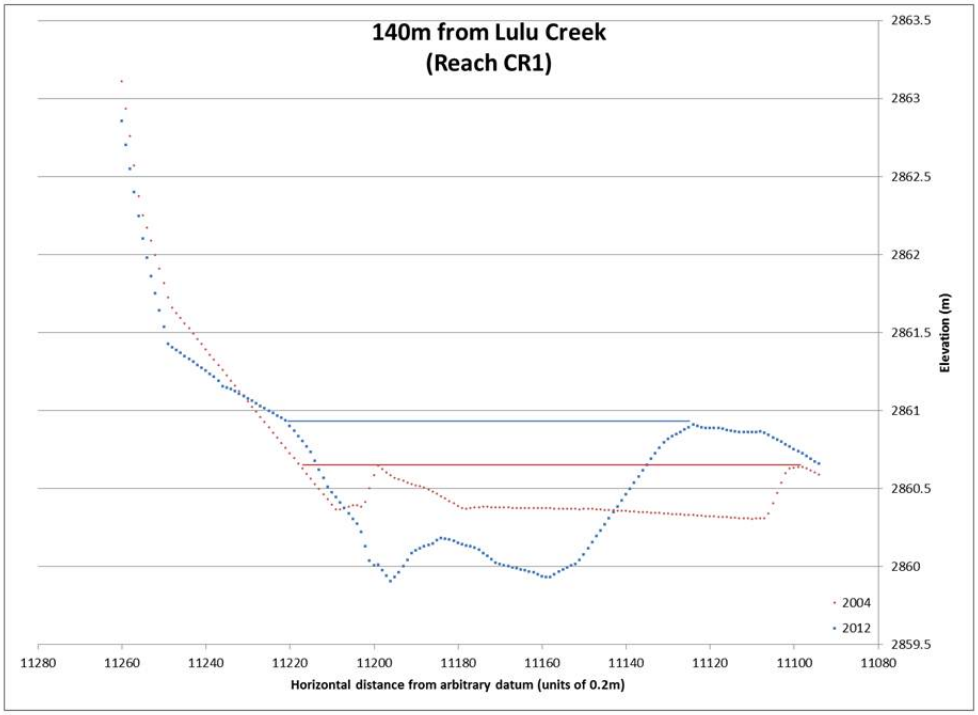
140m from Lulu Creek
(Reach CR1)
2863.5
2863
2862.5
2862
2861.5
2861
2860.5
2860
2859.5
Elevation (m)
2004
2012
11280
11260
11240
11220
11200
11180
11160
11140
11120
11100
11080
Horizontal distance from arbitrary datum (units of 0.2m)

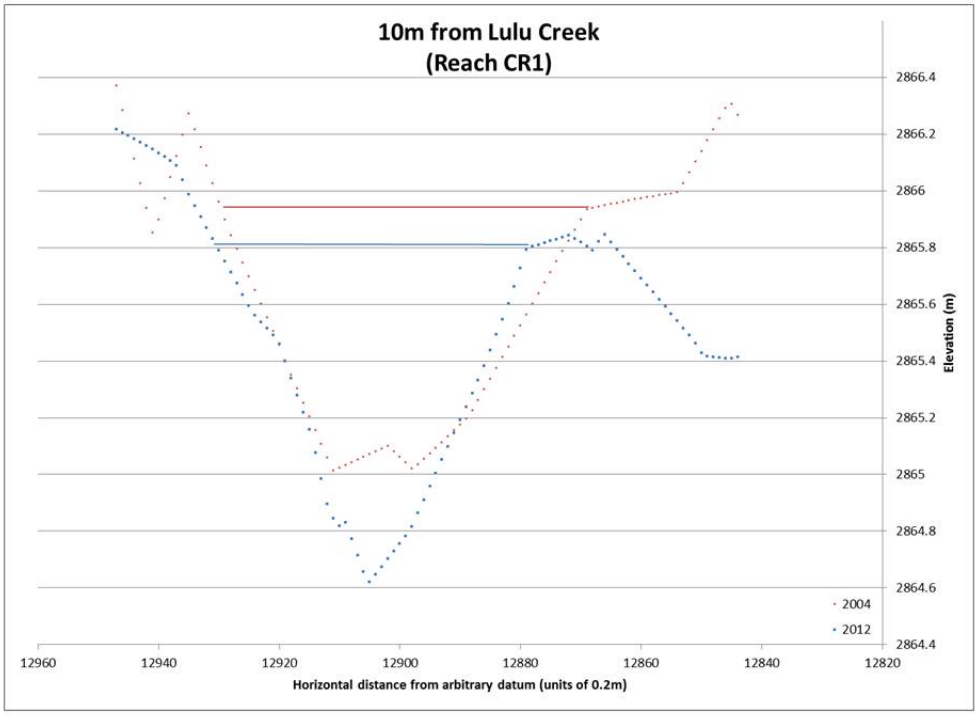
10m from Lulu Creek
(Reach CR1)
2866.4
2866.2
2866
2865.8
2865.6
2865.4
2865.2
2865
2864.8
2864.6
2864.4
Elevation (m)
2004
2012
12960
12940
12920
12900
12880
12860
12840
12820
Horizontal distance from arbitrary datum (units of 0.2m)

BEDLOAD FROM INVERSE METHOD CALCULATIONS

			Reach changes (from GCD)						Working from wetland up		Working from Lulu fan down							
									Sediment budget, no attrition		Sediment Budet, no attrition		Attrition, α = 0.01 (m3)		Attrition, α = 0.1 (m3)		Attrition, α = 0.5 (m3)	Attrition, α = 1.0 (m3)
Distance from fan (m)	Reach length (m)	Reach	Degradation (m³)	Aggradation (m³)	Net Sed Change (m³)	2004-2012 Water Volume Change (m³)	Sed gain from w ater loss (m³)	2004-2012 Total sediment change, ds/dt (m³)	Qo (m³)	Qi (m³)	Qo (m³)	Qi (m³)	Qo (grams)	Qo with attrition (α = 0.01) (m³)	Qo (grams)	Qo with attrition(α = 0.1) (m³)	Qo (grams)	Qo with attrition (α = 0.5) (m³)	Qo (grams)	Qo with attrition (α = 1.0) (m³)
0	0	LC			-1556			-1556	-40	-1208	1167		3093224	1167	3093224	1167	3093224	1167	3093224	1167
220	220	CR1	-1360	193	-1167	-37	37	-1131	808	-40	2015	1167	5333708	2013	5273198	1990	5018298	1894	4729652	1785
410	190	CR2	-604	0	-604	-19	19	-584	1246	808	2454	2015	6485207	2447	6335676	2391	5725127	2160	5072852	1914
620	210	CR3	-186	627	441	-94	94	535	845	1246	2063	2454	5409184	2041	5141499	1940	4092084	1544	3049556	1151
740	120	CR4	-250	42	-208	-40	40	-168	971	845	2179	2053	5736591	2165	5444063	2043	4187645	1580	3038607	1147
980	240	CR5	-72	679	607	-50	50	657	479	971	1686	2179	4417506	1667	3980339	1502	2408775	909	1084920	409
1200	220	WL			638			638	0	479	1208	1686	3139774	1185	2625703	991	889838	336	-397356	-150

APPENDIX E: REPEAT CROSS-SECTION PLOTS

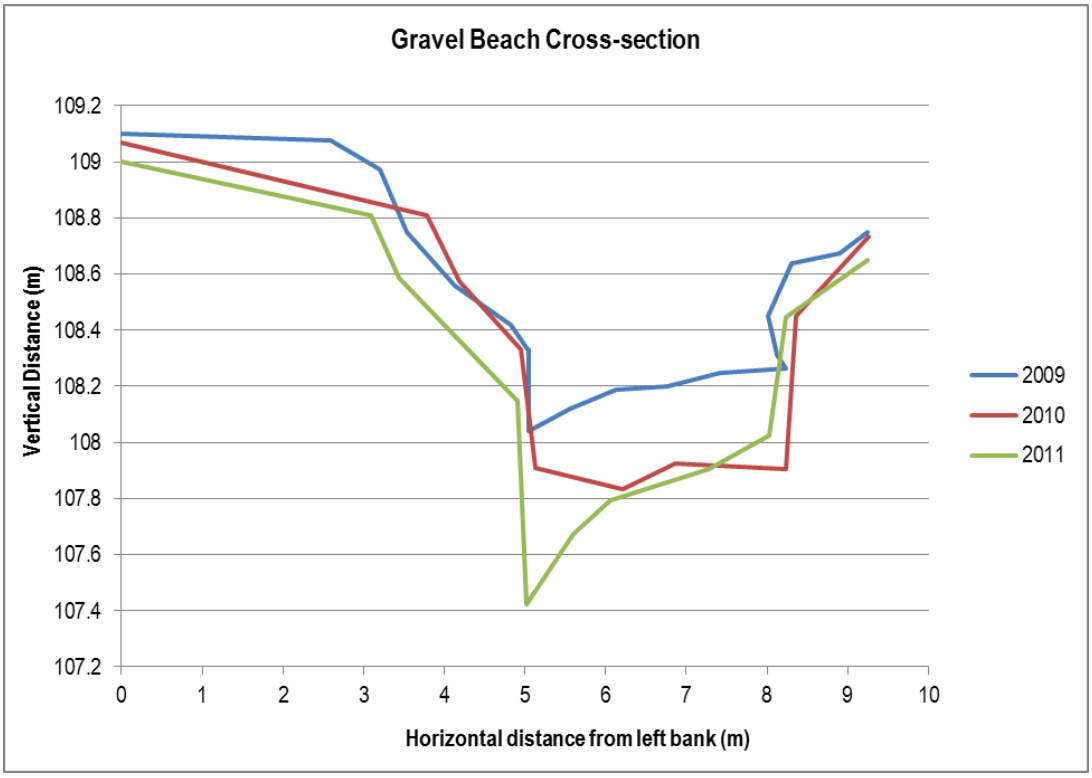

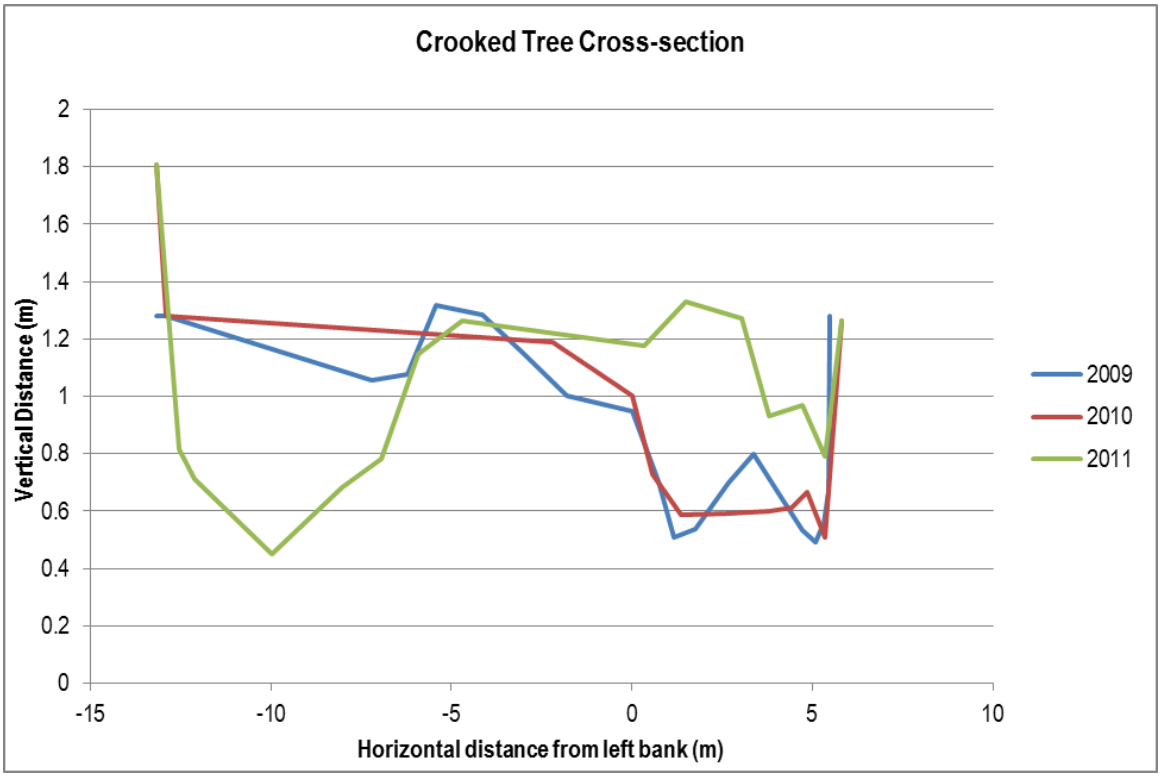

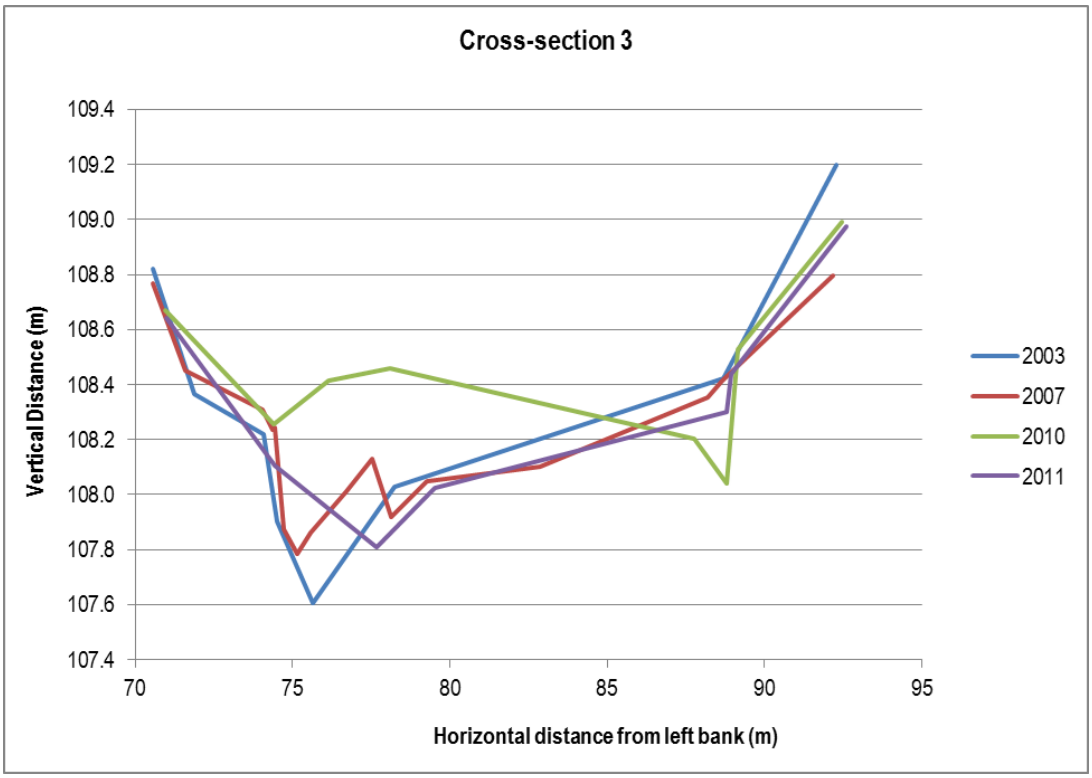
Cross-section 3
109.4
109.2
109.0
108.8
108.6
108.4
108.2
108.0
107.8
107.6
107.4
Vertical Distance (m)
70
75
80
85
90
95
Horizontal distance from left bank (m)
2003
2007
2010
2011

APPENDIX F: MORPHOLOGIC METRIC DATA TABLES

COLORADO RIVER MORPHOLOGIC METRICS DATA TABLE

Transect	Distance from Fan	Reach	Channel Elevation		2004 Water Surface Slope				2012 Water Surface Slope				Valley Elev.	Valley Slope		HAWS Width, at various 2012 HAWS heights						
TmsctID	DistFromFan	Reach	2004Elev	2012Elev	2004Length	2004WaterSlo pe1-1	2004WaterSlo pe5-5		2012Length	2012WaterSlo pe1-1	2012WaterSlo pe5-5		MEAN_ELEV2012_T (excluding channel and bar points)	Valley Slope, from five above to five below	Valley Slope, from five above to five below	25cmLength	50cmLength	75cmLength	100cmLength	125cmLength	150cmLength
#	m	#	m, asl	m, asl	m	m/m	m/m		m	m/m	m/m		m/m	m/m	m/m	m	m	m	m	m	m
89	1040												2842.54								
90	1030		2842.57	2842.72									2842.74			108.39	107.48	109.78	111.75	128.10	129.35
91	1020		2842.62	2842.86									2842.94			98.16	100.87	116.71	118.77	120.84	123.80
92	1010		2842.50	2842.88									2842.94			95.98	97.75	99.42	101.22	108.52	110.41
93	1000		2842.77	2842.99									2843.02			91.04	95.45	96.79	97.95	99.13	100.46
94	990		2842.89	2843.13									2843.22	0.019		75.78	90.78	92.22	93.67	95.02	96.31
95	980	5	2843.33	2843.21	10.27	0.04			10.05	0.01			2843.42	0.015		58.18	73.98	83.01	85.60	86.10	90.07
96	970	5	2842.95	2843.22	11.52	-0.03			10.29	0.00			2843.62	0.014		54.09	58.71	68.17	84.04	87.95	89.90
97	960	5	2843.12	2843.26	11.10	0.02			10.62	0.00			2843.86	0.016		42.20	46.00	54.64	67.91	86.42	88.70
98	950	5	2843.55	2843.20	10.87	0.04			10.40	-0.01			2844.15	0.016		38.19	42.44	50.32	83.21	78.66	92.06
99	940	5	2843.36	2843.64	10.06	-0.02	0.01		12.27	0.04	0.01		2844.44	0.014	0.015	38.01	47.35	52.28	58.32	68.40	90.74
100	930	5	2843.59	2843.67	10.13	0.02	0.01		10.11	0.00	0.01		2844.28	0.012	0.014	7.53	44.38	47.17	51.94	58.49	62.31
101	920	5	2843.71	2843.72	9.69	0.01	0.01		9.74	0.00	0.01		2844.39	0.014	0.014	8.43	33.99	42.65	52.78	58.61	63.26
102	910	5	2843.56	2843.84	10.68	-0.01	0.01		13.16	0.01	0.01		2844.51	0.013	0.015	22.14	35.71	41.12	48.82	53.27	63.52
103	900	5	2843.95	2843.93	15.24	0.03	0.01		11.26	0.01	0.01		2844.63	0.012	0.015	9.52	36.45	40.66	48.05	56.21	60.66
104	890	5	2843.87	2844.03	10.26	-0.01	0.01		10.67	0.01	0.01		2844.65	0.010	0.015	7.52	35.74	38.66	50.33	53.82	64.74
105	880	5	2844.10	2844.12	9.95	0.02	0.01		10.02	0.01	0.01		2844.66	0.013	0.015	5.53	43.83	49.13	57.20	66.05	71.78
106	870	5	2844.05	2844.24	10.54	0.00	0.01		10.06	0.01	0.01		2844.99	0.014	0.015	15.55	26.54	54.33	63.74	70.62	75.74
107	860	5	2844.28	2844.48	20.31	0.01	0.01		10.57	0.02	0.02		2845.20	0.014	0.014	12.30	26.84	58.47	68.47	72.14	78.95
108	850	5	2844.59	2844.54	10.40	0.03	0.01		10.11	0.01	0.02		2845.32	0.014	0.013	14.57	30.03	60.20	67.19	73.65	80.38
109	840	5	2844.57	2844.78	10.10	0.00	0.01		10.01	0.02	0.02		2845.48	0.016	0.012	9.56	36.35	45.76	64.69	73.15	86.27
110	830	5	2844.78	2844.93	14.07	0.02	0.01		10.05	0.02	0.02		2845.61	0.018	0.014	12.96	33.10	44.33	75.51	87.49	93.58
111	820	5	2844.86	2845.00	11.07	0.01	0.01		10.35	0.01	0.02		2845.81	0.015	0.014	9.71	24.25	38.62	89.69	96.96	111.50
112	810	5	2845.27	2845.13	26.94	0.02	0.02		12.14	0.01	0.02		2845.92	0.014	0.014	19.74	29.67	98.24	103.03	110.03	118.87
113	800	5	2845.65	2845.45	12.10	0.03	0.01		11.22	0.03	0.01		2846.02	0.014	0.014	29.98	39.48	111.90	115.30	119.28	125.95
114	790	5	2845.65	2845.73	10.54	0.00	0.01		10.42	0.03	0.02		2846.23	0.014	0.015	32.37	34.71	56.82	117.09	121.41	127.79
115	780	5	2845.66	2845.89	11.39	0.02	0.01		10.07	0.02	0.02		2846.43	0.015	0.015	13.91	29.93	40.37	115.00	129.81	132.94
116	770	5	2846.10	2845.86	12.46	0.02	0.02		10.74	0.00	0.02		2846.53	0.014	0.015	7.40	24.35	34.21	118.78	120.42	123.64
117	760	5	2846.29	2845.88	11.14	0.02	0.02		11.78	0.00	0.02		2846.60	0.014	0.014	7.47	21.89	28.49	76.07	126.87	128.25
118	750	5	2846.14	2845.97	10.49	-0.01	0.01		10.45	0.01	0.01		2846.72	0.014	0.015	8.22	11.29	28.72	90.92	137.12	139.86
119	740	4	2846.40	2846.19	10.67	0.02	0.01		10.52	0.02	0.01		2846.87	0.013	0.015	7.95	12.43	76.27	88.65	123.81	129.69
120	730	4	2846.46	2846.54	13.35	0.00	0.01		13.55	0.03	0.01		2847.13	0.013	0.015	15.36	24.82	90.89	120.02	131.91	151.98
121	720	4	2846.90	2846.67	12.73	0.03	0.01		12.49	0.01	0.01		2847.21	0.014	0.015	6.35	22.92	121.22	151.34	165.03	173.38
122	710	4	2847.28	2846.72	10.42	0.04	0.01		10.51	0.00	0.01		2847.30	0.015	0.016	7.30	23.69	104.37	162.11	168.59	172.44
123	700	4	2847.19	2846.87	8.74	-0.01	0.02		8.69	0.02	0.02		2847.40	0.015	0.016	7.85	18.43	155.62	159.46	162.44	165.10
124	690	4	2847.21	2847.11	10.14	0.00	0.02		9.92	0.02	0.02		2847.55	0.016	0.016	9.97	18.88	19.97	154.39	156.09	157.93
125	680	4	2847.39	2847.08	10.59	0.02	0.02		13.15	0.00	0.02		2847.70	0.015	0.016	10.81	18.61	36.30	149.35	150.48	152.40
126	670	4	2847.64	2847.40	10.40	0.02	0.01		10.42	0.03	0.01		2847.93	0.016	0.017	5.44	10.51	26.81	142.46	143.92	145.51
127	660	4	2847.82	2847.46	10.09	0.02	0.01		11.04	0.01	0.01		2848.09	0.018	0.018	9.17	17.56	27.68	136.22	138.07	139.52
128	650	4	2848.22	2847.62	10.23	0.04	0.02		11.19	0.01	0.02		2848.24	0.018	0.019	12.16	17.10	33.24	129.75	131.54	132.76
129	640	4	2848.53	2847.93	10.16	0.03	0.02		11.91	0.03	0.01		2848.44	0.018	0.020	6.38	16.80	99.21	124.95	126.55	127.86
130	630	4	2848.49	2848.20	10.95	0.00	0.02		11.47	0.02	0.02		2848.66	0.019	0.019	14.24	19.08	88.71	90.79	92.89	97.42
131	620	3	2848.44	2848.45	12.55	0.00	0.01		11.44	0.02	0.01		2848.84	0.020	0.019	15.51	56.73	84.28	85.47	86.65	87.75
132	610	3	2848.58	2848.60	11.44	0.01	0.01		11.97	0.01	0.01		2849.10	0.020	0.020	18.57	60.16	85.06	86.05	87.06	90.61
133	600	3	2848.91	2848.73	10.15	0.03	0.01		10.55	0.01	0.01		2849.20	0.022	0.021	9.46	28.08	99.36	100.71	102.09	103.26
134	590	3	2848.85	2848.93	10.24	-0.01	0.02		10.74	0.02	0.02		2849.39	0.024	0.021	15.96	36.46	53.46	95.84	97.34	98.81
135	580	3	2849.08	2849.04	12.47	0.02	0.01		11.03	0.01	0.01		2849.59	0.024	0.022	16.08	27.27	50.83	99.10	100.51	101.56
136	570	3	2849.17	2849.14	11.75	0.01	0.02		10.58	0.01	0.02		2849.88	0.023	0.021	8.55	13.99	38.36	47.19	90.17	91.63
137	560	3	2849.35	2849.30	10.18	0.02	0.02		10.65	0.02	0.02		2850.13	0.022	0.022	8.24	15.85	25.86	39.73	89.28	92.13
138	550	3	2849.67	2849.85	10.20	0.03	0.01		11.56	0.05	0.02		2850.48	0.023	0.022	13.32	24.00	29.02	82.34	84.89	88.27
139	540	3	2850.56	2850.22	10.73	0.08	0.02		11.77	0.03	0.02		2850.79	0.024	0.022	18.76	21.22	80.96	82.66	85.24	87.80
140	530	3	2850.05	2850.50	16.11	-0.03	0.02		12.14	0.02	0.02		2851.02	0.024	0.022	8.59	40.49	58.24	65.19	66.47	67.79
141	520	3	2850.45	2850.77	14.58	0.03	0.03		11.62	0.02	0.03		2851.10	0.023	0.023	4.15	52.37	61.07	68.09	68.95	69.73
142	510	3	2850.63	2851.12	10.62	0.02	0.02		11.06	0.03	0.02		2851.29	0.023	0.023	7.22	56.63	73.23	75.16	78.05	79.79
143	500	3	2850.66	2851.29	10.48	0.00	0.02		10.19	0.02	0.02		2851.51	0.022	0.024	8.68	61.61	72.47	74.07	75.17	76.10

COLORADO RIVER MORPHOLOGIC METRICS DATA TABLE

Transect	Distance from Fan	Reach	Channel Elevation		2004 Water Surface Slope			2012 Water Surface Slope			Valley Elev.	Valley Slope		HAWS Width, at various 2012 HAWS heights					
TmsctID	DistFromFan	Reach	2004Elev	2012Elev	2004Length	2004WaterSlope1-1	2004WaterSlope5-5	2012Length	2012WaterSlope1-1	2012WaterSlope5-5	MEAN_ELEV2012_T (excluding channel and bar points)	ValleySlope, from five above to five below	ValleySlope, from five above to five below	25cmLength	50cmLength	75cmLength	100cmLength	125cmLength	150cmLength
#	m	#	m, asl	m, asl	m	m/m	m/m	m	m/m	m/m	m/m	m/m	m/m	m	m	m	m	m	m
144	490	3	2851.09	2851.47	11.06	0.04	0.02	10.10	0.02	0.02	2851.78	0.021	0.024	7.43	53.97	64.66	66.08	67.20	68.11
145	480	3	2851.01	2851.65	10.21	-0.01	0.03	10.25	0.02	0.03	2852.02	0.020	0.024	8.83	13.41	56.96	57.92	58.69	59.57
146	470	3	2852.26	2851.81	11.56	0.11	0.03	10.24	0.02	0.03	2852.22	0.023	0.024	6.80	9.80	57.63	58.30	58.96	59.50
147	460	3	2851.64	2851.93	10.76	-0.06	0.03	10.55	0.01	0.03	2852.39	0.024	0.024	8.42	11.22	60.20	61.06	61.84	62.41
148	450	3	2852.26	2852.24	16.87	0.04	0.03	10.11	0.03	0.03	2852.67	0.024	0.024	13.53	14.82	16.38	65.73	66.99	68.11
149	440	3	2852.72	2852.38	12.47	0.04	0.03	10.17	0.01	0.03	2852.85	0.024	0.024	5.80	7.80	48.88	69.46	70.51	71.71
150	430	3	2853.10	2852.52	12.26	0.03	0.03	10.36	0.01	0.03	2853.03	0.024	0.024	5.59	8.53	66.96	74.28	75.34	76.05
151	420	3	2853.40	2852.90	10.52	0.03	0.02	11.62	0.03	0.02	2853.38	0.025	0.025	5.44	7.20	11.93	78.14	79.05	79.83
152	410	2	2853.80	2853.06	12.60	0.03	0.03	11.43	0.01	0.03	2853.68	0.025	0.025	6.18	8.56	15.53	65.86	81.07	82.04
153	400	2	2853.85	2853.27	10.10	0.01	0.02	10.39	0.02	0.03	2853.91	0.025	0.025	5.90	7.73	9.76	68.70	79.18	79.96
154	390	2	2854.17	2853.60	9.14	0.03	0.03	9.57	0.03	0.03	2854.14	0.028	0.025	4.93	7.21	8.93	82.10	84.48	85.68
155	380	2	2854.35	2853.68	9.76	0.02	0.02	10.01	0.01	0.02	2854.41	0.028	0.024	4.34	6.00	7.16	80.48	81.33	82.06
156	370	2	2854.59	2853.71	6.57	0.04	0.02	6.70	0.00	0.02	2854.69	0.027	0.023	4.47	5.38	6.23	7.22	73.91	75.05
157	360	2	2854.40	2853.91	6.85	-0.03	0.02	6.83	0.03	0.02	2854.94	0.026	0.023	4.56	5.24	5.94	6.74	59.70	66.46
158	350	2	2854.69	2854.28	8.45	0.03	0.02	8.38	0.04	0.02	2855.22	0.026	0.023	4.60	5.64	6.75	8.34	57.31	70.04
159	340	2	2855.25	2854.65	9.08	0.06	0.02	9.02	0.04	0.02	2855.62	0.026	0.023	4.47	5.81	7.01	47.11	62.32	85.52
160	330	2	2855.18	2854.64	10.23	-0.01	0.02	10.51	0.00	0.02	2855.82	0.024	0.026	5.99	6.99	8.47	21.43	52.42	56.56
161	320	2	2855.18	2854.90	10.15	0.00	0.02	10.14	0.03	0.02	2856.06	0.022	0.026	4.77	6.06	6.97	7.88	32.51	57.82
162	310	2	2855.75	2855.29	11.65	0.05	0.02	11.53	0.03	0.02	2856.32	0.021	0.025	5.59	7.13	8.71	10.35	15.66	59.97
163	300	2	2856.13	2855.58	10.48	0.04	0.02	10.64	0.03	0.02	2856.54	0.020	0.024	5.73	6.94	8.51	10.98	21.55	64.76
164	290	2	2856.09	2855.47	10.06	0.00	0.02	10.33	-0.01	0.02	2856.69	0.019	0.025	6.24	7.32	8.31	9.59	29.52	68.46
165	280	2	2856.55	2855.75	11.44	0.04	0.02	10.51	0.03	0.02	2856.82	0.023	0.027	5.17	6.95	8.80	24.07	25.43	27.01
166	270	2	2856.60	2855.75	10.15	0.01	0.03	10.41	0.00	0.03	2856.87	0.024	0.027	4.81	6.73	8.54	10.32	12.96	23.49
167	260	2	2856.90	2855.96	10.30	0.03	0.02	10.21	0.02	0.02	2857.02	0.023	0.027	4.22	5.30	6.55	8.43	11.60	28.04
168	250	2	2856.83	2856.39	10.21	-0.01	0.02	10.01	0.04	0.02	2857.25	0.022	0.026	4.19	6.32	8.29	10.24	12.76	30.04
169	240	2	2857.06	2856.69	11.00	0.02	0.03	11.02	0.03	0.02	2857.54	0.025	0.026	7.17	8.66	10.36	16.40	17.56	19.58
170	230	2	2857.76	2857.38	10.99	0.06	0.02	12.44	0.06	0.02	2858.15	0.030	0.026	6.13	12.61	13.84	14.59	15.60	18.58
171	220	1	2858.12	2857.92	10.46	0.03	0.03	11.18	0.05	0.03	2858.48	0.031	0.027	9.72	14.25	19.10	21.39	43.78	44.72
172	210	1	2858.33	2858.29	10.26	0.02	0.03	10.83	0.03	0.03	2858.58	0.033	0.027	7.82	21.39	38.74	40.01	40.96	41.93
173	200	1	2858.54	2858.29	10.28	0.02	0.03	10.69	0.00	0.03	2858.79	0.032	0.028	6.36	16.99	35.79	36.54	37.22	37.87
174	190	1	2858.75	2858.69	10.50	0.02	0.03	11.38	0.04	0.03	2859.22	0.033	0.028	9.56	12.46	36.83	37.69	38.44	38.98
175	180	1	2859.13	2859.10	11.77	0.03	0.03	10.93	0.04	0.03	2859.77	0.029	0.031	10.82	25.58	26.99	38.11	38.84	39.45
176	170	1	2859.90	2859.50	13.06	0.06	0.03	10.98	0.04	0.03	2859.99	0.030	0.032	10.43	26.06	37.26	38.28	39.17	39.81
177	160	1	2859.92	2859.44	10.39	0.00	0.03	10.57	-0.01	0.03	2860.32	0.031	0.033	9.86	21.03	24.49	34.93	36.71	38.00
178	150	1	2859.95	2859.75	10.77	0.00	0.03	10.25	0.03	0.03	2860.47	0.034	0.034	7.14	16.12	25.53	36.35	37.74	38.80
179	140	1	2860.39	2859.96	11.11	0.04	0.03	10.21	0.02	0.03	2860.81	0.031	0.035	12.04	14.41	16.60	31.89	35.53	37.31
180	130	1	2860.72	2860.42	11.54	0.03	0.03	10.26	0.04	0.03	2861.08	0.032	0.034	3.29	5.18	21.67	23.88	39.20	40.32
181	120	1	2861.28	2860.56	14.04	0.04	0.03	11.37	0.01	0.03	2861.47	0.033	0.034	6.32	9.69	25.84	27.44	46.51	46.91
182	110	1	2862.07	2860.96	11.09	0.07	0.03	13.56	0.03	0.03	2861.70	0.032	0.036	8.00	14.55	31.40	33.73	44.73	45.88
183	100	1	2861.75	2861.22	9.66	-0.03	0.03	11.34	0.02	0.03	2862.21	0.036	0.036	6.76	8.17	9.26	28.50	35.79	47.43
184	90	1	2862.23	2861.57	11.75	0.04	0.03	9.79	0.04	0.03	2862.27	0.038	0.039	7.59	15.63	17.98	40.98	49.60	51.38
185	80	1	2862.57	2861.83	10.06	0.03	0.04	9.76	0.03	0.03	2863.00	0.039	0.037	9.18	12.81	13.92	14.95	16.18	36.89
186	70	1	2863.02	2862.14	10.04	0.05	0.03	10.19	0.03	0.03	2863.30	0.037	0.038	7.20	8.62	9.83	12.05	29.48	32.74
187	60	1	2863.38	2862.52	10.15	0.04	0.03	10.69	0.04	0.03	2863.52	0.040	0.039	7.07	9.89	11.66	14.09	15.15	31.12
188	50	1	2863.30	2863.07	10.23	-0.01		11.65	0.05		2864.12	0.038	0.042	8.33	13.77	14.93	16.00	17.09	32.95
189	40	1	2863.86	2863.39	10.77	0.05		11.54	0.03		2864.59	0.047	0.043	5.10	7.04	9.72	16.62	26.32	28.47
190	30	1	2864.58	2863.74	11.75	0.06		10.95	0.03		2864.96	0.042	0.045	4.19	6.05	7.66	9.70	23.00	44.39
191	20	1	2864.97	2864.14	11.79	0.03		11.96	0.03		2865.21	0.042	0.046	5.60	6.79	8.33	11.36	23.31	36.12
192	10	1	2865.31	2864.86	10.70	0.03		10.79	0.07		2865.71	0.046	0.046	4.04	6.11	8.04	10.65	32.29	35.58
193	0		2865.79	2865.43							2865.98	0.047	0.045	12.40	16.81	29.33	40.28	42.28	44.67

COLORADO RIVER MORPHOLOGIC METRICS DATA TABLE

Transect	Distance from Fan	Reach	Migration			Proximity to			DOD			Bankful Width					Confinement Ratio, at various 2012 HAWS heights					
TmsctID	DistFromFan	Reach	MigLength	Migration, average one above to one below	Migration, average one above to one below	Confluence Bridge	Sawmill Bridge	Lulu Creek Fan	Negative Sum	Positive Sum	Both Sum	2004 Width	2012 Width	Width Difference	Width Difference	Include?	25cmHAWS	50cmHAWS	75cmHAWS	100cmHAWS	125cmHAWS	150cmHAWS
#	m	#	m	m	m	m	m	m	m^3	m^3	m^3	m	m	m	%	1 or 0	--	--	--	--	--	--
89	1040					1010	740	1040														
90	1030					1000	730	1030														
91	1020		0.54			990	720	1020														
92	1010		0.44	0.79		980	710	1010														
93	1000		1.38	3.08	2.87	970	700	1000														
94	990		7.43	4.46	2.97	960	690	990	-0.79	49.84	49.05											
95	980	5	4.57	4.34	2.89	950	680	980	-0.39	53.80	53.41	17.6	22.2	4.6	26%	1	2.6	3.3	3.7	3.9	4.0	4.1
96	970	5	1.02	1.87	2.88	940	670	970	0.00	42.60	42.60	19	20.2	1.2	6%	1	2.7	2.9	3.4	4.2	4.4	4.5
97	960	5	0.03	0.79	2.03	930	660	960	0.00	42.58	42.58	12.8	11.2	-1.6	-13%	1	3.8	4.1	4.9	6.1	7.7	7.9
98	950	5	1.33	1.53	1.55	920	650	950	-4.03	7.55	3.51	10.4	9.4	-1	-10%	1	4.1	4.5	5.4	6.7	8.4	9.8
99	940	5	3.22	2.24	1.53	910	640	940	-4.98	15.96	10.98	16	18	2	13%	1	2.1	2.6	2.9	3.2	3.8	5.0
100	930	5	2.16	2.10	2.20	900	630	930	0.00	36.17	36.17	18.8	21	2.2	12%	1	0.4	2.1	2.2	2.5	2.8	3.0
101	920	5	0.91	2.14	2.38	890	620	920	-6.18	31.24	25.06	17.8	19.8	2	11%	0	0.4	1.7	2.2	2.7	3.0	3.2
102	910	5	3.36	2.18	1.80	880	610	910	-1.34	29.48	28.14	14.8	15	0.2	1%	1	1.5	2.4	2.7	3.3	3.6	4.2
103	900	5	2.28	1.98	2.19	870	600	900	0.00	42.54	42.54	15.4	23.2	7.8	51%	0	0.4	1.6	1.8	2.1	2.4	2.6
104	890	5	0.32	2.23	3.28	860	590	890	-1.59	48.94	47.35	13.6	22	8.4	62%	1	0.3	1.6	1.8	2.3	2.4	2.9
105	880	5	4.11	3.58	5.26	850	580	880	-0.82	16.03	15.21	11.8	16.4	4.6	39%	0	0.3	2.7	3.0	3.5	4.0	4.4
106	870	5	6.32	7.90	7.23	840	570	870	-7.44	23.22	15.78	14.2	22.4	8.2	58%	1	0.7	1.3	2.4	2.8	3.2	3.4
107	860	5	13.27	10.58	8.78	830	560	860	-0.13	51.30	51.16	21	23.6	2.6	12%	1	0.5	1.1	2.5	2.9	3.1	3.3
108	850	5	12.15	11.17	8.32	820	550	850	-2.08	50.85	48.76	20.4	22.8	2.4	12%	1	0.6	1.3	2.6	2.9	3.2	3.5
109	840	5	8.08	7.34	8.31	810	540	840	-0.32	37.35	37.02	17.4	20.2	2.8	16%	1	0.5	1.8	2.3	3.2	3.6	4.3
110	830	5	1.79	5.37	7.67	800	530	830	-0.15	32.83	32.68	14.6	20.4	5.8	40%	1	0.6	1.6	2.2	3.7	4.3	4.6
111	820	5	6.25	6.05	7.53	790	520	820	0.00	38.02	38.02	18.8	18	-0.8	-4%	1	0.5	1.3	2.1	5.0	5.4	6.2
112	810	5	10.10	9.26	7.32	780	510	810	-2.14	29.80	27.66	25	27	2	8%	1	0.7	1.1	3.6	3.8	4.1	4.4
113	800	5	11.44	9.52	7.44	770	500	800	-2.22	22.73	20.50	19.6	24.6	5	26%	1	1.2	1.6	4.5	4.7	4.8	5.1
114	790	5	7.02	6.95	6.45	760	490	790	-0.45	11.81	11.36	23.4	15.2	-8.2	-35%	1	2.1	2.3	3.7	7.7	8.0	8.4
115	780	5	2.40	3.57	4.48	750	480	780	-5.46	4.33	-1.14	20.8	23	2.2	11%	1	0.6	1.3	1.8	5.0	5.6	5.8
116	770	5	1.28	1.31	2.19	740	470	770	-6.96	3.42	-3.54	16.4	12.6	-3.8	-23%	1	0.6	1.9	2.7	9.4	9.6	9.8
117	760	5	0.25	0.52	0.94	730	460	760	-16.99	4.35	-12.64	17.8	20.4	2.6	15%	1	0.4	1.1	1.4	3.7	6.2	6.3
118	750	5	0.03	0.35	0.59	720	450	750	-8.29	2.10	-6.19	12.2	10.8	-1.4	-11%	1	0.8	1.0	2.7	8.4	12.7	13.0
119	740	4	0.77	0.47	0.54	710	440	740	-8.03	0.61	-7.41	16	18.2	2.2	14%	1	0.4	0.7	4.2	4.9	6.8	7.1
120	730	4	0.60	0.81	0.62	700	430	730	-3.05	3.91	0.86	16.6	15.8	-0.8	-5%	1	1.0	1.6	5.7	7.6	8.3	9.6
121	720	4	1.04	0.77	0.74	690	420	720	-3.79	13.98	10.19	20.2	22	1.8	9%	1	0.3	1.0	5.5	6.9	7.5	7.9
122	710	4	0.66	0.77	0.81	680	410	710	-19.25	9.47	-9.77	21.4	22.6	1.2	6%	1	0.3	1.0	4.6	7.2	7.5	7.6
123	700	4	0.61	0.80	1.47	670	400	700	-28.00	3.29	-24.71	20	19.6	-0.4	-2%	1	0.4	0.9	7.9	8.1	8.3	8.4
124	690	4	1.14	1.88	2.05	660	390	690	-19.96	0.73	-19.23	20.4	19	-1.4	-7%	1	0.5	1.0	1.1	8.1	8.2	8.3
125	680	4	3.90	2.99	3.56	650	380	680	-18.48	0.70	-17.79	17	19.6	2.6	15%	1	0.6	0.9	1.9	7.6	7.7	7.8
126	670	4	3.95	5.35	4.52	640	370	670	-24.77	0.38	-24.39	19	21.2	2.2	12%	1	0.3	0.5	1.3	6.7	6.8	6.9
127	660	4	8.22	5.86	4.48	630	360	660	-31.01	0.23	-30.79	19.2	18.4	-0.8	-4%	1	0.5	1.0	1.5	7.4	7.5	7.6
128	650	4	5.41	4.85	4.18	620	350	650	-37.34	0.00	-37.34	17	17.8	0.8	5%	0	0.7	1.0	1.9	7.3	7.4	7.5
129	640	4	0.93	2.91	3.47	610	340	640	-41.93	1.03	-40.89	14.4	16.4	2	14%	0	0.4	1.0	6.0	7.6	7.7	7.8
130	630	4	2.40	1.24	2.08	600	330	630	-14.30	7.83	-6.48	14	19	5	36%	0	0.7	1.0	4.7	4.8	4.9	5.1
131	620	3	0.39	1.36	1.23	590	320	620	-8.54	1.87	-6.67	18.4	18.6	0.2	1%	1	0.8	3.1	4.5	4.6	4.7	4.7
132	610	3	1.29	0.93	1.70	580	310	610	-4.64	5.82	1.18	22.8	20.4	-2.4	-11%	1	0.9	2.9	4.2	4.2	4.3	4.4
133	600	3	1.12	1.91	1.34	570	300	600	-6.90	6.02	-0.87	21	26.4	5.4	26%	1	0.4	1.1	3.8	3.8	3.9	3.9
134	590	3	3.32	1.68	1.66	560	290	590	-3.85	1.21	-2.65	22.6	22.4	-0.2	-1%	0	0.7	1.6	2.4	4.3	4.3	4.4
135	580	3	0.60	1.97	1.43	550	280	580	-1.94	2.00	0.06	21.6	24.8	3.2	15%	1	0.6	1.1	2.0	4.0	4.1	4.1
136	570	3	1.98	0.90	2.29	540	270	570	-10.01	0.53	-9.49	7.8	12	4.2	54%	1	0.7	1.2	3.2	3.9	7.5	7.6
137	560	3	0.12	2.51	3.77	530	260	560	-2.39	0.55	-1.84	9.6	9.2	-0.4	-4%	1	0.9	1.7	2.8	4.3	9.7	10.0
138	550	3	5.44	5.42	4.87	520	250	550	-1.24	0.74	-0.50	19	18.2	-0.8	-4%	1	0.7	1.3	1.6	4.5	4.7	4.8
139	540	3	10.71	7.41	4.86	510	240	540	-8.91	9.65	0.74	20	22.8	2.8	14%	1	0.8	0.9	3.6	3.6	3.7	3.9
140	530	3	6.10	6.24	5.52	500	230	530	-12.46	22.03	9.57	14.6	9	-5.6	-38%	0	1.0	4.5	6.5	7.2	7.4	7.5
141	520	3	1.92	3.81	4.88	490	220	520	-3.76	92.14	88.38	18.6	5.6	-13	-70%	1	0.7	9.4	10.9	12.2	12.3	12.5
142	510	3	3.42	2.53	3.07	480	210	510	-2.12	81.89	79.77	7.4	8	0.6	8%	1	0.9	7.1	9.2	9.4	9.8	10.0
143	500	3	2.26	2.45	2.47	470	200	500	0.00	84.87	84.87	15.6	9.8	-5.8	-37%	1	0.9	6.3	7.4	7.6	7.7	7.8

COLORADO RIVER MORPHOLOGIC METRICS DATA TABLE

Transect	Distance from Fan	Reach	Migration			Proximity to			DOD			Bankful Width					Confinement Ratio, at various 2012 HAWS heights					
TmsctID	DistFromFan	Reach	MigLength	Migration, average one above to one below	Migration, average one above to one below	Confluence Bridge	Sawmill Bridge	Lulu Creek Fan	Negative Sum	Positive Sum	Both Sum	2004 Width	2012 Width	Width Difference	Width Difference	Include?	25cmHAWS	50cmHAWS	75cmHAWS	100cmHAWS	125cmHAWS	150cmHAWS
#	m	#	m	m	m	m	m	m	m^3	m^3	m^3	m	m	m	%	1 or 0	--	--	--	--	--	--
144	490	3	1.67	2.34	2.17	460	190	490	0.00	71.67	71.67	11	8.2	-2.8	-25%	1	0.9	6.6	7.9	8.1	8.2	8.3
145	480	3	3.10	1.73	1.52	450	180	480	0.00	55.63	55.63	13.4	13.8	0.4	3%	1	0.6	1.0	4.1	4.2	4.3	4.3
146	470	3	0.42	1.23	3.34	440	170	470	-0.54	47.10	46.57	13.6	11.8	-1.8	-13%	1	0.6	0.8	4.9	4.9	5.0	5.0
147	460	3	0.17	3.98	5.71	430	160	460	-8.63	40.91	32.28	20.4	15	-5.4	-26%	1	0.6	0.7	4.0	4.1	4.1	4.2
148	450	3	11.35	8.35	5.99	420	150	450	-2.84	69.40	66.56	8.6	6.8	-1.8	-21%	0	2.0	2.2	2.4	9.7	9.9	10.0
149	440	3	13.53	9.78	5.94	410	140	440	-10.40	31.31	20.91	13.6	9.4	-4.2	-31%	1	0.6	0.8	5.2	7.4	7.5	7.6
150	430	3	4.48	6.06	6.26	400	130	430	-46.07	0.15	-45.92	10.2	8.6	-1.6	-16%	1	0.6	1.0	7.8	8.6	8.8	8.8
151	420	3	0.16	2.15	4.24	390	120	420	-50.52	1.07	-49.45	9.4	9.6	0.2	2%	1	0.6	0.7	1.2	8.1	8.2	8.3
152	410	2	1.81	1.07	1.64	380	110	410	-54.08	0.35	-53.73	9.2	9.6	0.4	4%	1	0.6	0.9	1.6	6.9	8.4	8.5
153	400	2	1.24	1.19	0.77	370	100	400	-36.51	0.00	-36.51	10	11	1	10%	1	0.5	0.7	0.9	6.2	7.2	7.3
154	390	2	0.52	0.62	0.80	360	90	390	-36.42	0.00	-36.42	10	10.6	0.6	6%	1	0.5	0.7	0.8	7.7	8.0	8.1
155	380	2	0.09	0.32	0.52	350	80	380	-40.40	0.00	-40.40	9.2	8.2	-1	-11%	1	0.5	0.7	0.9	9.8	9.9	10.0
156	370	2	0.33	0.28	0.33	340	70	370	-25.11	0.00	-25.11	7.2	6.6	-0.6	-8%	1	0.7	0.8	0.9	1.1	11.2	11.4
157	360	2	0.40	0.35	0.25	330	60	360	-23.99	0.00	-23.99	7.2	7.6	0.4	6%	1	0.6	0.7	0.8	0.9	7.9	8.7
158	350	2	0.32	0.28	0.43	320	50	350	-16.03	0.00	-16.03	6.4	8.6	2.2	34%	1	0.5	0.7	0.8	1.0	6.7	8.1
159	340	2	0.12	0.47	0.51	310	40	340	-7.41	0.00	-7.41	7.8	8	0.2	3%	1	0.6	0.7	0.9	5.9	7.8	10.7
160	330	2	0.97	0.60	0.43	300	30	330	-28.64	0.00	-28.64	8.6	9.8	1.2	14%	1	0.6	0.7	0.9	2.2	5.3	5.8
161	320	2	0.73	0.57	0.47	290	20	320	-11.87	0.00	-11.87	7.4	8	0.6	8%	1	0.6	0.8	0.9	1.0	4.1	7.2
162	310	2	0.02	0.42	0.75	280	10	310	-17.15	0.00	-17.15	12.4	11	-1.4	-11%	1	0.5	0.6	0.8	0.9	1.4	5.5
163	300	2	0.52	0.69	0.69	270	0	300	-20.47	0.00	-20.47	10	10.2	0.2	2%	1	0.6	0.7	0.8	1.1	2.1	6.3
164	290	2	1.53	0.91	0.63	260		290	-27.63	0.00	-27.63	11.8	10.8	-1	-8%	1	0.6	0.7	0.8	0.9	2.7	6.3
165	280	2	0.68	0.88	0.85	250		280	-34.51	0.00	-34.51	17.4	8.6	-8.8	-51%	0	0.6	0.8	1.0	2.8	3.0	3.1
166	270	2	0.41	0.73	0.84	240		270	-36.43	0.00	-36.43	13.6	15.8	2.2	16%	1	0.3	0.4	0.5	0.7	0.8	1.5
167	260	2	1.11	0.66	0.74	230		260	-24.68	0.00	-24.68	8.6	11.4	2.8	33%	1	0.4	0.5	0.6	0.7	1.0	2.5
168	250	2	0.45	0.86	0.83	220		250	-30.73	0.00	-30.73	14.2	15.2	1	7%	1	0.3	0.4	0.5	0.7	0.8	2.0
169	240	2	1.03	0.88	0.93	210		240	-80.67	0.00	-80.67	13.2	21	7.8	59%	1	0.3	0.4	0.5	0.8	0.8	0.9
170	230	2	1.17	1.03	1.75	200		230	-51.32	0.00	-51.32	14.8	16.6	1.8	12%	1	0.4	0.8	0.8	0.9	0.9	1.1
171	220	1	0.90	2.43	3.76	190		220	-37.80	0.89	-36.92	14.2	17.2	3	21%	1	0.6	0.8	1.1	1.2	2.5	2.6
172	210	1	5.21	5.54	6.31	180		210	-32.08	3.07	-29.02	12.2	14.6	2.4	20%	1	0.5	1.5	2.7	2.7	2.8	2.9
173	200	1	10.50	9.83	7.66	170		200	-48.44	0.78	-47.66	16.4	18.6	2.2	13%	1	0.3	0.9	1.9	2.0	2.0	2.0
174	190	1	13.76	10.74	8.24	160		190	-79.92	10.00	-69.92	16.2	26.2	10	62%	1	0.4	0.5	1.4	1.4	1.5	1.5
175	180	1	7.95	8.50	8.95	150		180	-78.37	24.59	-53.78	21.8	28.2	6.4	29%	1	0.4	0.9	1.0	1.4	1.4	1.4
176	170	1	3.78	6.82	8.22	140		170	-36.51	18.35	-18.16	24.2	28	3.8	16%	1	0.4	0.9	1.3	1.4	1.4	1.4
177	160	1	8.74	6.46	5.73	130		160	-43.25	0.68	-42.57	26	24	-2	-8%	1	0.4	0.9	1.0	1.5	1.5	1.6
178	150	1	6.86	5.64	5.26	120		150	-39.46	2.87	-36.59	11.4	18.8	7.4	65%	1	0.4	0.9	1.4	1.9	2.0	2.1
179	140	1	1.30	4.59	6.58	110		140	-44.00	0.71	-43.29	23.4	19.2	-4.2	-18%	0	0.6	0.8	0.9	1.7	1.9	1.9
180	130	1	5.61	5.77	6.14	100		130	-46.74	0.00	-46.74	24.6	24.6	0	0%	1	0.1	0.2	0.9	1.0	1.6	1.6
181	120	1	10.39	7.51	4.95	90		120	-55.96	5.84	-50.12	21.4	25.2	3.8	18%	1	0.3	0.4	1.0	1.1	1.8	1.9
182	110	1	6.52	5.94	6.71	80		110	-80.67	0.00	-80.67	17.4	16	-1.4	-8%	1	0.5	0.9	2.0	2.1	2.8	2.9
183	100	1	0.92	5.85	8.10	70		100	-64.95	0.00	-64.95	13.6	10.4	-3.2	-24%	1	0.7	0.8	0.9	2.7	3.4	4.6
184	90	1	10.12	7.86	8.75	60		90	-52.33	0.09	-52.24	25	19	-6	-24%	1	0.4	0.8	0.9	2.2	2.6	2.7
185	80	1	12.54	12.11	10.22	50		80	-99.90	4.14	-95.75	22.4	16.2	-6.2	-28%	1	0.6	0.8	0.9	0.9	1.0	2.3
186	70	1	13.65	13.35	11.64	40		70	-67.20	21.41	-45.79	25.2	13.8	-11.4	-45%	1	0.5	0.6	0.7	0.9	2.1	2.4
187	60	1	13.84	11.84	11.16	30		60	-70.79	14.42	-56.37	23.6	14.4	-9.2	-39%	1	0.5	0.7	0.8	1.0	1.1	2.2
188	50	1	8.02	9.87	9.12	20		50	-116.24	28.58	-87.66	11.8	17	5.2	44%	1	0.5	0.8	0.9	0.9	1.0	1.9
189	40	1	7.75	6.03	6.62	10		40	-142.82	47.08	-95.73	16	13	-3	-19%	1	0.4	0.5	0.7	1.3	2.0	2.2
190	30	1	2.33	3.75	4.22	0		30	-60.28	8.84	-51.44	14.8	9.8	-5	-34%	1	0.4	0.6	0.8	1.0	2.3	4.5
191	20	1	1.18	1.77	2.97			20	-38.07	0.32	-37.75	20.6	9.8	-10.8	-52%	1	0.6	0.7	0.9	1.2	2.4	3.7
192	10	1	1.80	1.59	1.63			10	-24.33	0.00	-24.33	12.2	10.2	-2	-16%	1	0.4	0.6	0.8	1.0	3.2	3.5
193	0		1.78	1.55	1.28			0	-7.63	0.00	-7.63											

LULU CREEK MORPHOLOGIC METRIC DATA TABLE

Transect	Distance from Fan	Channel Elevation		HAWS Width, at various 2012 HAWS heights						Migration			DOD		
TrnsctID	DistFromFan	2004Elev	2012Elev	50cmLength	100cmLengt	150cmLengt	200cmLengt	250cmLengt	300cmLengt	MigLength	Migration, average one above to one below	Migration, average one above to one below	Negative Sum	Positive Sum	Both Sum
#	m	m, asl	m, asl	m	m	m	m	m	m	m	m	m	m^3	m^3	m^3
1	10	2865.77	2865.18	14.45	51.07	66.73	83.37	90.95	101.81	1.87			-57.0	0.0	-57.0
2	20	2867.04	2866.27	16.91	20.90	47.51	81.47	90.93	97.94	10.56	7.60		-115.6	14.5	-101.1
3	30	2867.60	2867.00	12.03	29.99	36.67	40.13	78.48	93.44	10.36	10.70	9.72	-105.7	9.2	-96.6
4	40	2868.58	2867.52	4.59	8.45	16.98	30.31	93.89	98.00	11.19	12.06	10.18	-139.6	0.5	-139.1
5	50	2869.83	2869.11	8.83	20.02	22.98	32.69	74.70	77.59	14.64	10.00	8.20	-75.6	1.0	-74.6
6	60	2870.88	2870.28	14.30	17.42	21.77	43.69	51.34	55.04	4.16	6.49	7.96	-68.5	0.7	-67.7
7	70	2872.60	2871.35	8.53	16.13	18.87	33.80	37.95	41.66	0.68	4.65	6.72	-57.4	0.0	-57.4
8	80	2873.55	2872.76	10.21	12.23	13.84	17.05	43.97	45.82	9.12	4.93	4.17	-94.4	0.2	-94.2
9	90	2875.75	2873.39	5.56	8.87	10.53	11.85	41.10	42.42	4.98	5.34	3.50	-63.5	0.3	-63.2
10	100	2875.54	2875.02	8.98	11.37	13.13	15.36	42.23	44.05	1.91	2.57	4.12	-15.7	0.0	-15.7
11	110	2876.31	2875.96	7.94	10.19	12.90	36.31	38.24	44.70	0.83	2.16	2.46	-48.4	0.0	-48.4
12	120	2879.51	2876.76	6.30	8.23	10.04	13.02	36.88	41.98	3.73	1.80	1.56	-78.5	0.6	-77.9
13	130	2878.38	2878.04	9.51	12.81	14.56	16.07	17.69	33.16	0.82	1.69	1.58	-82.3	0.7	-81.6
14	140	2879.66	2879.21	6.46	12.70	14.90	16.87	32.75	35.05	0.52	1.11	1.81	-25.5	4.3	-21.2
15	150	2881.44	2881.39	0.00	12.37	17.70	29.40	31.95	34.15	1.99	1.50	1.45	-39.1	0.0	-39.1
16	160	2883.04	2882.70	8.18	12.97	25.72	29.67	31.58	33.10	1.99	1.96	1.77	-33.9	2.9	-31.0
17	170	2885.71	2884.84	6.37	10.07	27.33	29.65	31.45	33.22	1.90	2.11	2.62	-40.6	9.6	-30.9
18	180	2886.75	2886.83	8.23	11.08	27.00	28.45	29.81	31.43	2.45	3.04	2.54	-15.1	2.3	-12.8
19	190	2888.92	2888.79	11.39	14.63	16.82	25.00	26.38	27.70	4.76	2.93	4.18	-27.4	0.0	-27.4
20	200	2891.19	2890.45	6.58	9.18	10.92	12.76	19.75	25.63	1.59	5.52	5.85	-30.3	0.7	-29.6
21	210	2892.93	2892.77	14.63	16.85	18.97	21.89	24.32	25.81	10.21	7.35	6.28	-78.9	0.8	-78.1
22	220	2894.86	2894.31	5.64	8.38	20.79	22.34	23.95	25.49	10.26	8.35	5.46	-81.5	0.0	-81.5
23	230	2896.90	2895.65	5.85	13.95	16.94	20.31	22.63	25.02	4.57	5.17	5.17	-45.9	0.0	-45.9
24	240	2898.21	2897.59	6.56	12.16	14.07	15.90	19.71	23.91	0.69	1.79	3.91	-22.3	0.6	-21.7
25	250	2899.43	2898.75	10.81	13.71	18.50	20.73	24.74	26.19	0.10	1.57	2.07	-77.8	1.0	-76.9
26	260	2901.73	2901.15	10.51	13.03	19.68	24.25	26.11	27.50	3.92	1.70	1.27	-47.1	0.2	-46.8
27	270	2902.94	2902.41	10.27	16.94	19.22	21.21	23.43	25.82	1.08	1.85	1.48			
28	280	2903.95	2904.02	5.34	9.59	16.81	19.91	21.88	24.22	0.56	1.13	2.39			
29	290	2906.84	2906.01	3.31	6.96	9.47	12.32	18.58	20.99	1.74	2.31	1.79			
30	300	2908.34	2907.97	7.09	9.73	12.08	14.48	15.95	17.46	4.64	2.43	2.10			
31	310	2910.41	2909.59	7.73	9.30	10.42	11.55	12.97	15.35	0.91	2.74	2.68			
32	320	2912.68	2912.06	5.43	9.08	12.67	15.55	16.80	18.34	2.68	2.35	4.76			
33	330	2914.86	2913.59	8.84	10.88	12.32	13.61	14.98	16.37	3.46	6.09	4.98			
34	340	2920.12	2915.51	6.09	7.69	9.14	11.00	13.11	14.81	12.13	7.10	5.04			
35	350	2919.47	2916.97	6.09	8.54	9.84	10.96	12.09	13.20	5.70	6.36	4.76			
36	360	2919.55	2918.67	4.18	6.47	8.04	9.34	10.47	11.58	1.26	2.74	4.53			
37	370	2921.52	2921.23	0.00	3.87	6.21	7.78	9.26	10.82	1.25	1.61	2.29			
38	380	2922.37	2922.45	5.33	7.28	9.19	11.17	13.14	14.63	2.34	1.49	1.36			
39	390	2923.50	2923.39	6.89	9.76	12.99	15.90	18.04	20.78	0.89	1.43	1.21			
40	400	2924.97	2924.52	7.82	10.84	13.65	15.63	17.26	18.87	1.06	0.83	1.36			
41	410	2926.02	2925.52	6.32	8.32	10.20	12.38	23.45	26.08	0.54	1.18				
42	420	2927.69	2927.11	5.75	10.06	12.65	16.49	27.38	29.47	1.95					
43	430		2928.34	8.52	10.75	12.89	15.49	20.40	25.02						
44	440		2929.80	8.60	10.61	12.55	15.17	24.82	27.93						
45	450		2931.41	4.34	9.72	12.78	17.20	20.77	32.16						
46	460		2932.55	6.85	11.51	14.21	16.21	17.92	19.50						
47	470		2933.90	7.65	9.80	16.29	18.22	20.72	28.31						
48	480		2936.02	6.63	9.95	22.76	24.64	26.54	47.73						
49	490		2937.49	8.92	13.90	18.25	21.02	31.38	46.71						
50	500		2939.73	3.76	5.97	8.12	10.42	13.27	38.06						
51	510		2942.02	6.58	10.28	12.31	13.93	16.06	38.28						
52	520		2945.18	5.26	7.07	8.65	10.27	33.39	35.81						
53	530		2947.20	17.39	24.50	26.42	28.31	31.19	35.73						
54	540		2949.03	4.56	14.86	17.56	23.79	29.40	31.28						
55	550		2950.49	6.10	9.92	14.86	18.13	20.64	22.81						
56	560		2952.77	6.72	13.51	16.61	19.17	21.24	22.98						